

DEFECTS IN CARBOHYDRATE-DEPENDENT LYSOSOMAL TARGETING LEAD  
TO ALTERATIONS IN GROWTH FACTOR SIGNALING

by

MEGAN AARNIO

(Under the Direction of Richard Steet)

ABSTRACT

**Lysosomal hydrolases are targeted to lysosomes by a carbohydrate-dependent mechanism. Following protein synthesis, mannose-6-phosphate (M6P) tags are added to N-glycans on lysosomal hydrolases by GlcNAc-1-phosphotransferase, allowing hydrolases to bind M6P receptors in the Golgi for trafficking to lysosomes. Mutations in *GNPTAB*, the gene encoding GlcNAc-1-phosphotransferase, cause the lysosomal storage disorder, mucopolysaccharidosis II (ML-II). Patients have abnormal skeletal, cartilage, and craniofacial development. While the genetic basis of ML-II is well defined, the drivers of early pathogenesis are not. Our laboratory has developed a zebrafish model for ML-II to explore this question. ML-II zebrafish embryos have altered craniofacial development, increased *col2a1* expression and elevated activity of the protease cathepsin K (CtsK). Recent work links the extracellular activity of CtsK to abnormal chondrogenesis by demonstrating that CtsK causes an imbalance in TGF $\beta$  and BMP growth factor signaling. Inhibition of CtsK activity normalizes this imbalance. Chapter two defines the mechanism whereby CtsK can cause altered growth factor signaling in ML-II cartilage. Using**

**in vitro studies, I show that CtsK directly cleaves and activates latent TGF $\beta$ . Conversely, CtsK is capable of cleaving and degrading mature BMP ligand. This signaling imbalance can be rescued by TGF $\beta$  inhibition, indicating that elevated TGF $\beta$  is likely the main driver of pathogenesis. In parallel studies, I used a HeLa-based model for ML-II to investigate how loss of lysosomal targeting impacts cell surface glycoproteins. This revealed changes in the abundance of multiple glycoproteins including uptake receptors, tyrosine kinases, and phosphatases. Further, loss of *GNPTAB* results in increased c-Met phosphorylation and localization to lysosomes. Normally, dephosphorylation of Met is controlled by protein tyrosine phosphatases (PTPs), which themselves are inactivated under oxidative conditions. *GNPTAB*-null cells have increased oxidative stress levels as measured by reactive oxygen species (ROS), likely due to impaired clearance of damaged mitochondria. Consistent with an ROS-dependent mechanism, antioxidant treatment restores phospho-Met levels whereas hydrogen peroxide treatment of HeLa cells elevates phospho-Met levels. Collectively, these results highlight two mechanisms whereby loss of carbohydrate-dependent lysosomal targeting alters signaling – one that arises from the action of secreted cathepsin proteases and one that arises from impaired cellular clearance and lysosomal storage.**

**INDEX WORDS:** Lysosomal storage disorder, cathepsin, zebrafish, growth factors, receptor tyrosine kinase, reactive oxygen species

DEFECTS IN CARBOHYDRATE-DEPENDENT LYSOSOMAL TARGETING LEAD  
TO ALTERATIONS IN GROWTH FACTOR SIGNALING

by

MEGAN AARNIO

BS, University of Georgia, 2009

A Dissertation Submitted to the Graduate Faculty of The University of Georgia in Partial  
Fulfillment of the Requirements for the Degree

DOCTOR OF PHILOSOPHY

ATHENS, GEORGIA

2017

© 2017

Megan Aarnio

All Rights Reserved

DEFECTS IN CARBOHYDRATE-DEPENDENT LYSOSOMAL TARGETING LEAD  
TO ALTERATIONS IN GROWTH FACTOR SIGNALING

by

MEGAN AARNIO

Major Professor: Richard Steet  
Committee: Heather Flanagan-Steet  
Michael Tiemeyer  
Kelley Moremen  
James Lauderdale

Electronic Version Approved:

Suzanne Barbour  
Dean of the Graduate School  
The University of Georgia  
August 2017

## DEDICATION

This work is dedicated to my wife, Claire Aarnio-Peterson and my parents, Alan and Laura Aarnio. I thank you for all of your love and support.

## ACKNOWLEDGEMENTS

I would like to thank Rich and Heather first for this opportunity. You both have been instrumental in my development as a scientist. Your drive and passion for science is unparalleled and you have instilled this in me. You encouraged me to always think critically and ask questions. You always pushed me to strive for more and treat every experiment as though it needed to be publication quality. I hope to make you proud!

To my committee members, Mike Tiemeyer, Kelley Moremen, and Jim Lauderdale, thank you for your suggestions and guidance. You have made meaningful contributions to my projects and my scientific development. Thank you for mentoring me throughout this process. Jim, thank you for your mentorship while I was a technician, and for introducing me to developmental biology. You inspired me to continue in academia and I will always be grateful for that.

To the Steet lab members and CCRC: you all are amazing! Noor, my cubby buddy, thank you for the long talks about science and life. I really appreciated your input and experimental advice and for your help in general. I will miss our snack drawer almost as much as you! You have been an amazing friend, and I'm so glad you joined the lab as a postdoc! Courtney, you are fabulous and will excel in graduate school. Cats, Star Wars, and fantasy/sci fi novels, that is all. Bob, thank you for the suitcase full of Hi-Chews and the weird fish snacks. Alex, thanks for keeping the fish alive and the giant chocolate bar. Michelle, you are now the only Steet lab graduate student! You got this! Also thank you for the cell culture chats. Alexina, thank you for your kindness. Seok-ho, you taught me

SEEL and how to do an IP and now I'm publishing that data! Thank you for all of your advice and help, and I will really miss getting in your way! To the thousands of zebrafish, thank you for your science sacrifice. I would also like to thank my colleagues and friends at the CCRC. This is a wonderful collaborative environment. I will really miss working here.

To my family and friends: your support has gotten me through this tiring process. Your constant motivation and love have kept me going when I thought I couldn't. Thank you Mom and Dad for always supporting me and giving me every opportunity you could. I'm getting my PhD because of you. Claire you are my everything. Long distance has been beyond tough and all of the hardships we have suffered would be enough to tear any couple apart, but here we are. Thank you for being you. To Maymay, you are a cute, adorable, dumb cat and I love you. Colleen, Cate, Susan, and Amanda, I will miss you all so much. Thanks for being amazing friends.

## TABLE OF CONTENTS

	Page
ACKNOWLEDGEMENTS .....	v
LIST OF TABLES .....	x
LIST OF FIGURES .....	xi
CHAPTER	
1 LITERATURE REVIEW AND INTRODUCTION .....	1
N-Linked Glycosylation Overview .....	1
Lysosomal Function .....	2
Mannose-6-Phosphate is the Common Recognition Marker on Lysosomal Enzymes .....	3
Carbohydrate-Dependent Lysosomal Targeting .....	4
GlcNAc-1-Phosphotransferase Enzyme .....	5
Uncovering Enzyme (UCE) .....	7
Mannose-6-Phosphate Receptors .....	8
Carbohydrate Independent Trafficking and Uptake .....	11
Cellular Consequences of Lysosomal Storage .....	13
MLII Clinical Characteristics .....	15
Animal Models of MLII .....	17
Chondrogenesis is a Growth Factor Driven Process .....	20

Transforming Growth Factor Beta (TGF $\beta$ ): Implications in Development and Disease .....	21
Bone Morphogenic Protein (BMP).....	25
Hepatocyte Growth Factor Receptor (c-Met) Function and Regulation....	26
Proteases in Extracellular Matrix Degradation and Growth Factor Regulation .....	30
Dissertation Overview .....	32
References.....	33
2 CATHEPSIN K PREFERENTIALLY ACTIVATES LATENT TGF $\beta$ GROWTH FACTORS, DRIVING CARTILAGE PATHOLOGY IN ZEBRAFISH MODEL OF MUCOLIPIDOSIS II.....	53
Abstract.....	54
Introduction.....	55
Results.....	57
Discussion.....	65
Materials and Methods.....	67
References.....	71
3 ALTERED MET RECEPTOR PHOSPHORYLATION AND LRP1 MEDIATED UPTAKE IN CELLS LACKING CARBOHYDRATE-DEPENDENT LYSOSOMAL TARGETING.....	81
Abstract.....	82
Introduction.....	83
Results.....	85

Discussion.....	92
Materials and Methods.....	96
Acknowledgements.....	100
References.....	102
4 DISCUSSION AND FUTURE PERSPECTIVES .....	113
The Contribution of Extracellular Cathepsins to Mucopolidosis II	
Pathology .....	113
Excessive TGF $\beta$ Signaling: A Hallmark of Disease.....	116
MLII Therapy.....	118
SEEL Applications and Future Studies in GNPTAB-null HeLa Cells....	120
Receptor Function and Activity is Modified by Glycosylation .....	122
References.....	124

## APPENDICES

A SUPPLEMENTAL TABLE.....	127
---------------------------	-----

## LIST OF TABLES

	Page
Table 1: Phenotype comparison between human MLII patients, feline MLII model, MLII mouse knock-in model, and morpholino generated MLII zebrafish.....	48

## LIST OF FIGURES

	Page
Figure 1.1: Normal and MLII Secretory Pathway .....	45
Figure 1.2: GlcNAc-1-Phosphotransferase Catalyzes the Biosynthesis of Mannose-6-phosphate .....	46
Figure 1.3: Domain Structure of GlcNAc-1-Phosphotransferase $\alpha\beta$ Subunit .....	47
Figure 1.4: Growth Factor Signaling Drives Chondrogenesis .....	49
Figure 1.5: Transforming Growth Factor Beta Synthesis and Processing.....	50
Figure 1.6: TGF $\beta$ and BMP Dependent Smad Signaling .....	51
Figure 1.7: c-Met Activation and Signaling .....	52
Figure 2.1: Amino acid sequence of human and zebrafish and TGF $\beta$ 1 precursor protein (LAP-TGF $\beta$ 1) .....	74
Figure 2.2: CTSK preferentially cleaves LAP .....	75
Figure 2.3: CTSK lowers the activation barrier for TGF $\beta$ ligand liberation from the Large Latent Complex (LLC) .....	76
Figure 2.4: CTSK degrades proBMP2.....	77
Figure 2.5: Pharmacological inhibition of TGF $\beta$ in MLII embryos rescues craniofacial morphology and chondrogenesis markers .....	78
Figure 2.6: TGF $\beta$ reduction in MLII embryos rescues TGF $\beta$ and BMP dependent genes and effectors.....	79
Figure 3.1: GNPTAB $^{-/-}$ cells have dynamic changes in cell surface sialoglycoproteins	107

Figure 3.2: Surface reduction of the reuptake receptor LRP1, results in decreased ligand uptake in GNPTAB <sup>-/-</sup> cells.....	108
Figure 3.3: GNPTAB <sup>-/-</sup> cells have increased levels of multiple phosphorylated receptor tyrosine kinases.....	109
Figure 3.4: Met and phospho-Met levels are increased in GNPTAB <sup>-/-</sup> cells.....	110
Figure 3.5: pMet increases are tied to elevated ROS in GNPTAB <sup>-/-</sup> cells.....	111
Figure 3.6: Wild type GlcNAc-1-phosphotransferase partially rescues lysosomal function in GNPTAB <sup>-/-</sup> cells .....	112
Figure 4.1: TGF $\beta$ reduction rescues zebrafish CtsL1a and CtsL1b transcript abundance in morphant zebrafish.....	126

## CHAPTER 1: LITERATURE REVIEW AND INTRODUCTION

### **N-Linked Glycosylation Overview**

Glycans serve essential cellular functions both on the interior and exterior of cells. They mediate protein interaction and function, protect against pathogens, transmit signals, facilitate protein stability, serve as recognition signals, and serve many other functions [1]. Glycans are classified by their linkage to the aglycone, which is the noncarbohydrate portion of the glycoconjugate [2]. Glycoproteins are either considered N-linked (attached via the nitrogen of an asparagine residue) or O-linked (attached via the hydroxyl of either a serine or threonine residue). Proteoglycans are a type of glycoconjugate that contain one or more glycosaminoglycan (GAG) chains. Glycans can also be attached to lipids thus forming glycolipids.

N-linked glycosylation takes place in the ER and Golgi apparatus. The process begins on the cytoplasmic face of ER with generation of the dolichol-p-p-glycan precursor [3]. Glycans are sequentially added in a stepwise fashion by glycosyltransferases to generate  $\text{Man}_5\text{GlcNAc}_2\text{-P-P-Dol}$ , which is translocated across the ER surface by a “flippase.” Further modifications take place to generate a 14-sugar glycan, which can then be transferred to asparagine residues in the Asn-X-Ser/Thr sequons of proteins translocated into the ER [4]. This transfer is mediated by the multisubunit oligosaccharyltransferase (OST). Following transfer, the glycan chain is

further processed within the ER and interacts with several chaperones to ensure proper folding of the glycoprotein [5]. Glycoproteins bearing either eight or nine mannose residues then exit the ER and enter the cis-Golgi [6]. Importantly, within the cis-Golgi, lysosomal hydrolases are recognized and modified by the GlcNAc-1-phosphotransferase enzyme (this will be described further in a subsequent section). Further processing takes place in the medial and Trans-Golgi leading to generate hybrid and complex N-glycans. Mature glycoproteins are then trafficked to the plasma membrane.

### **Lysosomal Function**

Lysosomes are dense acidic intracellular membrane-bound organelles that function to recycle and degrade macromolecules. Christian de Duve first described these dense acidic organelles in the 1950s [7]. Lysosomes are present in the majority of eukaryotic cells and are often located perinuclearly. They appear as spherical or tubular structures with a varying size that are typically greater than 1 $\mu$ m.

Lysosomes serve numerous cellular functions beyond cellular digestion, as evidenced by their importance in membrane repair, pathogen clearance, and bone remodeling [8]. Materials destined for the lysosome are received through multiple cellular mechanisms including, phagocytosis, autophagy, and the secretory pathway [9]. Cargo internalized from the plasma membrane is sorted through a series of endosomal compartments resulting in delivery of macromolecules to the lysosome for degradation. Autophagy is a process that involves the formation of double membrane autophagosome that sequesters and delivers cytosolic components to the lysosome [10]. This autophagic process serves as a cellular response to cell damage or starvation, and functions as a way

to conserve and reuse cellular material. The secretory pathway functions as a source of resident lysosomal components and is the route by which newly synthesized proteins reach the lysosome.

The secretory pathway originates with protein synthesis in the endoplasmic reticulum and proteins progress through the Golgi complex to subsequent transport vesicles destined for cellular organelles or the plasma membrane [11]. In order for lysosomal proteins to be separated from the bulk of secretory pathway proteins they are tagged with a unique carbohydrate moiety, mannose-6-phosphate (M6P), which will be discussed in the following section [12].

### **Mannose-6-Phosphate is the Common Recognition Marker on Lysosomal Enzymes**

Elizabeth Neufeld and colleagues performed early studies on genetic disorders characterized by the inability of disease cells to break down cellular components, resulting in lysosomal storage [13]. Interestingly, when they treated the disease cells with soluble factors (lysosomal hydrolases) from normal cells they could reverse cellular storage in a culture system. Using this cross correction approach Neufeld and colleagues determined that there were two types of secreted enzymes, “high-uptake” and “low-uptake” which differed in their ability to correct deficient cells. Further, cells from patients with severe lysosomal inclusions termed “I-cell disease,” were found to secrete large amounts of low-uptake enzymes, meaning that these enzymes were unable to be taken up by other cells (both diseased and normal) [14]. They also discovered that I-cells were able to internalize secreted factors from other cells [15]. From these findings they concluded that there was a common recognition marker on lysosomal enzymes that

resulted in their retention within the lysosome, and this marker was missing on lysosomal enzymes from I-cells. William Sly next discovered that secreted high-uptake enzyme endocytosis could be blocked through the addition of soluble mannose-6-phosphate (M6P), indicating that the recognition marker was M6P [16, 17]. I-cell disease is also known as Mucopolysaccharidosis II (ML-II), which is a severe lysosomal storage disorder caused by mutations in the enzyme that initiates M6P biosynthesis. The phenotypic and molecular characteristics of ML-II will be discussed later in this review.

### **Carbohydrate Dependent Lysosomal Targeting:**

As explained in the previous section, lysosomal enzymes contain M6P recognition markers that allow for proper sorting to the lysosomal compartment. M6P biosynthesis is initiated in the cis-Golgi by the enzyme N-acetylglucosamine-1-phosphotransferase (phosphotransferase) [18]. Phosphotransferase transfers GlcNAc-1-phosphate to high mannose oligosaccharides on the N-glycans of lysosomal proteins, specifically to the carbon-6 position of  $\alpha$ 1-2-linked mannose residues [3]. Further, this transfer happens en bloc and does not proceed through any intermediates [19]. The final step in M6P biosynthesis involves the removal of the external N-acetylglucosamine residues, yielding the mature M6P carbohydrate tag. The  $\alpha$ -N-acetylglucosaminidase enzyme, also termed “uncovering enzyme,” performs this second step.

The phosphotransferase enzyme identifies and modifies lysosomal enzymes with high affinity compared to non-lysosomal glycoproteins [18]. Lysosomal hydrolases are recognized by their protein conformation, since denatured and proteolytic fragments of

lysosomal hydrolases are not tagged with M6P [20]. It has also been demonstrated that specific lysine residues on lysosomal enzymes are important for phosphotransferase recognition [21]. Specifically, Kornfeld and colleagues showed that sequential mutation of specific lysines in the M6P modified enzyme, DNase I leads to a reduction in M6P modification. Similar studies have been performed with the lysosomal hydrolase cathepsin D, and show that mutation of two lysines within the mature portion of cathepsin D leads to a significant decrease in mannose phosphorylation [22]. Further, through gain-of-function studies, substitution of lysine residues and amino acids from a B loop region in cathepsin D to comparable regions in glycopepsinogen resulted in a significant increase in mannose phosphorylation and subsequent sorting to lysosomes [23-25].

### **GlcNAc-1-Phosphotransferase Enzyme**

The GlcNAc-1-phosphotransferase enzyme is a heterohexameric complex composed of two alpha, two beta, and two gamma subunits with a total molecular weight of 540kDa [26]. The  $\alpha$  and  $\beta$  subunits are composed of disulfide-linked homodimers with molecular weights of 166kDa and 51kDa respectively, while the  $\gamma$  subunit is formed by a noncovalently-associated homodimer, which is 56kDa. The GNPTAB gene encodes the  $\alpha$  and  $\beta$  subunits, while the GNPTG gene encodes the  $\gamma$  subunit [27, 28].

The  $\alpha\beta$  subunit makes up the catalytic portion of the phosphotransferase enzyme, and is composed of three domains, the stealth domain, two notch domains, and the DMAP domain, which are separated by spacer regions [29]. Importantly, the  $\alpha\beta$  subunit is synthesized in a catalytically inactive precursor form, and must undergo a cleavage

event between Lys-928 and Asp-929 by the site-1 protease in order to be active [30, 31]. The transmembrane domains of the  $\alpha\beta$  are essential for proper cleavage as shown through mutational studies that removed this portion of the protein. The stealth domain of the  $\alpha\beta$  subunit has similarities to bacterial proteins that function in cell wall biosynthesis and has been shown to act as a sugar-phosphate transferase [32]. A recent 2015 study used known mutations within the stealth domain to show that the stealth domain confers the catalytic activity of the subunit. Mutations within this region resulted in minimal activity towards  $\alpha$ -methylmannosidase, a known *in vitro* acceptor of GlcNAc-1-phosphate. This study also identified the Notch 1 domain as being important for recognition of lysosomal hydrolases. Mutations in this region lead to reduced M6P addition to lysosomal hydrolases but did not show a reduction in  $\alpha$ -methylmannosidase activity. Further mutational studies identified the DMAP interaction domain as being crucial for lysosomal hydrolase recognition and binding [29]. The DMAP domain mediates protein-protein interactions with lysosomal hydrolases, and is able to bind and immunoprecipitate lysosomal hydrolases. Interestingly, mutations within the DMAP domain resulted in normal localization and interaction with the  $\gamma$  subunit, as well as activity towards  $\alpha$ -methylmannosidase, although activity towards lysosomal hydrolases was reduced by about 85%. Using CRISPR mediated inactivation of either the GNPTAB gene or the GNPTG gene, the Kornfeld lab recently discovered that the two Notch regions and the DMAP domain in the  $\alpha$  subunit of the phosphotransferase enzyme facilitate recognition of lysosomal hydrolases [33]. This was accomplished by transfecting in mutant Notch or DMAP domains into CRISPR-null cells.

The  $\gamma$  subunit is a 30kDa soluble glycoprotein that is composed of two domains, a Man-6-P receptor homology domain (MRH) that includes regions necessary for mannose binding, and a DMAP interaction domain [33, 34]. As part of the phosphotransferase enzyme, the  $\gamma$  subunit enhances the rate and efficiency of GlcNAc-1-phosphate transfer to a selection of lysosomal hydrolases; mutational studies showed that  $\gamma$  does not have the ability to recognize and bind in a conformational dependent way to certain lysosomal hydrolases when mutated [35]. Further, the  $\gamma$  subunit also assists with the addition of the second GlcNAc-1-phosphate to high mannose oligosaccharides of acid hydrolases [36].

### **Uncovering Enzyme (UCE)**

After lysosomal hydrolases are tagged with GlcNAc-1-phosphate, the terminal GlcNAc residue must be removed in order to expose the mature M6P epitope. As stated previously, the “uncovering enzyme” or UCE, catalyzes the second step in the generation of M6P on acid hydrolases, which takes place in the trans-Golgi network [37]. UCE is synthesized as an inactive proenzyme that is only activated in the trans-Golgi network when it comes in contact with the endoprotease furin. Furin cleaves a RARLPR/D sequence and releases the 24-amino acid pro-inhibitory region of the UCE peptide. Mature UCE is a type I transmembrane glycoprotein that forms a tetramer composed of two disulfide-linked homodimers [38]. Known UCE mutations lead to increased proteosomal degradation and reduced enzyme activity [39]. Interestingly, mutations in UCE do not lead to Mucopolysaccharidosis II like phenotypes, but rather result in persistent stuttering.

## **Mannose-6-Phosphate Receptors**

After the mature M6P carbohydrate tag is uncovered on lysosomal hydrolases through the action of UCE, high affinity mannose-6-phosphate receptors (MPRs) recognize and bind hydrolases based on their M6P tag. There are two receptors, which are known as P-type lectins since they recognize phosphorylated mannose residues, the cation-dependent mannose 6-phosphate receptor (CD-MPR) and the cation-independent mannose 6-phosphate receptor (CI-MPR) [40, 41]. Both MPRs are type I transmembrane glycoproteins, but differ in molecular weight and structure, with the CD-MPR existing as 46kDa homodimer, and the CI-MPR existing as a 300kDa oligomer [42, 43].

MPRs cycle between the TGN, endosomes, and the plasma membrane, and have a half-life of approximately 20 hours [44]. Typically, 10% of the total CI-MPR within the cell is found at the plasma membrane, where it functions to uptake M6P containing ligands, which has important implications for enzyme replacement therapy. Both MPRs undergo different types of co- and posttranslational modifications that affect their intracellular transport, localization, and degradation. Both receptors bind M6P containing ligands at a pH optimum of 6.5 and release cargo at pH 5 or below, which is essential for lysosomal hydrolase trafficking and release. Importantly, both receptors are needed for effective transport of the more than 60 different lysosomal hydrolases. Knockout studies in fibroblasts and animal models indicate that neither receptor can totally compensate for the other, suggesting that the two receptors recognize different regions on lysosomal hydrolases or different hydrolases [45, 46].

CI-MPR is also known as the insulin-like growth factor II receptor since it can bind and internalize non-glycosylated IGFII, which is essential for controlling

extracellular signaling of IGFII in mammals [47]. As well as binding lysosomal hydrolases, the CI-MPR can bind and traffic non-lysosomal proteins bearing M6P tags such as the Leukemia Inhibitory Factor (LIF), although this is a less common mechanism. The CI-MPR binds with high affinity to lysosomal hydrolases containing two M6P moieties, and with less affinity to hydrolases containing only one M6P, while the receptor has very low affinity for covered M6P (GlcNAc 1-phosphate covered), which is interesting because UCE mutations are very mild [48]. The CI-MPR contains a large extracellular domain composed of 15 repetitive units that are 145 amino acids long and share partial similarity to each other and are termed Mannose 6-phosphate Receptor Homology (MRH) domains [49]. Each domain contains three or four disulfides and share approximately 14-38% homology to each other [44]. Of the 15 MHR domains, 3, 5, and 9 have been shown to participate in M6P binding, while domain 11 has a single IGFII binding site. These sites differ in their preference for binding to phosphomonoesters (domains 3 and 9) or phosphodiester (domain 5) [50]. Further, domains 3 and 5 have higher affinity for ligands when associated with adjacent domains, while additional domains are not needed for domain 9 binding affinity. Recently, domain 15 was identified as another M6P binding domain with the ability to recognize both mono and phosphodiester [51]. It was further shown that interaction with other domains increased the affinity of M6P binding to domain 15.

The cytoplasmic tail of CI-MPR serves two roles; endocytosis of extracellular lysosomal hydrolases, and sorting of newly synthesized hydrolases [52]. Based on mutational studies of the cytoplasmic tail of the CI-MPR, deletion of 40-89 residues from the carboxyl terminus resulted in impaired sorting of hydrolases but did not affect

endocytosis, while larger deletions removing most of the cytoplasmic domain lead to defects in endocytosis and sorting.

The cation-dependent mannose 6-phosphate receptor or CD-MPR was thus named based on its requirement of divalent cations for optimal M6P binding. It has a single extracellular MHR domain that is similar to the MHR domains of CI-MPR. The CD-MPR forms a stable homodimer, with each dimer binding one M6P, and shows greatest affinity for binding phosphomonoesters [44, 53]. Further, CD-MPR exists in two conformations, an “open” state with bound M6P and a “closed” state without bound ligand. Different from the CI-MPR, the CD-MPR does not bind M6P containing ligands at the cell surface.

Loss of function studies using targeted disruption of the CD-MPR in mice, showed slightly increased circulation of lysosomal enzymes, but mice appear phenotypically normal and are able to reproduce [48, 54]. Fibroblasts cultured from CD-MPR deficient mice have increased secretion of phosphorylated lysosomal enzymes in the medium, indicative of impaired sorting. Deletion of the CI-MPR gene is embryonic lethal in mice, as loss of CI-MPR inhibits IGFII uptake. Double knockouts of CI-MPR and IGFII are viable and but display a dwarf phenotype which is similar to IGFII knockouts [55]. Further, CI-MPR and IGF-II double knockouts have a higher level of mis-sorting than CD-MPR knockouts. Triple-deficient (CI-MPR, IGF-II, and CD-MPR) mouse mutants have been developed and show a similar phenotype to human ML-II patients, and have increased lethality, with high levels of lysosomal enzymes in serum and lysosomal storage [54]. Based on triple knockout studies, specific M6P modified

lysosomal hydrolases can be trafficked to lysosomes in a M6P independent manner, which appears to be cell type specific.

### **Carbohydrate Independent Trafficking and Uptake Mechanisms**

In the absence of carbohydrate dependent lysosomal targeting, as is the case with ML-II patients, multiple cell types and tissues have normal levels of lysosomal hydrolases [56]. These cell types include, lymphocytes, hepatocytes, leukocytes, and Kupffer cells, and the tissues, brain, spleen, kidney, and liver [15, 57]. Based on these observations, multiple mechanisms of M6P independent trafficking are present. Several carbohydrate independent pathways of lysosomal trafficking have been identified, and include the receptors LIMP2, sortilin, and LRP1. Further, the lysosomal associated membrane protein family (LAMP1, 2) are two integral membrane proteins that are localized to the lysosome are not sorted by M6P mechanisms. Instead, these lysosomal proteins use sorting signals in their cytoplasmic domains that function similarly to the two MPRs by associating with clathrin-coated vesicles [48]. The majority of newly synthesized and glycosylated Lamp is sorted to the lysosome directly from the trans-Golgi network, but a small percentage traffics to the plasma membrane before associating with the lysosome [58]. The sorting signal for Lamp has now been identified and a C-terminal isoleucine is essential for correct targeting of Lamp to lysosomes [59].

LIMP2, or lysosomal integral membrane protein-2, is a type III membrane glycoprotein that was identified as the key receptor for  $\beta$ -glucocerebrosidase ( $\beta$ GC), which is the enzyme implicated in Gaucher Disease [60-62]. In the absence of both MPRs, intracellular trafficking of  $\beta$ GC is unaffected, indicating an alternative trafficking

mechanism. Sortilin is another carbohydrate independent sorting receptor, and is a member of the Vps10 domain receptor family [63]. Sortilin is a 100kDa receptor that has been shown to transport sphingolipid activator proteins (SAPs), acid sphingomyelinase, and the two lysosomal cathepsins D and H [64]. Studies involving sortilin knockdown and truncation revealed that trafficking of the SAPs, GM2AP and prosaposin, were blocked, and thus dependent on sortilin function.

Another important pathway to the lysosome involves enzyme reuptake from the plasma membrane. Low-density lipoprotein receptor-related protein 1 (LRP1) is a transmembrane receptor that is synthesized as a large 600kDa precursor and is processed into two subunits [65]. Furin cleaves LRP1 in the *trans*-Golgi into two non-covalently linked subunits, a 515kDa  $\alpha$ -subunit and an 85kDa transmembrane  $\beta$ -subunit. The large extracellular  $\alpha$ -subunit is the ligand binding region, and the  $\beta$ -subunit is involved in cellular signaling [66]. The  $\alpha$ -subunit is composed of multiple segments that include, ligand binding regions enriched with cysteine repeats, EGF precursor homology domains, and YWTD domains [67]. The cytoplasmic  $\beta$ -subunit includes two NPxY domains and functions as a scaffold for adaptor binding and signaling pathways.

LRP1 recognizes more than 30 different proteins of many different ligand classes. Of particular interest, LRP1 binds protease inhibitors and multiple proteases including the Serpin superfamily of serine protease inhibitors, matrix metalloproteinases, and cathepsins B and D [67-70]. Multiple studies have shown that cathepsin D trafficking is M6P independent in certain tissues, such as breast cancer cells as ammonium chloride treatment does not promote cathepsin D secretion [71]. Further, pro-cathepsin D is internalized by breast cancer cells in the presence of M6P, indicating endocytosis is not

solely dependent on CI-MPR mediated uptake [68]. Interestingly, in double knockout cell lines of sortilin and GlcNAc-1-phosphotransferase, intracellular levels of cathepsin D were similar to GlcNAc-1-phosphotransferase knockout alone [72]. Further, medium secreted cathepsin D was not increased in double knockout cells, therefore indicating another sorting receptor was responsible for cathepsin D targeting. Both cathepsin D and B were shown to localize to Lamp1-positive vesicles in double knockout cells. These findings by Markmann and colleagues revealed that cathepsin D and B were targeted to the lysosome via a secretion and reuptake method by LRP1.

### **Cellular Consequences of Lysosomal Storage**

Lysosomal storage disorders (LSDs) have a prevalence of 1/8000 live births, and are classified as inherited disorders of dysfunctional metabolism [73, 74]. Lysosomes contain upwards of 60 acid hydrolases that perform diverse functions needed for cellular recycling and metabolism. Mutations in any one of the enzymes responsible for breakdown of cellular components can result in a lysosomal storage disorder. These disorders characteristically cause lysosomal storage and are progressive in nature with symptoms affecting multiple organ systems [75-77]. Many patients born with LSDs appear normal, and the hallmark clinical presentation of neurodegeneration occurs during infancy and early childhood [78]. Interestingly, the majority of LSDs affect the central nervous system and lead to neuropathology in multiple brain regions and neuronal subtypes.

At a cellular level, many processes are affected by lysosomal storage, including recycling and autophagy. Literature suggests that recycling is reduced in LSDs,

especially in the case of Nieman Pick, due to accumulation of cholesterol and impaired fusion of vesicles [79]. Similarly, autophagy is also affected as evidenced by an accumulation of autophagosomes in several mouse models of LSDs [80, 81]. Interestingly, MLII fibroblasts have a proliferation of lysosomes, suggesting alterations in TFEB nutrient sensing [82].

Lysosomal hydrolytic enzyme deficiency leads to accumulation of macromolecules which when severe can lead to secondary substrate accumulation due to inhibition of other enzymes. This buildup of substrates can impact turnover of defective organelles, such as mitochondria. Further, mitochondrial dysfunction has been linked to cellular increases in reactive oxygen species (ROS), and affects tissues with extensive ROS production [83]. Thus there is a tie between lysosomal storage and mitochondrial mediated ROS production. As an example of this, iPC derived vascular endothelial cells from the X-linked LSD, Fabry disease (FD), show an increase in ROS production [84]. Tseng and colleagues show that increases in ROS were caused by downregulation of the mitochondrial antioxidant superoxide dismutase 2 (SOD2). Further, suppression of SOD2 was caused by intracellular accumulation of globotriaosylceramide (Gb3), which is the undegraded metabolite in FD. The implications of lysosomal storage and ROS production will be discussed further in chapter 3.

Mucopolipidosis II is a severe pediatric lysosomal storage disorder that arises from mutations that affect the catalytic subunit of the GlcNAc-1-phosphotransferase enzyme, which is encoded by the GNPTAB gene [27, 28]. Mutations in the GNPTG gene that encodes the gamma subunit lead to the less severe lysosomal storage disorder, Mucopolipidosis III. Unlike other LSDs, which result from mutations in individual

lysosomal hydrolases, all enzymes are functional in ML-II, but fail to traffic to the lysosome [85, 86]. Specific loss of M6P carbohydrate dependent targeting can lead to massive lysosomal storage since macromolecules are not recycled or degraded. Certain tissues are affected more by lysosomal storage than others, which may be dependent on the presence of M6P independent targeting.

Approximately 100 autosomal recessive mutations have been identified in GNPTAB that lead to nonsense or frameshift mutations resulting in less than 1% GlcNAc-1-phosphotransferase activity, and are classified as ML-II alpha/beta [87-90]. Missense mutations leading to residual protein function are characterized as the less severe ML-III alpha/beta. Further, nonsense, frameshift, or missense mutations in GNPTG lead to ML-III gamma, with these mutations presenting a milder phenotype.

### **Mucopolipidosis II Clinical Characteristics**

ML-II is recognizable at birth and symptoms include characteristic skeletal phenotypes (termed dystosis multiplex), coarse facial features, gingival hyperplasia, short hands and fingers, thoracic deformity, and thick waxy skin [87, 91]. Patients have thickening of the mitral valve and progressive mucus secretion leading to airway thickening. Table 1.1 provides a phenotypic comparison between human MLII patients, feline MLII, a mouse knock-in model of MLII, and morpholino generated MLII zebrafish. Pregnancy abnormalities including growth delay and oligohydramnios can result in preterm delivery. Following phenotypic and radiographic analysis, a metabolic panel assaying for high enzyme plasma levels is used to diagnose patients, as well as genetic analysis. Patients have a failure to thrive and have severe developmental delay

with delayed and incomplete neuromotor development, often growth ceases within 24 months [92]. Unfortunately, ML-II patients rarely survive beyond the first decade, and succumb to numerous respiratory infections and suffer from cardiac abnormalities [93].

At a cellular level, patient fibroblasts contain large dense cytoplasmic inclusions composed of non-degraded material. Cells deficient in GlcNAc-1-phosphotransferase have lysosomal proliferation and enlargement, shown by increased Lamp-1 immunostaining [33, 94]. ML-II lysosomes contain increased concentrations of glycoproteins with terminal sialic acid, N-acetyl-glucosamine, and mannose residues, as well as increased cholesterol and phospholipid levels. Plasma concentrations of lysosomal enzymes are increased by 5-20% compared to control samples, which is indicative of hydrolase hypersecretion [87].

ML-III symptoms develop much slower and children are usually diagnosed several years after birth. This disorder is less severe but the impact on patients' lives is still debilitating. Most children develop joint stiffness and reduced range of motion as well as scoliosis [91].

Relatively few therapies are available to treat ML-II and other LSDs, and most therapies are aimed towards reducing symptoms, since these genetic disorders have no cure. Bisphosphonate, which decreases bone resorption, has shown some efficacy in reducing bone pain in a ML-II experimental trial [95]. While this therapy shows great promise, it has adverse side effects such as flu like symptoms, and does not prolong patient lifespan. Enzyme replacement therapy (ERT) is effective for some LSDs such as Gaucher disease [96], but efficacy is relatively low for most LSDs, as targeting to certain organelles or tissues can be difficult [97]. The aim of ERT is to reintroduce a functional

version of the enzyme that is defective in the LSD. The basis for ERT stems from the ability of the CIMPR to reuptake M6P tagged lysosomal hydrolases; therefore reintroduced enzymes are M6P modified. Unfortunately, ERT for ML-II would be ineffective because reintroduction of the numerous misstargeted hydrolases would be impractical. It is thus necessary to further our understanding of the disease in hopes of finding an effective treatment for ML-II.

### **Animals Models of Mucoipidosis II**

The first animal model of ML-II was a naturally occurring feline model identified in the mid 1990s [98, 99]. The leading symptoms were facial dysmorphism and dysotosis multiplex, and upon further investigation there was a deficiency of GlcNAc-1-phosphotransferase activity in cultured fibroblasts. Further, the cat fibroblasts had a striking similarity to the characteristic inclusions seen in human patients, as well as increased serum concentrations of lysosomal hydrolases. ML-II inheritance in affected kittens is consistent with the autosomal recessive mode of inheritance seen in patients [100]. Affected kittens suffered from upper respiratory infections and cardiac complication that lead to early mortality within 7 months of life.

Several mouse models of ML-II have also been developed recently. The first mouse model developed was a *Gnptab* gene trap model resulting in the deletion of the *Gnptab* gene [101]. These mice showed impaired growth, severe retinal degeneration, and elevated serum levels of lysosomal hydrolases, but did not have the characteristic skeletal abnormalities seen in patients. Further, these knockout mice had a normal life span. The Brulke lab has generated a ML-II mouse knock-in model by insertion of a

cytosine homologous to a mutation in an ML-II patient [102, 103]. This model shows many similarities to ML-II patients, especially the skeletal deformities, such as reduced bone size and volume. In general, the ML-II knock-in mice had decreased bone formation and an increase in bone reabsorption, further there was a marked decrease in mineralization of culture osteoblasts. Interestingly, ML-II osteoblasts showed decreased expression levels of differentiation markers, indicating impaired differentiation. Bräulke and colleagues demonstrated that osteoclastogenesis was increased while osteoblast activity was decreased in ML-II knock-in mice, which they suggest is the reason for low bone mass in these mice. Another ML-II mouse model has been recently generated via an ENU screen and contains the previously reported patient mutation Y888X [87, 104]. These ML-II mice displayed many of the pathological features seen in human patients such as, reduced growth, kyphosis, and facial abnormalities such as a flat profile and a reduced nasal bridge. Further, these ML-II mice had increased mortality. Mouse models are useful for studying the pathology and disease progression of ML-II, but are problematic for studying early developmental time points due to uterine development. As a way to study the early developmental time points in ML-II, a zebrafish model has been developed which recapitulates both the phenotypic and biochemical alterations seen in patients [105-107].

Zebrafish ML-II mutants or morphants are generated via morpholino knockdown of GlcNAc-1-phosphotransferase or TALEN mediated mutagenesis. Morphants have a short protracted jaw, impaired motility, and develop a significant heart edema [105]. Craniofacial chondrogenesis is severely affected in morphants, with many chondrocytes failing to intercalate. Further, type II collagen and Sox9, which are early markers of

chondrogenesis, have increased expression in morphant craniofacial elements, suggesting altered cartilage development and impaired extracellular matrix (ECM) production or turnover. This increase in type II collagen expression and deposition in the ECM arises from disrupted TGF $\beta$ -related signaling in morphants [107]. TGF $\beta$ -like Smad2,3 signaling is increased while BMP-like Smad1,5,8 signaling is reduced in morphant chondrocytes, which impedes the progression of chondrogenesis. This raises the question of whether reduction of TGF $\beta$  signaling can alleviate morphant phenotypes, which will be the focus of chapter two.

Interestingly, the lysosomal hydrolase cathepsin K had increased and sustained activity during the same developmental time points and tissues that type II collagen expression was increased [106]. Cathepsin K is a potent collagenase, but upon suppression of its activity in morphant zebrafish, there was a reduction in type II collagen accumulation. Reduction of cathepsin K to wild type levels also rescued many of the craniofacial phenotypes seen in morphants. Of note, inhibition of cathepsin K also rescued the cellular morphology of chondrocytes and resulted in chondrocyte intercalation. This finding suggests that excessive cathepsin K activity plays a role in the abnormal chondrogenesis of morphants.

Under normal conditions, cathepsin K is tagged with M6P, but loss of GlcNAc-1-phosphotransferase in morphants leads to the hypersecretion of cathepsin K to the ECM [107]. Affinity-binding assays showed that the level of mannose phosphorylation of cathepsin K in ML-II embryos was significantly reduced when compared to wild type embryos of the same age, indicating loss of M6P on cathepsin K. Further, enzyme assays performed on morphant chondrocytes showed that cathepsin K activity levels were 2-5

times lower than wild type cathepsin K activity within chondrocytes. Further evidence that cathepsin K is hypersecreted from ML-II chondrocytes was confirmed by immunohistochemical staining of craniofacial cartilage in WT and ML-II embryos. Recently published data links elevated cathepsin K activity to alterations in TGF $\beta$  growth factor signaling, which will be the focus of chapter three.

### **Chondrogenesis is a Growth Factor Driven Process**

Chondrogenesis is the process by which chondrocytes develop and form a mature cartilage structure, which in some locations is ossified to form bone. This process requires the precise oscillation of several growth factors, which mediate the expression of ECM components. Craniofacial chondrogenesis begins with the migration of non-differentiated mesenchymal neural crest cells into the presumptive facial region [108]. During maturation, chondroprogenitors express TGF $\beta$  as indicated by Smad2,3 in Figure 1 [109] [110]. TGF $\beta$  signaling in conjunction with Sox9 drive the deposition of type II collagen, and as stated earlier, is one of the earliest markers of chondrogenesis. Maturation of chondrocytes marks a stage of high proliferation and expression of TGF $\beta$  [108] [110]. This chondrocyte proliferation stage is followed by chondrocytic hypertrophy [111]. Pre-hypertrophic chondrocytes express the extracellular matrix proteins aggrecan and decorin and there is a marked switch from TGF $\beta$  signaling to BMP signaling, as indicated by Smad1,5 in figure 1.4. During hypertrophy, chondrocytes swell and begin to apoptose which corresponds to expression of type X collagen [110]. As chondrocytes undergo hypertrophy, osteoblasts enter the region and begin the ossification process.

Endochondral ossification is the process by which hypertrophic chondrocytes apoptose and are subsequently invaded by osteoclasts and osteoblasts that synthesize a calcified matrix [112]. The two transcription factors Runx2 and Osx promote this matrix ossification. At this time the extracellular matrix surrounding hypertrophic chondrocytes is degraded by proteases such as matrix metalloproteinases and cathepsins [113].

### **Transforming Growth Factor Beta (TGF $\beta$ ): Implications in Development and Disease**

Transforming growth factor beta (TGF $\beta$ ) is a member of the TGF $\beta$  superfamily and is a key cytokine involved in growth and development, tissue homeostasis, extracellular matrix synthesis/secretion, and apoptosis [114] [115]. There are four zebrafish TGF $\beta$  isoforms (1a, 1b, 2, and 3) and four latent TGF $\beta$  binding protein (LTBP) isoforms that all signal within different cellular contexts, which accounts for the great functional diversity of the TGF $\beta$  family [114, 116]. As shown in figure 1.5, TGF $\beta$  is synthesized as a propeptide dimer with the mature peptide attached to latency associated peptide (LAP) [114, 115]. Within the trans-Golgi, furin enzymes cleave LAP from the mature TGF $\beta$  dimer but the two proteins remain noncovalently associated forming the small latent complex (SLC), which functions to keep TGF $\beta$  inactive. LAP then associates with latent TGF $\beta$  binding protein (LTBP) through disulfide linkages to form the large latent complex (LLC). Upon secretion, LTBP is targeted to the matrix resulting in TGF $\beta$  sequestration within the ECM. LTBPs are structurally similar to fibrillins, which are components of microfibrils, and are considered important for the SLC to be targeted to the ECM [117].

TGF $\beta$  can be activated through many mechanisms one of which is mechanical release via matrix associated proteins such as integrins [114]. TGF $\beta$  can also be activated through thrombospondin or proteases. Specifically serine proteases and matrix metalloproteases have been implicated in activation of TGF $\beta$ . LTBP contains a protease sensitive hinge region that upon cleavage releases soluble LLC which then can be further cleaved to result in the release of TGF $\beta$  [118]. Specific cleavage of LAP by plasmin (serine protease) and to a lesser degree cathepsin D has been shown to release a low molecular weight protein with immunoreactivity to a TGF $\beta$  antibody [119]. Finally, treatment of latent TGF $\beta$  with acid in vitro has been shown to release active TGF $\beta$ . Thus activation of mature TGF $\beta$  is a complex process mediated by numerous factors.

As shown in figure 1.6, the ligand/mature growth factor activates Smad signaling by binding membrane receptor protein kinases which triggers the formation of a receptor complex that recruits and activates Smad transcription factors. There are two classes of receptors that recognize TGF $\beta$  family members, T $\beta$ R-I or Type I and T $\beta$ R-II or Type II serine/threonine protein kinase receptors. Both receptors are glycoproteins with a small extracellular region for binding the ligand [120]. The type I receptor contains a repeating GS region that is wedged within the kinase domain keeping the receptor catalytically inactive. TGF $\beta$  dimers activate signaling by first binding the T $\beta$ R-II receptor which then phosphorylates the GS region thereby dissociating it from the kinase domain and catalytically activating T $\beta$ R-I [120]. Therefore, type I receptors (T $\beta$ R-I) for TGF $\beta$  can only recognize and bind ligands when they are bound to the type II receptor (T $\beta$ R-II) first, and not free in solution. Type I receptors recognize and interact with receptor-regulated Smads or R-Smads on the intercellular surface to phosphorylate and transduce

the signal [121]. Signal transduction is also mediated through endocytosis of the activated receptor through clathrin coated pits or Caveolin-dependent endocytosis [122]. There are five vertebrate R-Smads; Smads 1,5, and 8 propagate BMP and anti-Muellerian signals, while Smads 2 and 3 propagate TGF $\beta$ , activin, and Nodal signals [121]. Smads6 and 7 serve as inhibitory Smads, with Smad6 blocking Smad1 and Smad4 interaction, and Smad7 functioning as a competitive inhibitor. Smad4 is a co-Smad and functions as a binding partner to all R-Smads. Upon phosphorylation, R-Smads translocate to the nucleus through interaction with nucleoporins and associate with DNA, dephosphorylation triggers the R-Smads to leave the nucleus. Further regulation in the basal unphosphorylated state is mediated by the cytosolic retention factor SARA [121]. The signaling system is therefore tightly controlled and linked to the activation state of the ligand receptor complex. Regulatory Smads form a complex with the Co-Smad (Smad4) once phosphorylation has occurred, either in the cytoplasm or within the nucleus [121]. Smad4 is thought to assist in the formation of transcription complexes on DNA and to help recruit cofactors. As indicated, Smad transcription factors transduce TGF $\beta$  family member signaling through an intricate process involving tightly regulated phosphorylation states and cofactor interactions.

Proper TGF $\beta$  signaling is essential for normal chondrogenesis, as it induces cartilage matrix synthesis and chondrocyte lineage committal [123]. This is evidenced by studies showing addition of exogenous TGF $\beta$  to undifferentiated mesenchymal cells induces chondrocyte development [124]. As mesenchymal cells begin to differentiate into chondrocytes, cells express type II collagen, which is an early chondrogenic differentiation marker [125]. TGF $\beta$  signaling stimulates type II collagen expression, and

this stimulation is mediated through Smad2/3 interaction with Sox9 on the type II collagen enhancer. PhosphoSmad2/3 translocates to the nucleus where it associates with Sox9 and its coactivator the histone acetylase CBP/p300. These factors form a complex on the type II collagen enhancer and consequentially promote type II collagen transcription. Further evidence for TGF $\beta$  required signaling in chondrogenesis is indicated by mouse knockout studies showing deformities in palatogenesis [126]. Recently, morpholino knockdown of TGF $\beta$ 2 in zebrafish caused craniofacial defects including a reduced palate and Meckel's cartilage [116].

TGF $\beta$  signaling dysregulation has been implicated in numerous disorders and diseases. For example, Myelodysplastic Syndrome (MDS), a disease resulting in anemias and cytopaenias, occurs from low levels of the inhibitory Smad7, which inhibits the TGF $\beta$  Type I receptor. Under reduced Smad7 levels, myeloid progenitor cells become sensitized to TGF $\beta$  signaling, so incremental levels of TGF $\beta$  leads to a large Smad2,3 response [127]. Another disorder, Marfan's Syndrome (MFS), is an autosomal dominant connective tissue disorder caused by a mutation in the fibrillin 1 gene [127, 128]. Within the ECM, fibrillin functions to sequester and control TGF $\beta$  signaling through binding of the LLC [127]. In MFS, TGF $\beta$  is abnormally activated and leads to muscle, skeletal, cardiovascular, and ocular issues. Another disorder characterized by excessive TGF $\beta$  signaling is Camurati-Engelmann Disease (CED) [129-132]. CED is caused by mutations in the latency associated peptide of TGF $\beta$ . LAP mutations lead to increased liberation of mature TGF $\beta$  ligand and thus increased signaling. CED patients have increased bone turnover and osteosclerosis, and suffer from severe leg pain, muscular weakness, and facial paralysis. These diseases highlight the importance of regulated TGF $\beta$  signaling in

normal tissue homeostasis, and were the first real demonstrations that ECM mediated growth factor latency and disruptions in ECM caused disease due to growth factor signaling.

### **Bone Morphogenetic Protein (BMP)**

BMPs are a subfamily of the TGF $\beta$  superfamily, and were first identified as mediators of ectopic bone formation, but now have been implicated in numerous cellular processes [133]. BMPs are synthesized with three domains, an N-terminal signaling peptide for directing the protein to the secretory pathway, followed by a prodomain which assists with proper folding, and finally the C-terminal mature peptide [122]. Serine proteases cleave the prodomain within the Trans Golgi to form the mature peptide. Signaling is primarily through homo and heterodimers that are linked via a disulfide bond. Individual monomers are formed around a cysteine knot motif. BMP ligands signal through BMP specific Type I (BMPRI) and Type II (BMPRII) serine threonine kinase receptors and activate Smads 1,5,8.

BMP signaling is tightly regulated by the secreted extracellular antagonists chordin and noggin [134]. Proteolytic activation also regulates BMP signaling, as BMP is synthesized as an inactive precursor, and is cleaved after the -R-S-K-R- motif. Cleavage via proprotein convertase endoproteases such as furin, results in a mature C-terminal BMP dimer. There are two cleavage sites within the prodomain of BMP4, which regulate the signaling range of the mature ligand. It is postulated that initial cleavage results in a noncovalent association of the prodomain with the mature ligand, similar to LAP-TGF $\beta$  cleavage. This differs from LAP-TGF $\beta$  in that this association targets the complex for

degradation. Following cleavage at the subsequent site, mature BMP is released and due to a conformational change is not targeted for degradation.

In mammals, there are twelve BMPs and they are divided into four groups, with BMPs 2 and 4 constituting the most relevant in craniofacial development. Zebrafish have two BMP2 homologues BMP2a and 2b and one BMP4 homolog that are both embryonically expressed and critical for proper development. BMP signaling is essential for chondrogenesis, as it promotes chondrocyte terminal differentiation [135]. This is shown by cell culture studies indicating that BMPs increase the expression of type X collagen, which marks hypertrophic chondrocytes. Additionally, inactivation of BMP type I receptors result in a severe cartilage phenotype, as there is a reduction in chondrocyte proliferation and an increase in chondrocyte apoptosis [136].

In addition to TGF $\beta$  dysregulation, BMP signaling is also implicated in Marfan's Syndrome (MFS) [128]. The level of phospho Smad 1,5 is decreased in MFS cells, as a function of increased TGF $\beta$  signaling. With the addition of exogenous BMP there was a restoration of cellular osteogenic behavior, suggesting cross talk between the two signaling molecules. Another example of decreased BMP signaling leading to a pathogenic state is osteoporosis [137]. In a mouse model of osteoporosis, loss of BMP2 leads to an osteoporosis like phenotype. Therefore, it is critical that proper growth factor signaling levels are maintained, since imbalances can lead to altered bone phenotypes.

### **Hepatocyte Growth Factor Receptor (c-Met): Function and Regulation**

Receptor tyrosine kinases (RTKs) are cell surface signaling receptors that serve essential roles during organismal development and tissue maintenance, but dysregulation

can lead to cancer development and progression [138-141]. Currently there are 58 known human RTKs that are grouped into 20 categories [142]. They share a conserved structure containing an extracellular ligand-binding domain followed by a single transmembrane domain and then an intracellular protein kinase domain. Further, signaling and mechanisms of action are very conserved across species. Most relevant to this literature review is the c-Met RTK, which is known for its potent morphogenic, motogenic and mitogenic signaling.

C-Met or mesenchymal epithelial transition factor, signals in conjunction with its ligand hepatocyte growth factor/scatter factor (HGF/SF) [141]. HGF is a pleiotropic growth factor that induces cell proliferation and survival, and functions to stimulate cell motility [143]. C-Met is expressed in many epithelial tissues during development, while HGF is mesenchymal in origin [144]. Signaling is essential for development of the liver, kidneys, muscles, and placenta, as loss of HGF or Met leads to embryonic lethality between E12.5 and E15.5 in mice.

The proto-oncogene c-Met, is transcriptionally regulated by several transcription factors including, Pax3, AP2, Tcf-4, and Ets [138, 145, 146]. The c-Met gene is located on chromosome 7q21-31, and transcription results in multiple isoforms and splice variants. C-Met is synthesized as a proprotein that is cleaved by furin or a furin-like protease in the Golgi. Met is composed of a 190 kDa  $\alpha$ - $\beta$  heterodimer with the extracellular  $\alpha$ -chain (50 kDa) forming a disulfide linkage with the transmembrane  $\beta$ -domain (145 kDa), and both domains are highly glycosylated [147, 148]. Mature HGF consists of a  $\alpha$  and  $\beta$  chain which is linked via a disulfide bond, similarly to c-Met. Once

secreted by mesenchymal cells, the HGF precursor is cleaved into its biologically active form.

The extracellular region of c-Met is composed of three domains, the N-terminal semaphoring (Sema) domain, the plex-in-semaphorin-integrin (PSI) domain, and then four immunoglobulin-plexin-transcription (IPT) domains [138]. The Sema domain encompasses all of the  $\alpha$ -chain and part of the  $\beta$ -chain, and is followed by the PSI domain that is much smaller and contains four disulfide bonds. The four IPT domain units share similarity to immunoglobulin-like domains.

The  $\beta$ -chain contains the intracellular tyrosine kinase activity, and undergoes autophosphorylation at tyrosines 1234 and 1235 of the activation loop upon binding of HGF and homo-dimerization [149]. The two tyrosines in the activation loop or catalytic domain (Tyr1234 and Tyr1235) of c-Met are essential for activation, and after autophosphorylation they initiate phosphorylation at Tyr1003 within the juxtamembrane domain [150]. The c-Met intracellular domain contains a conserved tandem-tyrosine docking domain that is required for signaling and contains the two tyrosines 1349 and 1356 which are phosphorylated following Tyr1234 and Tyr1235 activation [149]. Phosphorylation of this multifunctional docking site initiates interactions with Src homology 2 (SH2) domains, which are downstream effectors of Met regulated signaling [151]. Interestingly, mutation of Tyr1349 has little effect on Met activity, and only alters transformation induction [143]. Loss of Tyr1356 affects all Met-mediated cellular functions, which is caused by loss of its interaction with Grb2 and subsequent interaction with Ras. Further, loss of both Tyr1349 and Tyr1356 leads to complete loss of function and mimics Met KO.

C-Met signaling is mediated by adaptor and effector proteins upon phosphorylation of the various tyrosines within the cytoplasmic domain of the receptor [138, 141]. C-Met interacts with SH2 and SH3 containing adaptor proteins such as Grb2, CRK, and GAB1 which recruit the c-Met Src kinases signaling effectors PI3K, PLC- $\gamma$ 1, SHIP-2, STAT-3, and SOS. P44/42 Map kinase (ERK) is also a downstream effector of c-Met activation. As shown in figure 1.7, these signaling pathways lead to various cellular activities such as cell motility, cell proliferation, cell cycle progression, and cell survival. Importantly, c-Met can also be transactivated via members of the semaphorin receptor family, or directly by EGFR family members, or the RON RTK [152-154].

Tight control of Met signaling is essential for normal cellular function, and is therefore regulated at multiple levels. Met can be regulated at transcript level and further several miRNAs are known to target Met mRNA [155, 156]. At the protein level, Met is down regulated upon ligand binding, which is important for signal reduction. Ligand mediated receptor degradation takes place shortly after HGF binding (1 hour) and peaks around 8 hours before returning to the pre-induced state around 24 hours after ligand induction [157]. Ligand stimulation induces multimonoubiquitination and or polyubiquitination of the activated Met receptor, which promotes receptor internalization and degradation. Importantly, internalized Met still signals and has been shown to traffic to a perinuclear location in some cases following internalization. Met turnover and degradation is carried out by both the lysosome and proteasome, as evidenced by inhibition experiments [158]. Met is unique in the fact that it can be downregulated independently of ligand stimulation by cell surface shedding of the receptor through MMP mediated cleavage [159]. Generation of a soluble form of the external ligand-

binding portion of the receptor then competes with intact Met for HGF, thus downregulating signaling potential. Met signaling is further regulated by dephosphorylation of its c-terminal domain. This form of regulation is mediated by the action of protein-tyrosine phosphatases (PTPs), which serve to remove specific phosphates on the activated Met receptor. This mechanism is thought to regulate specificity and mitigate signaling rather than turning off the receptor as degradation would [160].

Aberrant c-Met signaling is often associated with cancer development and progression [161]. Approximately 40 mutations in Met have been identified in various tumor samples with mutations mostly localizing to the sema domain, juxtamembrane domain, and the kinase domain [157]. Many of these mutations result in continual activation of the receptor in the absence of ligand and lead to metastasis and poor prognosis.

### **Proteases in ECM Degradation and Growth Factor Regulation**

Cathepsin proteases are lysosomal hydrolases responsible for the degradation of lysosomal macromolecules, and are essential for normal cellular homeostasis. They are classified as either cysteine, serine, or aspartate proteases [162]. Cathepsins, like other lysosomal hydrolases, are targeted to the lysosome via M6P based recognition by M6PRs. Cathepsins are synthesized as inactive precursors containing a signal peptide and prodomain that assists in folding and functions as an inhibitor prior to removal [163]. The acidic pH of the lysosome triggers activation of cathepsin proteases either through

autocatalytic mechanisms or by other proteases [164-166]. Of note, certain cathepsins, such as cathepsin K, can also be processed to intermediate forms that retain some catalytic activity, which can play a role in normal and disease mechanisms [106, 107].

Cathepsins are mostly localized to the lysosome but under specific conditions, several cathepsin proteases have been shown to be involved in ECM degradation, namely cathepsins B, K, L, and S [167-170]. Cathepsins are secreted from macrophages, mast cells, smooth muscle cells, and osteoclasts, where they function to mediate ECM turnover [171-173]. For example, cathepsin K plays a key role in endochondral ossification and bone remodeling [174, 175]. During bone reabsorption, osteoclasts secrete cathepsin K to degrade the bone matrix [176, 177]. Another example of cathepsin mediated physiological ECM turnover involves adipogenesis or fat mass growth, which is driven by cathepsin S [178]. Further, cathepsins K and L have been shown to play a role in spermatogenesis by facilitating breakdown of ECM components to enable germ cell motility [179-181]. While cathepsins are essential for many normal cellular processes, increased expression or loss of expression result in pathological disorders.

In cancer, ECM breakdown is associated with tumor invasion and metastasis, which is mediated by the upregulation of proteases [182-184]. Further, overexpression of cathepsin proteases has been associated with poor cancer prognosis. Cathepsins have also been implicated in cardiovascular disease, with increases in cathepsins B, L, K, and S being common [185-188]. These increases lead to atherosclerotic plaque formation through collagen and elastin degradation and reduced cholesterol efflux, leading to plaque rupture via cathepsin S activity in late stage disease [189]. Cathepsin K in particular has been associated with the progression of osteoporosis and arthritis, through

the degradation of bone, collagen, and cartilage proteoglycans, and is unique in the fact that it has specificity for helical regions of type I and II collagens [190, 191]. Unlike other cathepsins, cathepsin K has a net positive charge due to a high density of basic positively charged amino acids [179]. This positive charge assists the protease in complex formation with negatively charged glycosaminoglycans to degrade collagen.

Cathepsins have been found to play a role in pathologic growth factor signaling through enhanced cathepsin expression or activation. For example, melanoma cells have increased mRNA and protein levels of cathepsin B and cathepsin L [192]. Cathepsin B in turn enhances TGF $\beta$  production and secretion from melanoma cells, and can also activate latent TGF $\beta$  [193, 194].

### **Dissertation Overview**

Significant advancement has been made since mannose-6-phosphate was discovered as a common recognition marker on lysosomal hydrolases. The genetic mechanisms leading to impaired carbohydrate dependent targeting have also been clearly defined in recent years. While we have an understanding of MLII progression, we are still determining the main drivers of pathogenesis. Further how does early MLII development differ from later disease stages? The cause of tissue specific differences in MLII pathology is also not understood. To look at early pathology of MLII and development of the disorder, our lab generated a zebrafish model of MLII. Early studies in the lab showed that disruption of M6P in zebrafish embryos leads to abnormal chondrogenesis. Recently we have tied abnormal chondrogenesis to impaired growth factor signaling and the increased activity of the lysosomal protease cathepsin K. Based on findings that

cathepsin K modulated TGF $\beta$  and BMP signaling in MLII zebrafish, we hypothesized that hypersecreted cathepsin K directly acts on latent growth factors in the extracellular matrix. The first part of this dissertation explores this interaction through in vitro digestions combining cathepsin K and latent growth factors. The findings presented show that cathepsin K preferentially cleaves latent TGF $\beta$  to help liberate a signaling competent ligand. I also show that increases in TGF $\beta$  signaling drive craniofacial pathogenesis in morphant zebrafish.

The consequence of lysosomal storage and impaired targeting on cell surface glycoproteins is currently undefined. To study these affects in a defined cell type without background mutations we used a CRISPR mediated GNPTAB knockout HeLa cell line. Based on cell surface glycoprotein labeling and proteomics we determined that GNPTAB-null cells have reduced surface abundance of several uptake receptors and increased abundance of several receptor tyrosine kinases. The findings presented in the second part of this dissertation describe a mechanism supporting deregulation of the c-Met receptor.

## REFERENCES

1. Varki, A. and J.B. Lowe, *Biological Roles of Glycans*, in *Essentials of Glycobiology*, A. Varki, et al., Editors. 2009: Cold Spring Harbor (NY).
2. Varki, A. and N. Sharon, *Historical Background and Overview*, in *Essentials of Glycobiology*, A. Varki, et al., Editors. 2009: Cold Spring Harbor (NY).
3. Stanley, P., H. Schachter, and N. Taniguchi, *N-Glycans*, in *Essentials of Glycobiology*, A. Varki, et al., Editors. 2009: Cold Spring Harbor (NY).
4. Kornfeld, R. and S. Kornfeld, *Assembly of asparagine-linked oligosaccharides*. *Annu Rev Biochem*, 1985. **54**: p. 631-64.

5. Hammond, C., I. Braakman, and A. Helenius, *Role of N-linked oligosaccharide recognition, glucose trimming, and calnexin in glycoprotein folding and quality control*. Proc Natl Acad Sci U S A, 1994. **91**(3): p. 913-7.
6. Fleischer, B., *Mechanism of glycosylation in the Golgi apparatus*. J Histochem Cytochem, 1983. **31**(8): p. 1033-40.
7. Appelmans, F., R. Wattiaux, and C. De Duve, *Tissue fractionation studies. 5. The association of acid phosphatase with a special class of cytoplasmic granules in rat liver*. Biochem J, 1955. **59**(3): p. 438-45.
8. Appelqvist, H., et al., *The lysosome: from waste bag to potential therapeutic target*. J Mol Cell Biol, 2013. **5**(4): p. 214-26.
9. Sardiello, M., et al., *A gene network regulating lysosomal biogenesis and function*. Science, 2009. **325**(5939): p. 473-7.
10. Li, X., et al., *A molecular mechanism to regulate lysosome motility for lysosome positioning and tubulation*. Nat Cell Biol, 2016. **18**(4): p. 404-17.
11. Rothman, J.E. and L. Orci, *Molecular dissection of the secretory pathway*. Nature, 1992. **355**(6359): p. 409-15.
12. Kornfeld, S., *Trafficking of lysosomal enzymes in normal and disease states*. J Clin Invest, 1986. **77**(1): p. 1-6.
13. Neufeld, E.F., *The biochemical basis for mucopolysaccharidoses and mucolipidoses*. Prog Med Genet, 1974. **10**: p. 81-101.
14. Hickman, S. and E.F. Neufeld, *A hypothesis for I-cell disease: defective hydrolases that do not enter lysosomes*. Biochem Biophys Res Commun, 1972. **49**(4): p. 992-9.
15. Owada, M. and E.F. Neufeld, *Is there a mechanism for introducing acid hydrolases into liver lysosomes that is independent of mannose 6-phosphate recognition? Evidence from I-cell disease*. Biochem Biophys Res Commun, 1982. **105**(3): p. 814-20.
16. Natowicz, M.R., et al., *Enzymatic identification of mannose 6-phosphate on the recognition marker for receptor-mediated pinocytosis of beta-glucuronidase by human fibroblasts*. Proc Natl Acad Sci U S A, 1979. **76**(9): p. 4322-6.
17. Kaplan, A., et al., *Phosphohexosyl recognition is a general characteristic of pinocytosis of lysosomal glycosidases by human fibroblasts*. J Clin Invest, 1977. **60**(5): p. 1088-93.
18. Reitman, M.L. and S. Kornfeld, *Lysosomal enzyme targeting. N-Acetylglucosaminylphosphotransferase selectively phosphorylates native lysosomal enzymes*. J Biol Chem, 1981. **256**(23): p. 11977-80.
19. Reitman, M.L. and S. Kornfeld, *UDP-N-acetylglucosamine:glycoprotein N-acetylglucosamine-1-phosphotransferase. Proposed enzyme for the phosphorylation of the high mannose oligosaccharide units of lysosomal enzymes*. J Biol Chem, 1981. **256**(9): p. 4275-81.
20. Lang, L., et al., *Lysosomal enzyme phosphorylation. Recognition of a protein-dependent determinant allows specific phosphorylation of oligosaccharides present on lysosomal enzymes*. J Biol Chem, 1984. **259**(23): p. 14663-71.
21. Nishikawa, A., et al., *The phosphorylation of bovine DNase I Asn-linked oligosaccharides is dependent on specific lysine and arginine residues*. J Biol Chem, 1997. **272**(31): p. 19408-12.

22. Cuozzo, J.W., et al., *Lysine-based structure responsible for selective mannose phosphorylation of cathepsin D and cathepsin L defines a common structural motif for lysosomal enzyme targeting*. J Biol Chem, 1998. **273**(33): p. 21067-76.
23. Baranski, T.J., P.L. Faust, and S. Kornfeld, *Generation of a lysosomal enzyme targeting signal in the secretory protein pepsinogen*. Cell, 1990. **63**(2): p. 281-91.
24. Baranski, T.J., et al., *Mapping and molecular modeling of a recognition domain for lysosomal enzyme targeting*. J Biol Chem, 1991. **266**(34): p. 23365-72.
25. Steet, R., W.S. Lee, and S. Kornfeld, *Identification of the minimal lysosomal enzyme recognition domain in cathepsin D*. J Biol Chem, 2005. **280**(39): p. 33318-23.
26. Bao, M., et al., *Bovine UDP-N-acetylglucosamine:lysosomal-enzyme N-acetylglucosamine-1-phosphotransferase. I. Purification and subunit structure*. J Biol Chem, 1996. **271**(49): p. 31437-45.
27. Kudo, M., et al., *The alpha- and beta-subunits of the human UDP-N-acetylglucosamine:lysosomal enzyme N-acetylglucosamine-1-phosphotransferase [corrected] are encoded by a single cDNA*. J Biol Chem, 2005. **280**(43): p. 36141-9.
28. Raas-Rothschild, A., et al., *Molecular basis of variant pseudo-hurler polydystrophy (mucopolidosis IIIC)*. J Clin Invest, 2000. **105**(5): p. 673-81.
29. Qian, Y., et al., *The DMAP interaction domain of UDP-GlcNAc:lysosomal enzyme N-acetylglucosamine-1-phosphotransferase is a substrate recognition module*. Proc Natl Acad Sci U S A, 2013. **110**(25): p. 10246-51.
30. Marschner, K., et al., *A key enzyme in the biogenesis of lysosomes is a protease that regulates cholesterol metabolism*. Science, 2011. **333**(6038): p. 87-90.
31. Kudo, M. and W.M. Canfield, *Structural requirements for efficient processing and activation of recombinant human UDP-N-acetylglucosamine:lysosomal-enzyme-N-acetylglucosamine-1-phosphotransferase*. J Biol Chem, 2006. **281**(17): p. 11761-8.
32. Qian, Y., et al., *Analysis of mucopolidosis II/III GNPTAB missense mutations identifies domains of UDP-GlcNAc:lysosomal enzyme GlcNAc-1-phosphotransferase involved in catalytic function and lysosomal enzyme recognition*. J Biol Chem, 2015. **290**(5): p. 3045-56.
33. van Meel, E., et al., *Multiple Domains of GlcNAc-1-phosphotransferase Mediate Recognition of Lysosomal Enzymes*. J Biol Chem, 2016. **291**(15): p. 8295-307.
34. Castonguay, A.C., L.J. Olson, and N.M. Dahms, *Mannose 6-phosphate receptor homology (MRH) domain-containing lectins in the secretory pathway*. Biochim Biophys Acta, 2011. **1810**(9): p. 815-26.
35. Pohl, S., et al., *Compensatory expression of human N-acetylglucosaminyl-1-phosphotransferase subunits in mucopolidosis type III gamma*. Biochim Biophys Acta, 2009. **1792**(3): p. 221-5.
36. Qian, Y., et al., *Functions of the alpha, beta, and gamma subunits of UDP-GlcNAc:lysosomal enzyme N-acetylglucosamine-1-phosphotransferase*. J Biol Chem, 2010. **285**(5): p. 3360-70.
37. Do, H., et al., *Human mannose 6-phosphate-uncovering enzyme is synthesized as a proenzyme that is activated by the endoprotease furin*. J Biol Chem, 2002. **277**(33): p. 29737-44.

38. Kornfeld, R., et al., *Purification and multimeric structure of bovine N-acetylglucosamine-1-phosphodiester alpha-N-acetylglucosaminidase*. J Biol Chem, 1998. **273**(36): p. 23203-10.
39. Lee, W.S., et al., *Analysis of mannose 6-phosphate uncovering enzyme mutations associated with persistent stuttering*. J Biol Chem, 2011. **286**(46): p. 39786-93.
40. Hoflack, B. and S. Kornfeld, *Lysosomal enzyme binding to mouse P388D1 macrophage membranes lacking the 215-kDa mannose 6-phosphate receptor: evidence for the existence of a second mannose 6-phosphate receptor*. Proc Natl Acad Sci U S A, 1985. **82**(13): p. 4428-32.
41. Junghans, U., A. Waheed, and K. von Figura, *The 'cation-dependent' mannose 6-phosphate receptor binds ligands in the absence of divalent cations*. FEBS Lett, 1988. **237**(1-2): p. 81-4.
42. Dahms, N. and M.K. Hancock, *P-type lectins*. Biochim Biophys Acta, 2002. **1572**(2-3): p. 317-40.
43. Dahms, N.M., P. Lobel, and S. Kornfeld, *Mannose 6-phosphate receptors and lysosomal enzyme targeting*. J Biol Chem, 1989. **264**(21): p. 12115-8.
44. Dahms, N.M., L.J. Olson, and J.J. Kim, *Strategies for carbohydrate recognition by the mannose 6-phosphate receptors*. Glycobiology, 2008. **18**(9): p. 664-78.
45. Ludwig, T., et al., *Targeted disruption of the mouse cation-dependent mannose 6-phosphate receptor results in partial missorting of multiple lysosomal enzymes*. EMBO J, 1993. **12**(13): p. 5225-35.
46. Koster, A., et al., *Targeted disruption of the M(r) 46,000 mannose 6-phosphate receptor gene in mice results in misrouting of lysosomal proteins*. EMBO J, 1993. **12**(13): p. 5219-23.
47. Kasper, D., et al., *Neither type of mannose 6-phosphate receptor is sufficient for targeting of lysosomal enzymes along intracellular routes*. J Cell Biol, 1996. **134**(3): p. 615-23.
48. Varki, A. and S. Kornfeld, *P-type Lectins*. 2009.
49. Munro, S., *The MRH domain suggests a shared ancestry for the mannose 6-phosphate receptors and other N-glycan-recognising proteins*. Curr Biol, 2001. **11**(13): p. R499-501.
50. Bohnsack, R.N., et al., *Cation-independent mannose 6-phosphate receptor: a composite of distinct phosphomannosyl binding sites*. J Biol Chem, 2009. **284**(50): p. 35215-26.
51. Olson, L.J., et al., *Identification of a fourth mannose 6-phosphate binding site in the cation-independent mannose 6-phosphate receptor*. Glycobiology, 2015. **25**(6): p. 591-606.
52. Lobel, P., et al., *Mutations in the cytoplasmic domain of the 275 kd mannose 6-phosphate receptor differentially alter lysosomal enzyme sorting and endocytosis*. Cell, 1989. **57**(5): p. 787-96.
53. Kim, J.J., L.J. Olson, and N.M. Dahms, *Carbohydrate recognition by the mannose-6-phosphate receptors*. Curr Opin Struct Biol, 2009. **19**(5): p. 534-42.
54. Dittmer, F., et al., *Alternative mechanisms for trafficking of lysosomal enzymes in mannose 6-phosphate receptor-deficient mice are cell type-specific*. J Cell Sci, 1999. **112** ( Pt 10): p. 1591-7.

55. Sohar, I., et al., *Mouse mutants lacking the cation-independent mannose 6-phosphate/insulin-like growth factor II receptor are impaired in lysosomal enzyme transport: comparison of cation-independent and cation-dependent mannose 6-phosphate receptor-deficient mice*. *Biochem J*, 1998. **330 ( Pt 2)**: p. 903-8.
56. Glickman, J.N. and S. Kornfeld, *Mannose 6-phosphate-independent targeting of lysosomal enzymes in I-cell disease B lymphoblasts*. *J Cell Biol*, 1993. **123**(1): p. 99-108.
57. Waheed, A., et al., *Deficiency of UDP-N-acetylglucosamine:lysosomal enzyme N-acetylglucosamine-1-phosphotransferase in organs of I-cell patients*. *Biochem Biophys Res Commun*, 1982. **105**(3): p. 1052-8.
58. Carlsson, S.R. and M. Fukuda, *The lysosomal membrane glycoprotein lamp-1 is transported to lysosomes by two alternative pathways*. *Arch Biochem Biophys*, 1992. **296**(2): p. 630-9.
59. Akasaki, K., et al., *COOH-terminal isoleucine of lysosome-associated membrane protein-1 is optimal for its efficient targeting to dense secondary lysosomes*. *J Biochem*, 2010. **148**(6): p. 669-79.
60. Fujita, H., et al., *Isolation and sequencing of a cDNA clone encoding 85kDa sialoglycoprotein in rat liver lysosomal membranes*. *Biochem Biophys Res Commun*, 1991. **178**(2): p. 444-52.
61. Reczek, D., et al., *LIMP-2 is a receptor for lysosomal mannose-6-phosphate-independent targeting of beta-glucocerebrosidase*. *Cell*, 2007. **131**(4): p. 770-83.
62. Coutinho, M.F., et al., *Molecular and computational analyses of genes involved in mannose 6-phosphate independent trafficking*. *Clin Genet*, 2015. **88**(2): p. 190-4.
63. Willnow, T.E., C.M. Petersen, and A. Nykjaer, *VPS10P-domain receptors - regulators of neuronal viability and function*. *Nat Rev Neurosci*, 2008. **9**(12): p. 899-909.
64. Lefrancois, S., et al., *The lysosomal trafficking of sphingolipid activator proteins (SAPs) is mediated by sortilin*. *EMBO J*, 2003. **22**(24): p. 6430-7.
65. Willnow, T.E., et al., *RAP, a specialized chaperone, prevents ligand-induced ER retention and degradation of LDL receptor-related endocytic receptors*. *EMBO J*, 1996. **15**(11): p. 2632-9.
66. Owen, J.B., et al., *Oxidative modification to LDL receptor-related protein 1 in hippocampus from subjects with Alzheimer disease: implications for Abeta accumulation in AD brain*. *Free Radic Biol Med*, 2010. **49**(11): p. 1798-803.
67. Herz, J. and D.K. Strickland, *LRP: a multifunctional scavenger and signaling receptor*. *J Clin Invest*, 2001. **108**(6): p. 779-84.
68. Laurent-Matha, V., et al., *Endocytosis of pro-cathepsin D into breast cancer cells is mostly independent of mannose-6-phosphate receptors*. *J Cell Sci*, 1998. **111 ( Pt 17)**: p. 2539-49.
69. Beaujouin, M., et al., *Pro-cathepsin D interacts with the extracellular domain of the beta chain of LRP1 and promotes LRP1-dependent fibroblast outgrowth*. *J Cell Sci*, 2010. **123**(Pt 19): p. 3336-46.
70. Derocq, D., et al., *Cathepsin D is partly endocytosed by the LRP1 receptor and inhibits LRP1-regulated intramembrane proteolysis*. *Oncogene*, 2012. **31**(26): p. 3202-12.

71. Capony, F., et al., *Specific mannose-6-phosphate receptor-independent sorting of pro-cathepsin D in breast cancer cells*. Exp Cell Res, 1994. **215**(1): p. 154-63.
72. Markmann, S., et al., *Lrp1/LDL Receptor Play Critical Roles in Mannose 6-Phosphate-Independent Lysosomal Enzyme Targeting*. Traffic, 2015. **16**(7): p. 743-59.
73. Schultz, M.L., et al., *Clarifying lysosomal storage diseases*. Trends Neurosci, 2011. **34**(8): p. 401-10.
74. Burton, B.K., *Inborn errors of metabolism in infancy: a guide to diagnosis*. Pediatrics, 1998. **102**(6): p. E69.
75. Fuller, M., P.J. Meikle, and J.J. Hopwood, *Epidemiology of lysosomal storage diseases: an overview*, in *Fabry Disease: Perspectives from 5 Years of FOS*, A. Mehta, M. Beck, and G. Sunder-Plassmann, Editors. 2006: Oxford.
76. Ballabio, A., *Disease pathogenesis explained by basic science: lysosomal storage diseases as autophagocytic disorders*. Int J Clin Pharmacol Ther, 2009. **47 Suppl 1**: p. S34-8.
77. Ballabio, A. and V. Gieselmann, *Lysosomal disorders: from storage to cellular damage*. Biochim Biophys Acta, 2009. **1793**(4): p. 684-96.
78. Platt, F.M., B. Boland, and A.C. van der Spoel, *The cell biology of disease: lysosomal storage disorders: the cellular impact of lysosomal dysfunction*. J Cell Biol, 2012. **199**(5): p. 723-34.
79. Mbua, N.E., et al., *Abnormal accumulation and recycling of glycoproteins visualized in Niemann-Pick type C cells using the chemical reporter strategy*. Proc Natl Acad Sci U S A, 2013. **110**(25): p. 10207-12.
80. Settembre, C., et al., *A block of autophagy in lysosomal storage disorders*. Hum Mol Genet, 2008. **17**(1): p. 119-29.
81. Boonen, M., et al., *Vacuolization of mucopolipidosis type II mouse exocrine gland cells represents accumulation of autolysosomes*. Mol Biol Cell, 2011. **22**(8): p. 1135-47.
82. Abe, M., et al., *An assay for transforming growth factor-beta using cells transfected with a plasminogen activator inhibitor-1 promoter-luciferase construct*. Anal Biochem, 1994. **216**(2): p. 276-84.
83. Terman, A., et al., *Mitochondrial turnover and aging of long-lived postmitotic cells: the mitochondrial-lysosomal axis theory of aging*. Antioxid Redox Signal, 2010. **12**(4): p. 503-35.
84. Tseng, W.L., et al., *Imbalanced Production of Reactive Oxygen Species and Mitochondrial Antioxidant SOD2 in Fabry Disease-Specific Human Induced Pluripotent Stem Cell-Differentiated Vascular Endothelial Cells*. Cell Transplant, 2017. **26**(3): p. 513-527.
85. Kornfeld, S., *Trafficking of lysosomal enzymes*. FASEB J, 1987. **1**(6): p. 462-8.
86. Cathey, S.S., et al., *Molecular order in mucopolipidosis II and III nomenclature*. Am J Med Genet A, 2008. **146A**(4): p. 512-3.
87. Cathey, S.S., et al., *Phenotype and genotype in mucopolipidoses II and III alpha/beta: a study of 61 probands*. J Med Genet, 2010. **47**(1): p. 38-48.
88. Bargal, R., et al., *When Mucopolipidosis III meets Mucopolipidosis II: GNPTA gene mutations in 24 patients*. Mol Genet Metab, 2006. **88**(4): p. 359-63.

89. Kollmann, K., et al., *Mannose phosphorylation in health and disease*. Eur J Cell Biol, 2010. **89**(1): p. 117-23.
90. Kudo, M., M.S. Brem, and W.M. Canfield, *Mucopolipidosis II (I-cell disease) and mucopolipidosis IIIA (classical pseudo-hurler polydystrophy) are caused by mutations in the GlcNAc-phosphotransferase alpha / beta -subunits precursor gene*. Am J Hum Genet, 2006. **78**(3): p. 451-63.
91. Liu, S., et al., *Mutation Analysis of 16 Mucopolipidosis II and III Alpha/Beta Chinese Children Revealed Genotype-Phenotype Correlations*. PLoS One, 2016. **11**(9): p. e0163204.
92. Leroy, J.G., S. Cathey, and M.J. Friez, *Mucopolipidosis II*, in *GeneReviews(R)*, R.A. Pagon, et al., Editors. 1993: Seattle (WA).
93. Patriquin, H.B., et al., *Neonatal mucopolipidosis II (I-cell disease): clinical and radiologic features in three cases*. AJR Am J Roentgenol, 1977. **129**(1): p. 37-43.
94. Sandoval, I.V., et al., *Lysosomal integral membrane glycoproteins are expressed at high levels in the inclusion bodies of I-cell disease fibroblasts*. Arch Biochem Biophys, 1989. **271**(1): p. 157-67.
95. Robinson, C., et al., *The osteodystrophy of mucopolipidosis type III and the effects of intravenous pamidronate treatment*. J Inher Metab Dis, 2002. **25**(8): p. 681-93.
96. Barton, N.W., et al., *Therapeutic response to intravenous infusions of glucocerebrosidase in a patient with Gaucher disease*. Proc Natl Acad Sci U S A, 1990. **87**(5): p. 1913-6.
97. Futerman, A.H. and G. van Meer, *The cell biology of lysosomal storage disorders*. Nat Rev Mol Cell Biol, 2004. **5**(7): p. 554-65.
98. Bosshard, N.U., et al., *Spontaneous mucopolipidosis in a cat: an animal model of human I-cell disease*. Vet Pathol, 1996. **33**(1): p. 1-13.
99. Hubler, M., et al., *Mucopolipidosis type II in a domestic shorthair cat*. J Small Anim Pract, 1996. **37**(9): p. 435-41.
100. Mazrier, H., et al., *Inheritance, biochemical abnormalities, and clinical features of feline mucopolipidosis II: the first animal model of human I-cell disease*. J Hered, 2003. **94**(5): p. 363-73.
101. Gelfman, C.M., et al., *Mice lacking alpha/beta subunits of GlcNAc-1-phosphotransferase exhibit growth retardation, retinal degeneration, and secretory cell lesions*. Invest Ophthalmol Vis Sci, 2007. **48**(11): p. 5221-8.
102. Kollmann, K., et al., *Decreased bone formation and increased osteoclastogenesis cause bone loss in mucopolipidosis II*. EMBO Mol Med, 2013. **5**(12): p. 1871-86.
103. Schweizer, M., et al., *Ultrastructural analysis of neuronal and non-neuronal lysosomal storage in mucopolipidosis type II knock-in mice*. Ultrastruct Pathol, 2013. **37**(5): p. 366-72.
104. Paton, L., et al., *A novel mouse model of a patient mucopolipidosis II mutation recapitulates disease pathology*. J Biol Chem, 2014. **289**(39): p. 26709-21.
105. Flanagan-Steet, H., C. Sias, and R. Steet, *Altered chondrocyte differentiation and extracellular matrix homeostasis in a zebrafish model for mucopolipidosis II*. Am J Pathol, 2009. **175**(5): p. 2063-75.

106. Petrey, A.C., et al., *Excessive activity of cathepsin K is associated with cartilage defects in a zebrafish model of mucopolidosis II*. *Dis Model Mech*, 2012. **5**(2): p. 177-90.
107. Flanagan-Steet, H., et al., *Cathepsin-Mediated Alterations in TGF $\beta$ s-Related Signaling Underlie Disrupted Cartilage and Bone Maturation Associated With Impaired Lysosomal Targeting*. *J Bone Miner Res*, 2016. **31**(3): p. 535-48.
108. van der Kraan, P.M., et al., *TGF-beta signaling in chondrocyte terminal differentiation and osteoarthritis: modulation and integration of signaling pathways through receptor-Smads*. *Osteoarthritis Cartilage*, 2009. **17**(12): p. 1539-45.
109. Lee, Y.H. and J.P. Saint-Jeannet, *Sox9 function in craniofacial development and disease*. *Genesis*, 2011. **49**(4): p. 200-8.
110. Goldring, M.B., K. Tsuchimochi, and K. Ijiri, *The control of chondrogenesis*. *J Cell Biochem*, 2006. **97**(1): p. 33-44.
111. DeLise, A.M., L. Fischer, and R.S. Tuan, *Cellular interactions and signaling in cartilage development*. *Osteoarthritis Cartilage*, 2000. **8**(5): p. 309-34.
112. Mackie, E.J., et al., *Endochondral ossification: how cartilage is converted into bone in the developing skeleton*. *Int J Biochem Cell Biol*, 2008. **40**(1): p. 46-62.
113. Soderstrom, M., et al., *Cathepsin expression during skeletal development*. *Biochim Biophys Acta*, 1999. **1446**(1-2): p. 35-46.
114. Horiguchi, M., M. Ota, and D.B. Rifkin, *Matrix control of transforming growth factor-beta function*. *J Biochem*, 2012. **152**(4): p. 321-9.
115. Annes, J.P., J.S. Munger, and D.B. Rifkin, *Making sense of latent TGFbeta activation*. *J Cell Sci*, 2003. **116**(Pt 2): p. 217-24.
116. Swartz, M.E., et al., *Examination of a palatogenic gene program in zebrafish*. *Dev Dyn*, 2011. **240**(9): p. 2204-20.
117. Todorovic, V., et al., *Long form of latent TGF-beta binding protein 1 (Ltbp1L) is essential for cardiac outflow tract septation and remodeling*. *Development*, 2007. **134**(20): p. 3723-32.
118. Taipale, J., et al., *Latent transforming growth factor-beta 1 associates to fibroblast extracellular matrix via latent TGF-beta binding protein*. *J Cell Biol*, 1994. **124**(1-2): p. 171-81.
119. Lyons, R.M., J. Keski-Oja, and H.L. Moses, *Proteolytic activation of latent transforming growth factor-beta from fibroblast-conditioned medium*. *J Cell Biol*, 1988. **106**(5): p. 1659-65.
120. Massague, J., *TGF-beta signal transduction*. *Annu Rev Biochem*, 1998. **67**: p. 753-91.
121. Massague, J., J. Seoane, and D. Wotton, *Smad transcription factors*. *Genes Dev*, 2005. **19**(23): p. 2783-810.
122. Sieber, C., et al., *Recent advances in BMP receptor signaling*. *Cytokine Growth Factor Rev*, 2009. **20**(5-6): p. 343-55.
123. Allen, J.L., M.E. Cooke, and T. Alliston, *ECM stiffness primes the TGFbeta pathway to promote chondrocyte differentiation*. *Mol Biol Cell*, 2012. **23**(18): p. 3731-42.

124. Yang, X., et al., *TGF-beta/Smad3 signals repress chondrocyte hypertrophic differentiation and are required for maintaining articular cartilage*. J Cell Biol, 2001. **153**(1): p. 35-46.
125. Furumatsu, T., et al., *Smad3 induces chondrogenesis through the activation of SOX9 via CREB-binding protein/p300 recruitment*. J Biol Chem, 2005. **280**(9): p. 8343-50.
126. Kaartinen, V., et al., *Abnormal lung development and cleft palate in mice lacking TGF-beta 3 indicates defects of epithelial-mesenchymal interaction*. Nat Genet, 1995. **11**(4): p. 415-21.
127. Akhurst, R.J. and A. Hata, *Targeting the TGFbeta signalling pathway in disease*. Nat Rev Drug Discov, 2012. **11**(10): p. 790-811.
128. Quarto, N., et al., *Exogenous activation of BMP-2 signaling overcomes TGFbeta-mediated inhibition of osteogenesis in Marfan embryonic stem cells and Marfan patient-specific induced pluripotent stem cells*. Stem Cells, 2012. **30**(12): p. 2709-19.
129. Janssens, K., et al., *Mutations in the gene encoding the latency-associated peptide of TGF-beta 1 cause Camurati-Engelmann disease*. Nat Genet, 2000. **26**(3): p. 273-5.
130. Janssens, K., et al., *Transforming growth factor-beta 1 mutations in Camurati-Engelmann disease lead to increased signaling by altering either activation or secretion of the mutant protein*. J Biol Chem, 2003. **278**(9): p. 7718-24.
131. McGowan, N.W., et al., *A mutation affecting the latency-associated peptide of TGFbeta1 in Camurati-Engelmann disease enhances osteoclast formation in vitro*. J Clin Endocrinol Metab, 2003. **88**(7): p. 3321-6.
132. Vanhoenacker, F.M., et al., *Camurati-Engelmann disease. Review of radioclinical features*. Acta Radiol, 2003. **44**(4): p. 430-4.
133. Bragdon, B., et al., *Bone morphogenetic proteins: a critical review*. Cell Signal, 2011. **23**(4): p. 609-20.
134. Cui, Y., et al., *The activity and signaling range of mature BMP-4 is regulated by sequential cleavage at two sites within the prodomain of the precursor*. Genes Dev, 2001. **15**(21): p. 2797-802.
135. Yoon, B.S. and K.M. Lyons, *Multiple functions of BMPs in chondrogenesis*. J Cell Biochem, 2004. **93**(1): p. 93-103.
136. Derynck, R. and K.ç. Miyazono, *The TGF-[beta] family*. 2008: Cold Spring Harbor Laboratory Press Cold Spring Harbor, NY.
137. Bandyopadhyay, A., P.S. Yadav, and P. Prashar, *BMP signaling in development and diseases: a pharmacological perspective*. Biochem Pharmacol, 2013. **85**(7): p. 857-64.
138. Organ, S.L. and M.S. Tsao, *An overview of the c-MET signaling pathway*. Ther Adv Med Oncol, 2011. **3**(1 Suppl): p. S7-S19.
139. Qiu, S., Z. Lu, and P. Levitt, *MET receptor tyrosine kinase controls dendritic complexity, spine morphogenesis, and glutamatergic synapse maturation in the hippocampus*. J Neurosci, 2014. **34**(49): p. 16166-79.
140. Emaduddin, M., et al., *Cell growth, global phosphotyrosine elevation, and c-Met phosphorylation through Src family kinases in colorectal cancer cells*. Proc Natl Acad Sci U S A, 2008. **105**(7): p. 2358-62.

141. Hass, R., et al., *c-Met expression and activity in urogenital cancers - novel aspects of signal transduction and medical implications*. Cell Commun Signal, 2017. **15**(1): p. 10.
142. Lemmon, M.A. and J. Schlessinger, *Cell signaling by receptor tyrosine kinases*. Cell, 2010. **141**(7): p. 1117-34.
143. Maina, F., et al., *Uncoupling of Grb2 from the Met receptor in vivo reveals complex roles in muscle development*. Cell, 1996. **87**(3): p. 531-42.
144. Sonnenberg, E., et al., *Scatter factor/hepatocyte growth factor and its receptor, the c-met tyrosine kinase, can mediate a signal exchange between mesenchyme and epithelia during mouse development*. J Cell Biol, 1993. **123**(1): p. 223-35.
145. Epstein, J.A., et al., *Pax3 modulates expression of the c-Met receptor during limb muscle development*. Proc Natl Acad Sci U S A, 1996. **93**(9): p. 4213-8.
146. Gambarotta, G., et al., *Ets up-regulates MET transcription*. Oncogene, 1996. **13**(9): p. 1911-7.
147. Comoglio, P.M., *Structure, biosynthesis and biochemical properties of the HGF receptor in normal and malignant cells*. EXS, 1993. **65**: p. 131-65.
148. Bardelli, A., C. Ponzetto, and P.M. Comoglio, *Identification of functional domains in the hepatocyte growth factor and its receptor by molecular engineering*. J Biotechnol, 1994. **37**(2): p. 109-22.
149. Schiering, N., et al., *Crystal structure of the tyrosine kinase domain of the hepatocyte growth factor receptor c-Met and its complex with the microbial alkaloid K-252a*. Proc Natl Acad Sci U S A, 2003. **100**(22): p. 12654-9.
150. Longati, P., et al., *Tyrosines 1234-1235 are critical for activation of the tyrosine kinase encoded by the MET proto-oncogene (HGF receptor)*. Oncogene, 1994. **9**(1): p. 49-57.
151. Ponzetto, C., et al., *A multifunctional docking site mediates signaling and transformation by the hepatocyte growth factor/scatter factor receptor family*. Cell, 1994. **77**(2): p. 261-71.
152. Sierra, J.R., et al., *Tumor angiogenesis and progression are enhanced by Sema4D produced by tumor-associated macrophages*. J Exp Med, 2008. **205**(7): p. 1673-85.
153. Jo, M., et al., *Cross-talk between epidermal growth factor receptor and c-Met signal pathways in transformed cells*. J Biol Chem, 2000. **275**(12): p. 8806-11.
154. Follenzi, A., et al., *Cross-talk between the proto-oncogenes Met and Ron*. Oncogene, 2000. **19**(27): p. 3041-9.
155. Migliore, C., et al., *MicroRNAs impair MET-mediated invasive growth*. Cancer Res, 2008. **68**(24): p. 10128-36.
156. Yan, D., et al., *MicroRNA-1/206 targets c-Met and inhibits rhabdomyosarcoma development*. J Biol Chem, 2009. **284**(43): p. 29596-604.
157. Lefebvre, J., et al., *Met degradation: more than one stone to shoot a receptor down*. FASEB J, 2012. **26**(4): p. 1387-99.
158. Hammond, D.E., et al., *Down-regulation of MET, the receptor for hepatocyte growth factor*. Oncogene, 2001. **20**(22): p. 2761-70.
159. Prat, M., et al., *C-terminal truncated forms of Met, the hepatocyte growth factor receptor*. Mol Cell Biol, 1991. **11**(12): p. 5954-62.

160. Palka, H.L., M. Park, and N.K. Tonks, *Hepatocyte growth factor receptor tyrosine kinase met is a substrate of the receptor protein-tyrosine phosphatase DEP-I*. J Biol Chem, 2003. **278**(8): p. 5728-35.
161. Schmidt, L., et al., *Germline and somatic mutations in the tyrosine kinase domain of the MET proto-oncogene in papillary renal carcinomas*. Nat Genet, 1997. **16**(1): p. 68-73.
162. Brömme, D., *Papain-like cysteine proteases*. Current protocols in protein science / editorial board, John E. Coligan ... [et al.], 2001. **Chapter 21**.
163. Chapman, H.A., R.J. Riese, and G.P. Shi, *Emerging roles for cysteine proteases in human biology*. Annu Rev Physiol, 1997. **59**: p. 63-88.
164. McQueney, M.S., et al., *Autocatalytic activation of human cathepsin K*. J Biol Chem, 1997. **272**(21): p. 13955-60.
165. Menard, R., et al., *Autocatalytic processing of recombinant human procathepsin L. Contribution of both intermolecular and unimolecular events in the processing of procathepsin L in vitro*. J Biol Chem, 1998. **273**(8): p. 4478-84.
166. Pungercar, J.R., et al., *Autocatalytic processing of procathepsin B is triggered by proenzyme activity*. FEBS J, 2009. **276**(3): p. 660-8.
167. Maciewicz, R.A. and S.F. Wotton, *Degradation of cartilage matrix components by the cysteine proteinases, cathepsins B and L*. Biomed Biochim Acta, 1991. **50**(4-6): p. 561-4.
168. Hou, W.S., et al., *Cleavage site specificity of cathepsin K toward cartilage proteoglycans and protease complex formation*. Biol Chem, 2003. **384**(6): p. 891-7.
169. Baumgrass, R., M.K. Williamson, and P.A. Price, *Identification of peptide fragments generated by digestion of bovine and human osteocalcin with the lysosomal proteinases cathepsin B, D, L, H, and S*. J Bone Miner Res, 1997. **12**(3): p. 447-55.
170. Buck, M.R., et al., *Degradation of extracellular-matrix proteins by human cathepsin B from normal and tumour tissues*. Biochem J, 1992. **282** ( Pt 1): p. 273-8.
171. Punturieri, A., et al., *Regulation of elastinolytic cysteine proteinase activity in normal and cathepsin K-deficient human macrophages*. J Exp Med, 2000. **192**(6): p. 789-99.
172. Wolters, P.J., et al., *Regulated expression, processing, and secretion of dog mast cell dipeptidyl peptidase I*. J Biol Chem, 1998. **273**(25): p. 15514-20.
173. Sukhova, G.K., et al., *Expression of the elastolytic cathepsins S and K in human atheroma and regulation of their production in smooth muscle cells*. J Clin Invest, 1998. **102**(3): p. 576-83.
174. Drake, F.H., et al., *Cathepsin K, but not cathepsins B, L, or S, is abundantly expressed in human osteoclasts*. J Biol Chem, 1996. **271**(21): p. 12511-6.
175. Kamiya, T., et al., *Fluorescence microscopic demonstration of cathepsin K activity as the major lysosomal cysteine proteinase in osteoclasts*. J Biochem, 1998. **123**(4): p. 752-9.
176. Fuller, K., et al., *Cathepsin K inhibitors prevent matrix-derived growth factor degradation by human osteoclasts*. Bone, 2008. **42**(1): p. 200-11.

177. Delaisse, J.M., et al., *Matrix metalloproteinases (MMP) and cathepsin K contribute differently to osteoclastic activities*. *Microsc Res Tech*, 2003. **61**(6): p. 504-13.
178. Taleb, S., et al., *Cathepsin s promotes human preadipocyte differentiation: possible involvement of fibronectin degradation*. *Endocrinology*, 2006. **147**(10): p. 4950-9.
179. Lecaille, F., D. Bromme, and G. Lalmanach, *Biochemical properties and regulation of cathepsin K activity*. *Biochimie*, 2008. **90**(2): p. 208-26.
180. Anway, M.D., et al., *Expression and localization of cathepsin k in adult rat sertoli cells*. *Biol Reprod*, 2004. **70**(3): p. 562-9.
181. Wright, W.W., et al., *Mice that express enzymatically inactive cathepsin L exhibit abnormal spermatogenesis*. *Biol Reprod*, 2003. **68**(2): p. 680-7.
182. Liotta, L.A., C.N. Rao, and U.M. Wewer, *Biochemical interactions of tumor cells with the basement membrane*. *Annu Rev Biochem*, 1986. **55**: p. 1037-57.
183. Woodhouse, E.C., R.F. Chuaqui, and L.A. Liotta, *General mechanisms of metastasis*. *Cancer*, 1997. **80**(8 Suppl): p. 1529-37.
184. Nomura, T. and N. Katunuma, *Involvement of cathepsins in the invasion, metastasis and proliferation of cancer cells*. *J Med Invest*, 2005. **52**(1-2): p. 1-9.
185. Chen, J., et al., *In vivo imaging of proteolytic activity in atherosclerosis*. *Circulation*, 2002. **105**(23): p. 2766-71.
186. Liu, J., et al., *Cathepsin L expression and regulation in human abdominal aortic aneurysm, atherosclerosis, and vascular cells*. *Atherosclerosis*, 2006. **184**(2): p. 302-11.
187. Lutgens, E., et al., *Disruption of the cathepsin K gene reduces atherosclerosis progression and induces plaque fibrosis but accelerates macrophage foam cell formation*. *Circulation*, 2006. **113**(1): p. 98-107.
188. Rodgers, K.J., et al., *Destabilizing role of cathepsin S in murine atherosclerotic plaques*. *Arterioscler Thromb Vasc Biol*, 2006. **26**(4): p. 851-6.
189. Lutgens, S.P., et al., *Cathepsin cysteine proteases in cardiovascular disease*. *FASEB J*, 2007. **21**(12): p. 3029-41.
190. Dejica, V.M., et al., *Cleavage of type II collagen by cathepsin K in human osteoarthritic cartilage*. *Am J Pathol*, 2008. **173**(1): p. 161-9.
191. Kafienah, W., et al., *Human cathepsin K cleaves native type I and II collagens at the N-terminal end of the triple helix*. *Biochem J*, 1998. **331** ( Pt 3): p. 727-32.
192. Yin, M., et al., *TGF-beta signaling, activated stromal fibroblasts, and cysteine cathepsins B and L drive the invasive growth of human melanoma cells*. *Am J Pathol*, 2012. **181**(6): p. 2202-16.
193. Guo, M., et al., *Phorbol ester activation of a proteolytic cascade capable of activating latent transforming growth factor-betaL a process initiated by the exocytosis of cathepsin B*. *J Biol Chem*, 2002. **277**(17): p. 14829-37.
194. Andl, C.D., et al., *Cathepsin B is the driving force of esophageal cell invasion in a fibroblast-dependent manner*. *Neoplasia*, 2010. **12**(6): p. 485-98.

**FIGURES**

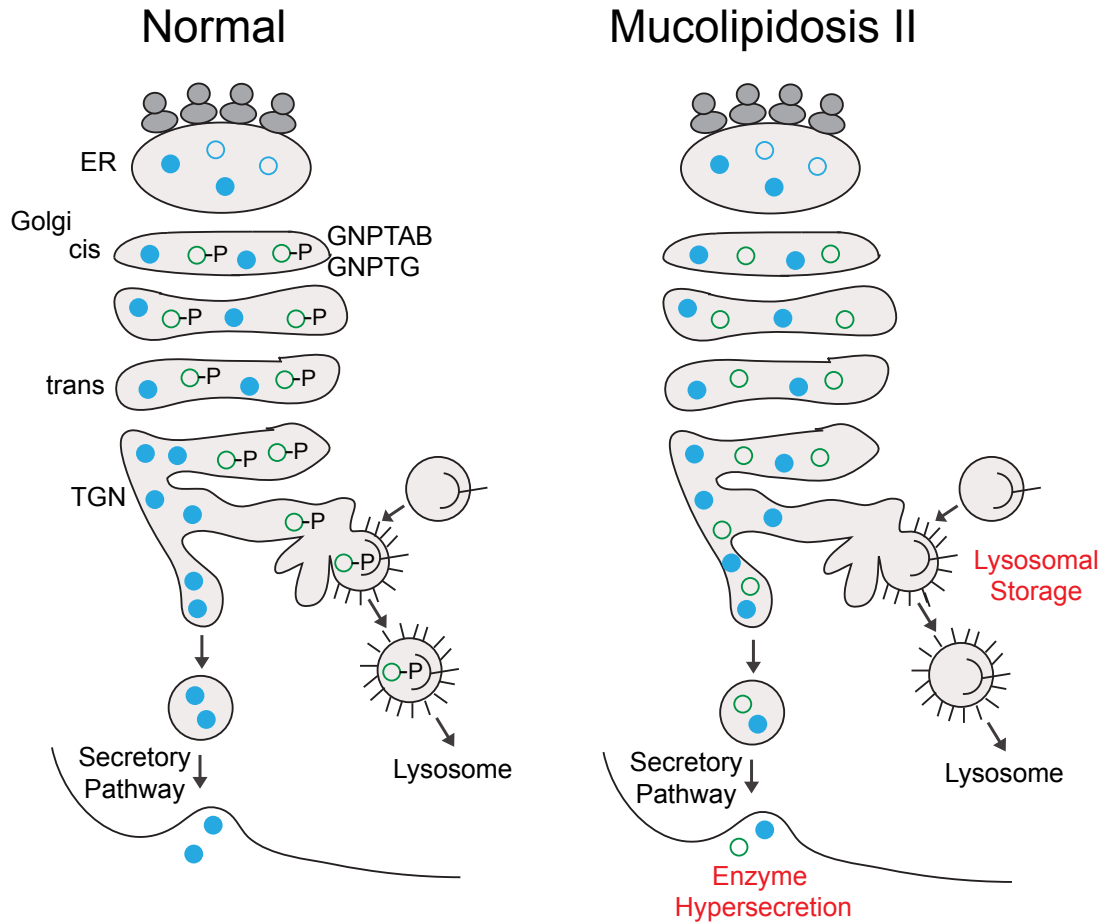


**Figure 1.1. Normal and MLII Secretory Pathway.** Lysosomal hydrolases shown as green outlined circles, acquire mannose-6-phosphate residues in the cis-Golgi by GlcNAc-1-phosphotransferase in normal cells. Two genes encode GlcNAc-1-phosphotransferase, GNPTAB and GNPTG. Within the TGN, M6P labeled lysosomal hydrolases are separated from secretory proteins (shown as blue circles) by binding with high affinity to M6P receptors. M6P receptors then traffic hydrolases to the lysosome. In MLII, loss of GNPTAB leads to loss of M6P addition to lysosomal hydrolases. Hydrolases are no longer separated from secretory proteins and are secreted from the cell. Pathology results from enzyme hypersecretion and lysosomal storage.

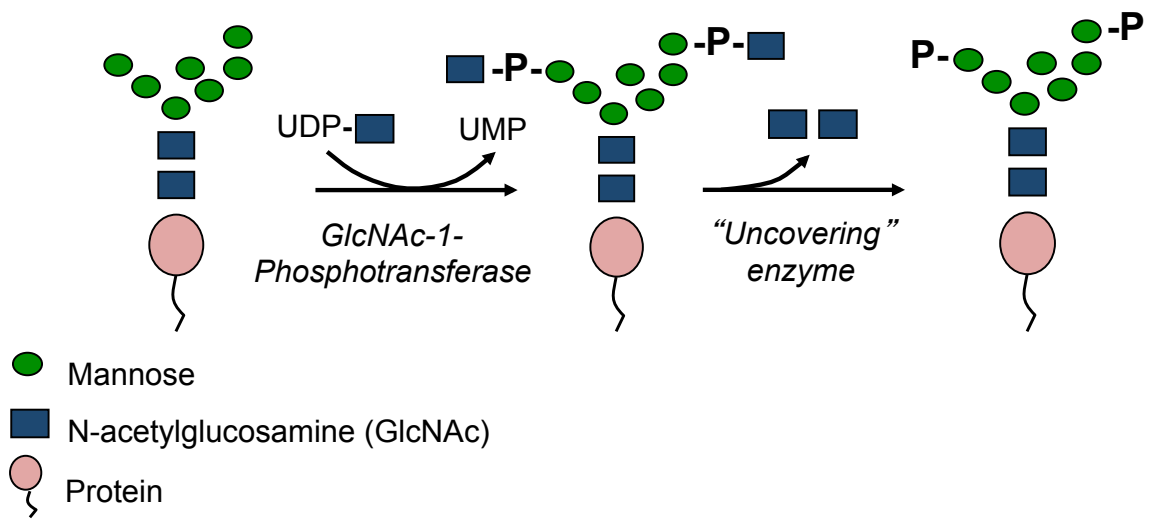


**Figure 1.2. GlcNAc-1-phosphotransferase catalyzes the biosynthesis of mannose-6-phosphate.** Schematic of GlcNAc-1-phosphate addition to N-glycans on lysosomal hydrolases, followed by removal of terminal GlcNAc residues by uncovering enzyme.



<b>Phenotype</b>	<b>Patients</b>	<b>Feline</b>	<b>Mouse (knock-in model)</b>	<b>Zebrafish</b>
Growth	Slow and stops before age 2	Retarded growth	Reduced growth	Smaller head
Onset of symptoms	Birth to early infancy	Birth	Birth	2-3 dpf
Limbs	Short hands and fingers	Difficulty walking, enlarged paws	Decreased femur length	N/A, but less ossification in fins
Skeleton	Generalized bone loss	Reduced bone volume	Bone loss, increased osteoclastogenesis	Reduced osteogenesis
Cardiac and respiratory	Congenital heart defects, recurrent respiratory infections	Cardiac complications and upper respiratory infections	Not determined	Heart edema, valve malformation, improper heart looping, blood backflow
Craniofacial features	Coarse features including, round cheeks, shallow orbits, and depressed nasal bridge	Flat, broad face	Facial dysmorphism with flat face	Short protracted jaw
Ocular	No phenotype reported	Retinal degeneration	Retinal degeneration and storage in retina	Smaller eyes
Lifespan	Early mortality less than 10 years	Early mortality within 7 months of life	Early mortality around 64 weeks	Early mortality, rarely longer than a week
Lysosomal storage	Yes	Yes	Yes	No
Enzyme secretion	Yes	Yes	Yes	Yes

**Table 1.1: Phenotype comparison between human MLII patients, feline MLII model, MLII mouse knock-in model, and morpholino generated MLII zebrafish.**

\*Adapted from Cathey, S.S., [76]

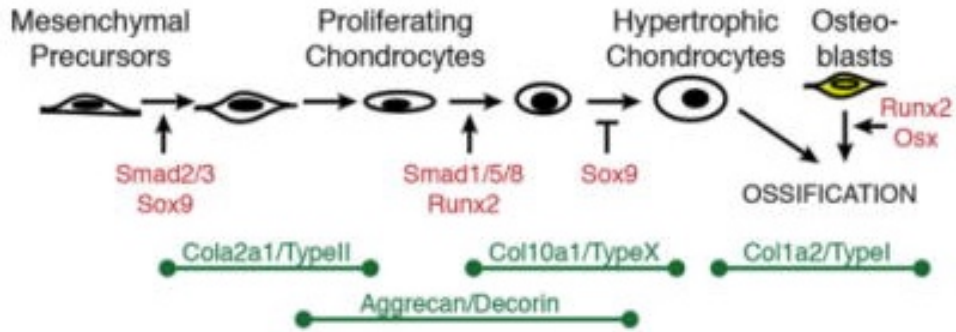


**Figure 1.4. Growth Factor Signaling Drives Chondrogenesis.** Schematic of chondrogenesis showing the transcriptional drivers and ECM proteins involved in cartilage development. Taken from Flanagan-Steet, et al. [99].

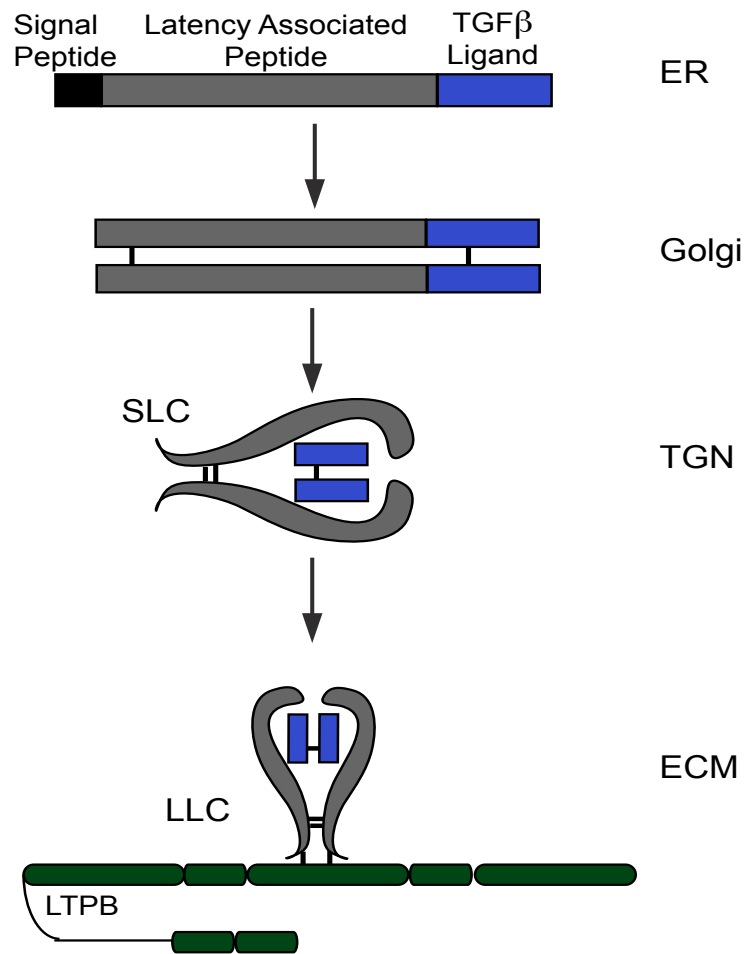


**Figure 1.5. Transforming Growth Factor Beta Synthesis and Processing.** TGFβ is synthesized as a precursor protein in the ER, that undergoes co-translational modification and removal of the signal peptide. The latency associated peptide (gray) is cleaved from the mature TGFβ ligand (blue) in the Golgi. The latency associated peptide remains noncovalently bound to TGFβ and forms the small latent complex (SLC). The SLC can associate with the latent TGFβ binding protein (LTBP), which mediates incorporation into the ECM.

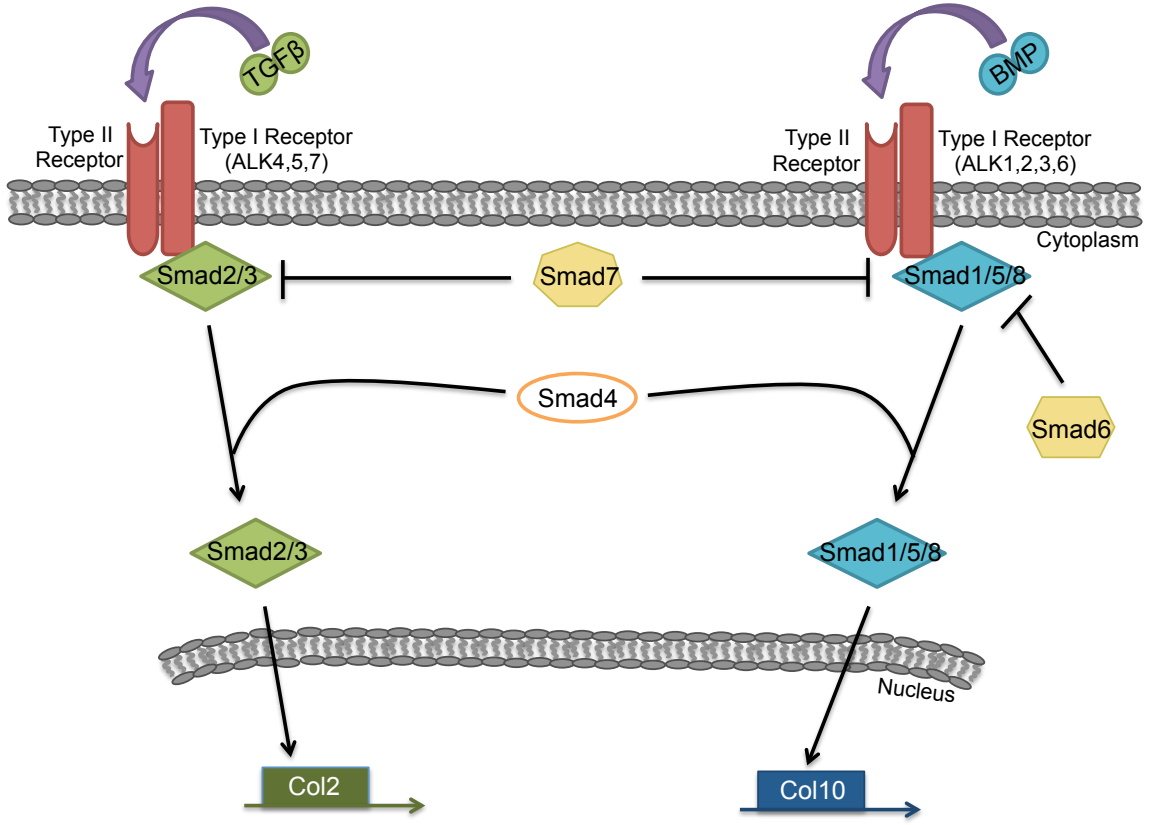


**Figure 1.6. TGFβ and BMP Dependent Smad Signaling.** Cellular schematic of TGFβ and BMP mediated Smad signaling.

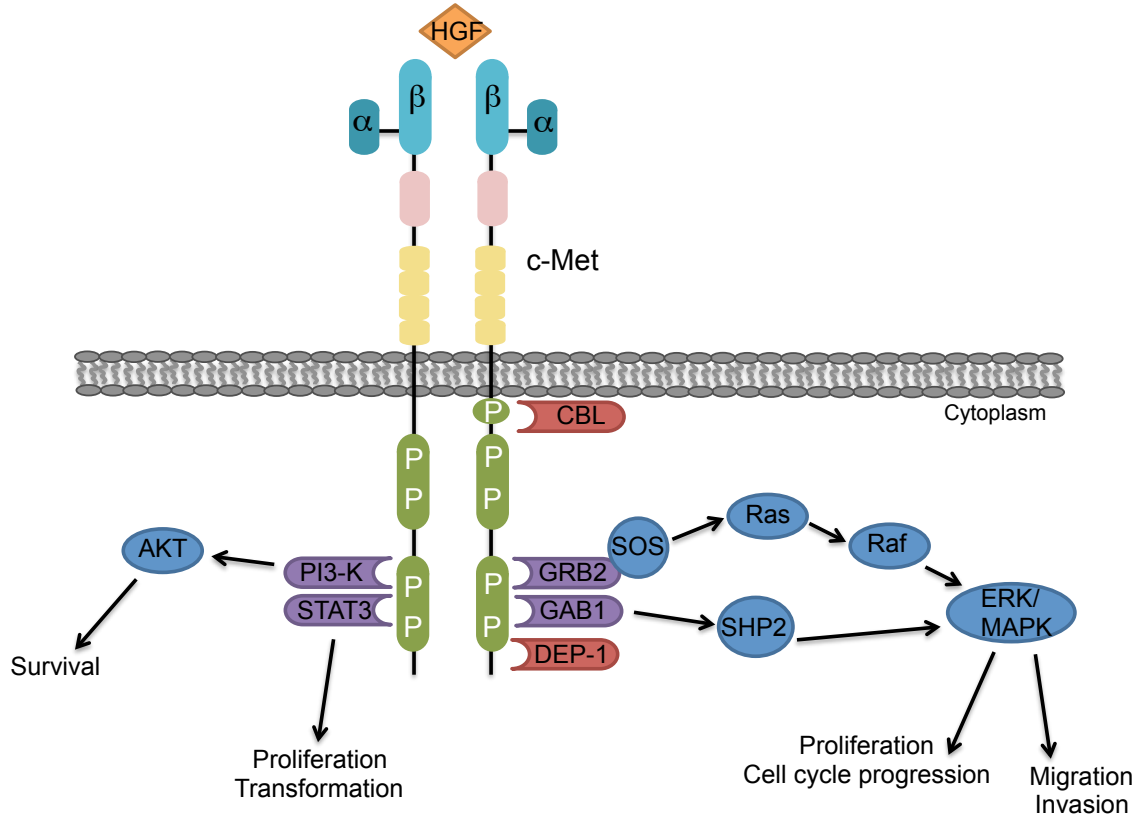


**Figure 1.7. c-Met Activation and Signaling.** Cellular schematic of c-Met signaling following HGF ligand binding. Adaptors are shown in purple, negative regulators are in red, and signaling pathways are in blue.

**CHAPTER 2: CATHEPSIN K PREFERENTIALLY ACTIVATES LATENT TGF $\beta$   
GROWTH FACTORS, DRIVING CARTILAGE PATHOLOGY IN ML-II  
ZEBRAFISH**

Aarnio, Megan. To be submitted to Disease Models and Mechanisms

## **Abstract**

**Loss of carbohydrate dependent targeting leads to the severe lysosomal storage disorder Mucopolysaccharidosis II (MLII). MLII is characterized by abnormal skeletal development, lysosomal storage, and enzyme hypersecretion. In a zebrafish model of MLII, hypersecretion of the lysosomal protease, cathepsin K (CtsK), leads to abnormal cartilage development. Abnormal chondrogenesis in MLII zebrafish is characterized by increased expression of TGF $\beta$  dependent Smad2,3 signaling and decreased BMP dependent Smad1,5,8 signaling. Inhibition of CtsK in MLII zebrafish rescues cartilage development and restores TGF $\beta$  and BMP dependent Smad signaling. This indicates a link between abnormal CtsK activity and imbalanced growth factor signaling in MLII embryos. Due to its extracellular location, CtsK is in proximity to latent growth factors in the extracellular matrix such as latent TGF $\beta$ . Based on in vitro digestions, we show that CTSK preferentially cleaves the latency associated peptide of TGF $\beta$  while sparing the mature ligand. Further, latent TGF $\beta$  pretreated with CTSK lowers the activation barrier to release signaling competent TGF $\beta$ . This finding suggests that hypersecreted CtsK could mediate direct activation of latent TGF $\beta$  leading to altered signaling. Our results also show that elevated TGF $\beta$  signaling drives ML-II pathology in zebrafish. Through pharmacological inhibition of TGF $\beta$  we were able to rescue MLII phenotypes and normalize TGF $\beta$  and BMP driven gene expression. These findings and previous studies show that both CtsK and TGF $\beta$  drive MLII zebrafish pathology, and support a gain of function by CtsK.**

## INTRODUCTION

Lysosomal targeting is a carbohydrate dependent process that is driven through the coordinated action of several enzymes. The heterohexameric enzyme, GlcNAc-1-phosphotransferase (phosphotransferase), recognizes and initiates tagging of lysosomal hydrolases with mannose 6-phosphate (M6P) [1, 2]. These hydrolases are then trafficked to the lysosome via high affinity mannose 6-phosphate receptors (MPRs), which recognize and bind M6P [3-5]. Two genes, *GNPTAB* and *GNPTG*, encode the phosphotransferase enzyme with the gene products from *GNPTAB* generating the catalytic  $\alpha\beta$  subunit [6]. Mutations in *GNPTAB* lead to the severe lysosomal storage disorder, Mucopolysaccharidosis II (MLII), which is characterized by altered craniofacial and skeletal development (dystosis multiplex) [7-9]. Patients suffer from cardiac defects and multiple recurrent respiratory infections, leading to early mortality. At the cellular level, loss of mannose phosphorylation on acid hydrolases can lead to profound lysosomal storage and secretion of lysosomal enzymes [10, 11].

In order to study the early developmental defects associated with loss of carbohydrate dependent targeting, Flanagan-Steet and colleagues developed a zebrafish model of MLII targeting the GlcNAc-1-phosphotransferase enzyme. Morpholino generated MLII embryos (morphants) display abnormal craniofacial cartilage development [12, 13]. Based on expression analysis of chondrogenic markers, chondrocytes remain in an immature state compared to wild type (WT) embryos. This is shown by sustained expression of the early chondrogenic markers *col2a1* and *sox9a* in morphant (see figure 1.5 for a schematic of chondrogenesis). WT embryos express high levels of aggrecan and decorin at 4 days post fertilization (dpf). Aggrecan and decorin are

two chondroitin sulfate proteoglycans that are expressed by mature chondrocytes [14-16]. In comparison, aggrecan and decorin expression is decreased in morphants. Osteogenesis is also affected in morphant embryos, as shown by decreased expression of type X collagen (*col10a1*). The two osteogenic transcription factors, runt-related transcription factor *runx2a* and osterix (*osx*), are also reduced in morphants [17-19].

Chondrogenesis is a growth factor mediated process with TGF $\beta$  dependent Smad2,3 signaling and Sox9a driving early stages leading to the deposition of type II collagen. As chondrogenesis progresses, there is a decline in TGF $\beta$  signaling and a concomitant increase in BMP dependent Smad1,5,8 signaling. As shown in figure 1.4, BMP drives expression of the hypertrophic marker, *col10a*. Based on immunohistochemical data, activated Smad2,3 is increased in morphant chondrocytes while activated Smad1,5,8 is decreased. This indicates an imbalance in growth factor signaling in morphants leading to altered chondrogenesis. Further, based on transcript analysis of TGF $\beta$  (TGF $\beta$ 1a, TGF $\beta$ 2, and TGF $\beta$ 3) and BMP (BMP2a, BMP2b, and BMP4) genes, there is no change in transcript abundance between WT and MLII embryos, indicating that the signaling defects are post-translational.

In the absence of M6P, lysosomal hydrolases are not recognized by M6PRs and can be secreted from the cell. One example of this is the lysosomal hydrolase cathepsin K (CtsK), which is hypersecreted from chondrocytes in MLII zebrafish cartilage [13]. CtsK activity is sustained and increased in ML-II embryos, and localized outside of chondrocytes [20]. Interestingly, inhibition of CtsK in morphants leads to reduced type II collagen accumulation and rescue of altered craniofacial development. This finding is unexpected because CtsK is a potent collagenase [21-25]. Further, TGF $\beta$  and BMP levels

are also normalized following CtsK inhibition in MLII zebrafish embryos. These findings suggest that CtsK plays a critical role in MLII pathogenesis.

In this study we show that human recombinant CtsK can cleave and liberate signaling competent TGF $\beta$  from its latency associated peptide and latent binding protein in an in vitro system. This suggests a direct mechanism of growth factor activation. CtsK inhibition is sufficient to rescue MLII craniofacial phenotypes and regulate signaling, and is a driving factor in MLII pathology, placing it upstream of a pathogenic cascade. As a way to assess whether TGF $\beta$  also drives MLII cartilage pathology we pharmacologically inhibited TGF $\beta$  signaling using a TGF $\beta$  receptor specific inhibitor. Through this we show that reduction of TGF $\beta$  signaling in morphants rescues craniofacial cartilage elements and expression of *col2a1*, *coll10a1*, and *sox9a*. Further, this reduction restores *smad 2,3* and *smad1* transcript abundance. These findings cast light on the interaction between various signaling pathways during early development, and further our understanding of MLII pathogenesis.

## **RESULTS**

### **Human and zebrafish latent TGF $\beta$ contain CtsK cleavage sites**

Previous studies have shown that suppression of CtsK activity in MLII embryos results in rescue of morphant phenotypes, and further leads to restoration of TGF $\beta$  family member signaling, indicating aberrant CtsK activity contributes to abnormal MLII chondrogenesis [13, 20]. In establishing that CtsK is a mediator of aberrant TGF $\beta$  signaling and is localized outside of the cell in proximity to latent growth factors, we

wanted to ask whether CtsK has the ability to physically act on TGF $\beta$ . The ability of active CtsK to liberate and or degrade latent growth factors *in vivo* is dependent on the recognition of certain consensus cleavage sites. Based on the established minimal recognition sequence of CTSK (leucine-arginine) we mapped the amino acid sequences of human and zebrafish TGF $\beta$ 1 [22, 23, 26]. As shown in figure 2.1, human TGF $\beta$ 1 has five LR residues in the latency-associated peptide (LAP) of TGF $\beta$ 1, and no LR residues within the mature ligand. Zebrafish TGF $\beta$ 1a, which shares approximately 80% homology with human TGF $\beta$ 1, has four LR residues within the LAP region and none in the mature ligand. This is important because the LAP region of TGF $\beta$  forms a straightjacket like domain around the mature TGF $\beta$  ligand, and in order for signaling, TGF $\beta$  must be released from LAP (see figure 1.5 for a schematic of LAP-TGF $\beta$  structure) [27, 28]. Humans and zebrafish have two other *TGF $\beta$*  genes, *TGF $\beta$ 2* and *TGF $\beta$ 3*. Based on expression analysis, *tgfb2* and *3* are expressed in the palate and in Meckel's cartilage in developing zebrafish, and are essential for proper palate development ([29] and unpublished). By amino acid sequence, zebrafish TGF $\beta$ 2 has one LR site within the LAP region while TGF $\beta$ 3 has three, and both TGF $\beta$ 2 and TGF $\beta$ 3 have one LR site within the mature TGF $\beta$  ligand region. This indicates that zebrafish TGF $\beta$ 2 and TGF $\beta$ 3 could potentially be more sensitive to proteolysis. We also mapped the amino acid sequences of human and zebrafish BMP2 and found one LR site in the human sequence and two sites in zebrafish BMP2. Both residues were within the proprotein region of the protein. Based on these consensus cleavage sites, it is possible that CtsK can recognize and cleave these latent growth factors *in vitro*.

### **The latency associated peptide (LAP) of TGF $\beta$ is a substrate for CTSK**

To address CtsK's activity towards latent growth factors we incubated active recombinant human CTSK with the latency associated peptide of TGF $\beta$ 1 (of note, the following experiments were performed using recombinant human growth factors rather than zebrafish proteins, based on commercial availability). Digestions shown in figure 2.2A compare the substrate specificity for LAP by the aspartate protease cathepsin D and the cysteine protease CTSK. In MLII mouse and zebrafish models CtsD and CtsK are differentially trafficked [13, 30]. These digestions indicate a difference in the pH sensitivity between CTSD and K, as only CTSK can cleave LAP at a neutral pH. Importantly, untreated LAP is stable at an acidic pH and is not degraded when both cathepsins are inhibited. These results suggest that CTSK has the potential to operate at an extracellular-like pH and cleave LAP.

Liberation of mature TGF $\beta$  from LAP is essential for receptor binding and TGF $\beta$  signaling. For a direct mechanism of cathepsin-mediated activation of TGF $\beta$ , CTSK would need to differently cleave LAP and spare the mature ligand. Figure 2.2B shows CTSK in vitro digestion experiments comparing LAP susceptibility to mature TGF $\beta$  susceptibility. Active CTSK in increasing amounts was incubated with recombinant LAP over a pH range. At pH 5, LAP was mostly degraded by CTSK, but was cleaved into distinct fragments at 7.5. pH 6 shows an intermediate cleavage and degradation pattern, suggesting that the level of LAP degradation or cleavage by CTSK is pH dependent. Digestions were performed under identical conditions incubating activated recombinant human CTSK with purified TGF $\beta$  ligand. As seen in Figure 2.2B, TGF $\beta$  is stable when

combined with CTSK, indicating a difference in substrate specificity between LAP and mature TGF $\beta$  ligand.

### **CTSK can release signaling competent TGF $\beta$ from the large latent complex**

The large latent complex (LLC) of TGF $\beta$  is composed of the small latent complex plus the latent TGF $\beta$  binding protein (LTBP), and is the primary form of TGF $\beta$  in the extracellular matrix (ECM) (see figure 1.5 for a schematic). LTBP serves to direct TGF $\beta$  to the ECM and confer latency, and studies indicate its importance in proper TGF $\beta$  signaling regulation [31-33]. Based on this we asked if CTSK could act on LTBP or LAP in the LLC to release signaling-competent TGF $\beta$ . LLC was generated from PMA differentiated human erythroleukemia cells (HELs) [34]. Following PMA stimulated differentiation, cells were serum starved and media-containing LLC was collected and concentrated. Figure 2.3A shows an immunoblot probing for LTBP using an antibody that detects non-reduced LTBP. In this experiment, *in vitro* digestions containing concentrated LLC from media was incubated at pH 5, 6, and 7.5 with two amounts of active recombinant human CTSK. Digestion with CTSK causes a 100kDa molecular weight shift at both amounts tested (15ng and 46ng of CTSK). At higher amounts of CTSK, LTBP signal is reduced indicating potential degradation of the protein. Additionally, the same digestions were immunoblotted for LAP (figure 2.3A). The 100kDa band represents the unreduced form and the 40kDa band is the reduced form of LAP. Addition of the reducing agent DTT fully reduces the complex, interestingly, incubation with a lower amount of CTSK at all pHs tested did not alter the mobility of the complex. In contrast, the higher amounts of CTSK (46ng) lead to a reduction in signal

of the 100kDa band for all pHs. As a control, LLC was also incubated with the known latent TGF $\beta$  activator, plasmin, which cleaves LTBP (figure 2.3B). As seen in figure 2.3B, using an antibody that detects reduced and nonreduced LTBP, digestion with plasmin at two concentrations (.5U and 1U), results in total degradation of LTBP. In vitro digestions were also performed with another lysosomal hydrolase, cathepsin L (CtsL), which has elevated and sustained activity in ML-II zebrafish embryos. Incubation with CTSK and CTSL lead to molecular weight shifts and a differential cleavage pattern. Figure 2.3B shows that plasmin does not affect LAP, but digestion with CTSK and CTSL lead to a reduction in LAP signal. These results suggest that LTBP of the LLC is more susceptible to CTSK activity, as indicated by its change in mobility and degradation upon CTSK incubation. The LAP portion of the LLC was less affected by CTSK activity, and was only degraded with the higher amount of CTSK. Alternatively, based on the presentation of the LLC, CTSK may come in contact with LTBP before LAP, which could explain its preferential cleavage.

As a measure of bioactive TGF $\beta$  signaling we used a TGF $\beta$  reporter cell line that expresses firefly luciferase upon TGF $\beta$  stimulation [35]. For these experiments we used heat treatment to liberate TGF $\beta$  ligand. Figure 2.3C shows heat dependent activation of TGF $\beta$  in relative fluorescence units (RLU). Heating LLC for 10 minutes at 80°C yields maximal activation, while the suboptimal temperature 75°C, results in 35%-40% of the maximal activation. To assess proteolytic activation of LLC, we performed in vitro digestions with LLC and either plasmin or CTSK (figure 2.3D). No induction was found after digestion with either plasmin or CTSK alone, but post treatment at 75°C resulted in a synergistic increase in TGF $\beta$  signaling induction. This suggests that by compromising

LLC's stability, CTSK lowers the activation energy needed for TGF $\beta$  liberation and signaling.

### **BMP is a substrate for CTSK**

To look at the susceptibility of BMP to CTSK activity we performed in vitro digestions at acidic and neutral pH with increasing concentrations of CTSK. Under the same in vitro digestion conditions tested with LAP and LLC, CTSK degrades BMP2 (Figure 2.4A). Further, it does not appear that CTSK activates proBMP into a signaling competent form. This is shown in figure 2.4B where incubation with CTSK leads to a decrease in reporter induction. This is important because BMP regulated signaling (Smad1,5,8) is decreased in MLII morphants, suggesting a potential direct relationship between decreased BMP signaling.

### **Inhibition of TGF $\beta$ signaling rescues ML-II craniofacial phenotypes**

Zebrafish express multiple TGF $\beta$  genes and isoforms during early craniofacial development, with TGF $\beta$ 2 and TGF $\beta$ 3 playing the largest role [29]. In order to look at the effects of TGF $\beta$  expression to MLII craniofacial pathogenesis, we used a TGF $\beta$  receptor specific inhibitor to reduce TGF $\beta$  signaling. SB505124 is an ATP-competitive reversible inhibitor that targets the TGF $\beta$  type I receptors Alk4, Alk5, and Alk7 receptors specifically in a concentration dependent manner [36, 37]. 3 days post fertilization (3dpf) WT and MLII embryos were treated with 1 $\mu$ M SB505124 (which showed the best phenotypic rescue) for 24 hours. This time point was chosen because ML-II embryos begin to display dramatically altered *col2*, *coll10*, and *sox9a* expression. Following

treatment, Alcian Blue staining was used to assess for phenotypic changes in cartilage morphology. For all treatments, control embryos (either WT or MLII) were treated with the same concentration of DMSO as SB treated embryos. Figure 2.5A shows representative Alcian Blue stains of WT, MLII, and MLII treated embryos. 100% of WT embryos resembled the photograph, with Meckel's cartilage reaching the palate and the ceratohyal forming an acute angle. In comparison, morphants have a protracted jaw and a ceratohyal angle greater than 90°. Following TGF $\beta$  inhibition, 35% of treated embryos were significantly rescued and resembled WT embryos, with a reduced ceratohyal angle, elongated trabeculum, and Meckel's cartilage meeting the palate.

Examination of molecular rescue was assessed using in situ hybridization towards the TGF $\beta$  effector gene *col2a1* and the BMP effector gene *coll0a1*, as well as the chondrogenic regulator *sox9a*. *Sox9* is an HMG-box transcription factor that is required for the early stages of chondrogenesis, but prolonged expression inhibits further maturation [38, 39]. As published previously, RNA expression levels of *col2a1* and *sox9a* are elevated at 4dpf in MLII embryos, while *coll0a1* is dramatically reduced [13]. Treatment with the TGF $\beta$ R specific inhibitor SB505124 reduced *col2a1* expression in the palate, Meckel's cartilage, and the ceratohyal in 46% of MLII treated embryos (Figure 2.5B). Further, approximately half of treated embryos gained pectoral fin expression of *col2a1* (data not shown). For *sox9a* in situ hybridizations, 54% of MLII SB505124 treated embryos showed significant rescue as shown by reduced expression of *sox9a* in Meckel's and the palatoquadrate. *Coll0a1* rescue progressed in a posterior to anterior direction, with posterior structures recovering before anterior, beginning with lengthened cleithrum and elongated parasphenoid followed by gain of expression in the following

anterior structures, entopterygoid, dentary, and maxilla. 51% of treated embryos were significantly rescued and resembled the representative MLII + SB image in figure 2.5B. These findings indicate that reduction of TGF $\beta$  signaling in morphant embryos leads to significant restoration of TGF $\beta$  and BMP regulated genes. Further, the reduction in *sox9a* expression was also interesting and suggests a tie between TGF $\beta$  and *sox9a*.

### **TGF $\beta$ and BMP effector expression is rescued following TGF $\beta$ inhibition.**

Since reduction of TGF $\beta$  signaling in morphants improved phenotypes and significantly recovered *col2a1*, *coll10*, and *sox9a* expression, we wanted see how modulation of TGF $\beta$  signaling affected transcript abundance of Smads2,3 and Smad1. Quantitative PCR was performed on 4dpf embryos following 24 hours of SB505124 treatment at three different concentrations. These concentrations were determined based on previous reports in zebrafish and through concentration gradient assessment [40]. In order to detect changes in transcript levels, only phenotypically rescued embryos were used for all genes. As shown in figure 2.6A, elevated *col2a1* expression significantly decreases upon SB505124 treatment and recovers to WT levels. The other early chondrogenesis marker, *sox9a*, has slightly decreased transcript abundance at .5 $\mu$ M and 1 $\mu$ M, but increases when embryos are treated at the higher concentration of 2 $\mu$ M (figure 2.6B). As shown in figure 2.6C, the BMP regulated hypertrophic chondrocyte marker, *coll10a1*, has reduced abundance in ML-II embryos, and is significantly restored upon TGF $\beta$  inhibition, with levels exceeding WT at .5 $\mu$ M. The TGF $\beta$  effectors *smad2* and *smad3a* have increased transcript abundance in morphants, and both genes respond to TGF $\beta$  inhibition (figure 2.6D,E). As shown in figure 2.6D, *smad2* significantly recovers

to WT levels following TGF $\beta$  inhibition. *Smad3a* responds similarly to *smad2*, with inhibition decreasing transcript abundance close to WT levels (figure 2.6F). *Smad1*, which is a BMP effector, has reduced levels in ML-II embryos, and upon TGF $\beta$  reduction *smad1* transcript abundance reaches and surpasses WT levels (figure 2.6F). These data suggest that inhibition of elevated TGF $\beta$  signaling in morphants rescues cartilage defects and restores the molecular alterations caused by imbalanced growth factor signaling.

## DISCUSSION

CtsK is a driving factor of the craniofacial pathogenesis seen in MLII zebrafish. This stems from both a gain in the extracellular availability and increased activation of CtsK. This is caused by loss of M6P targeting, rather than loss of its intracellular localization, which has been demonstrated by the lack of MLII like phenotypes following CtsK knockdown in WT embryos [13]. To tie the extracellular activity of CtsK to altered TGF $\beta$  and BMP signaling, we performed in vitro digestions to assess the specificity of CtsK for latent or mature growth factors that reside in the extracellular matrix. Based on in vitro digestions combining recombinant activated CTSK with various components of the latent TGF $\beta$  complex, we showed that CTSK has a higher specificity for LTBP and LAP than the mature TGF $\beta$  ligand. Further, CTSK was able to cleave and liberate a signaling competent version of TGF $\beta$  following in vitro digestion and subsequent heat activation. Interestingly, under the same in vitro digestion conditions, BMP2 was degraded by CTSK and unable to signal. These findings suggest that hypersecreted CtsK

could degrade and liberate latent TGF $\beta$  localized in the ECM while degrading BMP, leading to signaling imbalance in morphant cartilage.

Based on the extracellular location of CtsK and its ability to activate latent growth factors, we propose that the cartilage pathogenesis in morphants is mediated by CtsK gain of function. Under normal conditions, CtsK is segregated from latent growth factors, but in MLII loss of M6P targeting leads to hypersecretion of CtsK, which puts it in proximity to latent growth factors. This gain of function mimics the effects of enhanced TGF $\beta$  signaling seen in Camurati-Engelmann Disease (CED) [41-43]. CED is caused by mutations in the latency associated peptide portion of TGF $\beta$ , and leads to increased TGF $\beta$  activation. This is thought to occur because mutations in LAP render it less stable and able to remain tightly associated with the mature TGF $\beta$  ligand. Thus in the context of ML-II, destabilization of latent TGF $\beta$  by CtsK could result in the enhanced signaling seen in morphants.

Previous research by Flanagan-Steet and colleagues showed that *sox9a* reduction in the ML-II background was sufficient to phenotypically rescue MLII zebrafish embryos [13]. Further, reduction of CtsK via genetic or pharmacological means in MLII morphants normalized TGF $\beta$  and BMP signaling. Based on these findings, we sought to elucidate the role of elevated TGF $\beta$  signaling in abnormal MLII chondrogenesis, and learn if TGF $\beta$  drives disease pathogenesis. Pharmacologic inhibition of TGF $\beta$  signaling in morphants rescued craniofacial cartilage abnormalities and resulted in an elongated palatoquadrate and Meckel's cartilage, and restoration of the ceratohyal angle. Further, expression of *col2a1* and *coll10a1* were restored as indicated by in situ hybridization and qPCR analysis. Interestingly, TGF $\beta$  inhibition significantly rescued *sox9a* expression via

in situ hybridization, but little rescue was seen in qPCR transcript abundance. This suggests that potentially little change in *sox9a* expression is needed to initiate phenotypic rescue, which might not be reflected in transcript abundance. TGF $\beta$  inhibition also rescued the downstream signaling effectors *smad2* and *smad3a*, as well as the BMP effector *smad1*. Based on these results we show that TGF $\beta$  as well as CtsK drives MLII pathology in zebrafish. This is an important finding that has clinical implications for MLII treatment.

Many studies have detailed the interaction between TGF $\beta$  and BMP signaling through genetic ablation of the smad effectors or TGF $\beta$ /BMP receptors in an in vitro system. For example, Smad3-deficient chondrocytes showed enhanced BMP signaling and increased hypertrophy, suggesting elevated TGF $\beta$  signaling is necessary to modulate BMP signaling [44]. Similar to these findings, our results support the role of signaling cross talk between TGF $\beta$  and BMP in normal and pathological development, and specifically demonstrate that reduction of TGF $\beta$  signaling restores BMP signaling in vivo.

## **MATERIALS AND METHODS**

### **Zebrafish strains and husbandry**

Zebrafish were maintained according to standard protocols. Zebrafish strains were obtained from Fish 2U (F2U; Gibsonton, FL, USA) and the Zebrafish International Resource Center (ZIRC, Eugene, OR, USA) (TL and AB). Embryo staging was performed according to established criteria [45]. To inhibit pigmentation, 0.003% 1-

phenyl 2-thiourea (PTU) was added to embryo growth media. Handling and euthanasia of all experimental fish was in compliance with the University of Georgia policies, as approved by the UGA Institutional Animal Care and Use Committee (permit #A2013-8-144).

### **Morpholinos and inhibition of gene expression**

Morpholino knockdown of GlcNAc-1-phosphotransferase was performed and assessed as previously published [12, 20].

### **In vitro analyses and reporter assays**

Recombinant human LAP dimer, TGF $\beta$  ligand, and proBMP2 ligand were used for in vitro experiments. 40 $\mu$ g of recombinant protein was digested for 30 or 60 minutes at RT with active human recombinant CTSK at pH 5, 6, and 7.5. CTSK activity was normalized using a fluorescent substrate to ensure the same amount of activity was added for each experiment. HEL cells were differentiated for 72 hours in the presence of PMA, and LLC media was collected in serum free media. LLC containing media was concentrated using centricon spin columns. LLC samples were digested for 30 minutes and then heat activated for 10 minutes at 75C or 80C. Following digestions and heat activation, samples were added to reporter cells for 16 hours and luciferase induction was measured.

### **In situ hybridization**

In situ hybridization experiments were performed according to Thisse and Thisse [46]. The following probes were made as described, *col2a1*, *coll10a1*, and *sox9a* [47]. Images

were captured on an Olympus SZ16 microscope with a Retiga 2000R camera using Q-capture software.

### **Quantitative RT-PCR analysis**

QPCR and data analysis was performed as previously described [20]. The primer sequences used are as follows:

RPL4: forward primer (5' to 3') - GTGCCCCGACCGTTAATCTC

reverse primer (5' to 3') – ACACTGCTGGCATAACCACAT

Col2a1: forward primer (5' to 3') – GAACTTCCTCAGGCTGCTGT

reverse primer (5' to 3') – TGTAAGCCACGCTGTTCTTG

Col10a1: forward primer (5' to 3') – TGCCCATGGTGAGAGATATGT

reverse primer (5' to 3') – CGGAGTAAGGCTGGTACTGC

Sox9a: forward primer (5' to 3') – GCATCTCCAGCATTACAGCA

reverse primer (5' to 3') – CTGGTGGCTGTCGGAATAGT

Smad1: forward primer (5' to 3') – CAGCCAAGCAATTGTGTCAC

reverse primer (5' to 3') – GAAGCACCTTTCGGTGTGAT

Smad2: forward primer (5' to 3') – AAACATTCCACGCCTCTCAG

reverse primer (5' to 3') – GCAGAATCGCTCTGAATTGG

Smad3a: forward primer (5' to 3') – CTTACAGACCCGTCCAACCT

reverse primer (5' to 3') – CAGCGTTTCGGTTCACATT

### **TGF $\beta$ inhibition**

Embryos were treated with 0.5 $\mu$ M, 1 $\mu$ M, or 2 $\mu$ M of SB505124 reconstituted in DMSO for 24 hours beginning at 3dpf. As a control, DMSO was added to growth media at the same concentration as SB treated embryos.

## REFERENCES

1. Kornfeld, S., et al., *Steps in the phosphorylation of the high mannose oligosaccharides of lysosomal enzymes*. Ciba Found Symp, 1982(92): p. 138-56.
2. Reitman, M.L. and S. Kornfeld, *Lysosomal enzyme targeting. N-Acetylglucosaminylphosphotransferase selectively phosphorylates native lysosomal enzymes*. J Biol Chem, 1981. **256**(23): p. 11977-80.
3. Dahms, N.M., P. Lobel, and S. Kornfeld, *Mannose 6-phosphate receptors and lysosomal enzyme targeting*. J Biol Chem, 1989. **264**(21): p. 12115-8.
4. Griffiths, G., et al., *The mannose 6-phosphate receptor and the biogenesis of lysosomes*. Cell, 1988. **52**(3): p. 329-41.
5. Hoflack, B., K. Fujimoto, and S. Kornfeld, *The interaction of phosphorylated oligosaccharides and lysosomal enzymes with bovine liver cation-dependent mannose 6-phosphate receptor*. J Biol Chem, 1987. **262**(1): p. 123-9.
6. Kudo, M., et al., *The alpha- and beta-subunits of the human UDP-N-acetylglucosamine:lysosomal enzyme N-acetylglucosamine-1-phosphotransferase [corrected] are encoded by a single cDNA*. J Biol Chem, 2005. **280**(43): p. 36141-9.
7. Cathey, S.S., et al., *Phenotype and genotype in mucopolidoses II and III alpha/beta: a study of 61 probands*. J Med Genet, 2010. **47**(1): p. 38-48.
8. Herman, T.E. and W.H. McAlister, *Neonatal mucopolidosis II (I-cell disease) with dysharmonic epiphyseal ossification and butterfly vertebral body*. J Perinatol, 1996. **16**(5): p. 400-2.
9. Sprigz, R.A., et al., *Neonatal presentation of I-cell disease*. J Pediatr, 1978. **93**(6): p. 954-8.
10. Kornfeld, S. and W.S. Sly, *Lysosomal storage defects*. Hosp Pract (Off Ed), 1985. **20**(8): p. 71-5, 78-82.
11. Platt, F.M., B. Boland, and A.C. van der Spoel, *The cell biology of disease: lysosomal storage disorders: the cellular impact of lysosomal dysfunction*. J Cell Biol, 2012. **199**(5): p. 723-34.
12. Flanagan-Steet, H., C. Sias, and R. Steet, *Altered chondrocyte differentiation and extracellular matrix homeostasis in a zebrafish model for mucopolidosis II*. Am J Pathol, 2009. **175**(5): p. 2063-75.
13. Flanagan-Steet, H., et al., *Cathepsin-Mediated Alterations in TGFs-Related Signaling Underlie Disrupted Cartilage and Bone Maturation Associated With Impaired Lysosomal Targeting*. J Bone Miner Res, 2016. **31**(3): p. 535-48.
14. Takahashi, I., et al., *Compressive force promotes sox9, type II collagen and aggrecan and inhibits IL-1beta expression resulting in chondrogenesis in mouse embryonic limb bud mesenchymal cells*. J Cell Sci, 1998. **111** ( Pt 14): p. 2067-76.
15. Grunder, T., et al., *Bone morphogenetic protein (BMP)-2 enhances the expression of type II collagen and aggrecan in chondrocytes embedded in alginate beads*. Osteoarthritis Cartilage, 2004. **12**(7): p. 559-67.
16. Knudson, C.B. and W. Knudson, *Cartilage proteoglycans*. Semin Cell Dev Biol, 2001. **12**(2): p. 69-78.

17. Dalcq, J., et al., *RUNX3, EGR1 and SOX9B form a regulatory cascade required to modulate BMP-signaling during cranial cartilage development in zebrafish*. PLoS One, 2012. **7**(11): p. e50140.
18. Flores, M.V., et al., *A hierarchy of Runx transcription factors modulate the onset of chondrogenesis in craniofacial endochondral bones in zebrafish*. Dev Dyn, 2006. **235**(11): p. 3166-76.
19. Kim, E.J., et al., *Ihh and Runx2/Runx3 signaling interact to coordinate early chondrogenesis: a mouse model*. PLoS One, 2013. **8**(2): p. e55296.
20. Petrey, A.C., et al., *Excessive activity of cathepsin K is associated with cartilage defects in a zebrafish model of mucopolidosis II*. Dis Model Mech, 2012. **5**(2): p. 177-90.
21. Li, Z., et al., *Collagenase activity of cathepsin K depends on complex formation with chondroitin sulfate*. J Biol Chem, 2002. **277**(32): p. 28669-76.
22. Lecaille, F., et al., *Selective inhibition of the collagenolytic activity of human cathepsin K by altering its S2 subsite specificity*. Biochemistry, 2002. **41**(26): p. 8447-54.
23. Lecaille, F., et al., *The S2 subsites of cathepsins K and L and their contribution to collagen degradation*. Protein Sci, 2007. **16**(4): p. 662-70.
24. Li, Z., et al., *The crystal and molecular structures of a cathepsin K:chondroitin sulfate complex*. J Mol Biol, 2008. **383**(1): p. 78-91.
25. Selent, J., et al., *Selective inhibition of the collagenase activity of cathepsin K*. J Biol Chem, 2007. **282**(22): p. 16492-501.
26. Lecaille, F., D. Bromme, and G. Lalmanach, *Biochemical properties and regulation of cathepsin K activity*. Biochimie, 2008. **90**(2): p. 208-26.
27. Shi, M., et al., *Latent TGF-beta structure and activation*. Nature, 2011. **474**(7351): p. 343-9.
28. Buscemi, L., et al., *The single-molecule mechanics of the latent TGF-beta1 complex*. Curr Biol, 2011. **21**(24): p. 2046-54.
29. Swartz, M.E., et al., *Examination of a palatogenic gene program in zebrafish*. Dev Dyn, 2011. **240**(9): p. 2204-20.
30. Kollmann, K., et al., *Decreased bone formation and increased osteoclastogenesis cause bone loss in mucopolidosis II*. EMBO Mol Med, 2013. **5**(12): p. 1871-86.
31. Annes, J.P., J.S. Munger, and D.B. Rifkin, *Making sense of latent TGFbeta activation*. J Cell Sci, 2003. **116**(Pt 2): p. 217-24.
32. Horiguchi, M., M. Ota, and D.B. Rifkin, *Matrix control of transforming growth factor-beta function*. J Biochem, 2012. **152**(4): p. 321-9.
33. Hyytiainen, M., C. Penttinen, and J. Keski-Oja, *Latent TGF-beta binding proteins: extracellular matrix association and roles in TGF-beta activation*. Crit Rev Clin Lab Sci, 2004. **41**(3): p. 233-64.
34. Miyazono, K., et al., *A role of the latent TGF-beta 1-binding protein in the assembly and secretion of TGF-beta 1*. EMBO J, 1991. **10**(5): p. 1091-101.
35. Abe, M., et al., *An assay for transforming growth factor-beta using cells transfected with a plasminogen activator inhibitor-1 promoter-luciferase construct*. Anal Biochem, 1994. **216**(2): p. 276-84.

36. DaCosta Byfield, S., et al., *SB-505124 is a selective inhibitor of transforming growth factor-beta type I receptors ALK4, ALK5, and ALK7*. Mol Pharmacol, 2004. **65**(3): p. 744-52.
37. Vogt, J., R. Traynor, and G.P. Sapkota, *The specificities of small molecule inhibitors of the TGFs and BMP pathways*. Cell Signal, 2011. **23**(11): p. 1831-42.
38. Bi, W., et al., *Sox9 is required for cartilage formation*. Nat Genet, 1999. **22**(1): p. 85-9.
39. Olsen, B.R., A.M. Reginato, and W. Wang, *Bone development*. Annu Rev Cell Dev Biol, 2000. **16**: p. 191-220.
40. Jazwinska, A., R. Badakov, and M.T. Keating, *Activin-betaA signaling is required for zebrafish fin regeneration*. Curr Biol, 2007. **17**(16): p. 1390-5.
41. Janssens, K., et al., *Mutations in the gene encoding the latency-associated peptide of TGF-beta 1 cause Camurati-Engelmann disease*. Nat Genet, 2000. **26**(3): p. 273-5.
42. McGowan, N.W., et al., *A mutation affecting the latency-associated peptide of TGFbeta1 in Camurati-Engelmann disease enhances osteoclast formation in vitro*. J Clin Endocrinol Metab, 2003. **88**(7): p. 3321-6.
43. Janssens, K., et al., *Transforming growth factor-beta 1 mutations in Camurati-Engelmann disease lead to increased signaling by altering either activation or secretion of the mutant protein*. J Biol Chem, 2003. **278**(9): p. 7718-24.
44. Li, T.F., et al., *Smad3-deficient chondrocytes have enhanced BMP signaling and accelerated differentiation*. J Bone Miner Res, 2006. **21**(1): p. 4-16.
45. Kimmel, C.B., et al., *Stages of embryonic development of the zebrafish*. Dev Dyn, 1995. **203**(3): p. 253-310.
46. Thisse, C. and B. Thisse, *High-resolution in situ hybridization to whole-mount zebrafish embryos*. Nat Protoc, 2008. **3**(1): p. 59-69.
47. Li, N., et al., *Tracking gene expression during zebrafish osteoblast differentiation*. Dev Dyn, 2009. **238**(2): p. 459-66.

## FIGURES

### Human TGF- $\beta$ 1 precursor

MPPSG**LR**LLPLLPLLLWLLVLTTPGRPAAGLSTCKTIDMELVKKRIEAIRGQILSK**LRL**ASPPS  
QGEVPPGPLPEAVLALYNSTRDRVAGESAEPEPEPEADYYAKEVTRVLMVETHNEIYDKFKQST  
HSIYMFNTSEL**LR**EAVPEPVLLSRAE**LRLLR**LKLKVEQHVELYQKYSNNSWRYLSNRLAPSDS  
PEWLSFDVTGVVRQWLSRGGEIEGFRLSAHCSCDSRDNTLQVDINGFTTGRRGDLATIHGMNRP  
FLLMATPLERAQHLQSSRHRRALDTNYCFSSSTEKNCCVRQLYIDFRKDLGWKWIHEPKGYHAN  
FCLGPCPYIWSLDTQYSKVLALYNQHNPGASAAPCCVPQALEPLPIVYYYVGRKPKVEQLSNMIV  
RSCKCS

### Zebrafish TGF- $\beta$ 1a precursor

MRLVCLVLTALCLVTGTGSMSTCKTLDLELVVRKKRIEAIRGQILSK**LR**MAKEPESGADDDGQKI  
PDSL~~SL~~YNSTVELSEEMKTKIYPVQDEDEDYFGKEVHKFVFQQAQNNTKHQMFNVSEMKRSI  
PDYRLLSQAE**LRLR**IKNPTMDQEQRLELYRGVGDQARYLGTRFVSKDLSNRWLSFDVKQTMIEW  
LQSEDEETLE**LRL**YCDCKANQQSTDKFLFTISGLDKQRGDTAGLADMMVKPYILALSLPSNGN  
SLASVRKRRAVGTDETCDEKTETCCMRKLYIDFRKDLGWKWIHKPKGYFANYCMGSC~~TY~~IWNAE  
NKYSQILALYKHHNPGASAQPCCVPAILDPLPIIYYVGRQHKVEQLSNMVVRNCKCS

**Figure 2.1. Amino acid sequence of human and zebrafish TGF $\beta$ 1 precursor protein (LAP-TGF $\beta$ 1).** Highlighted regions indicate putative cathepsin K cleavage sites, and the underlined portion is the mature TGF $\beta$  ligand.

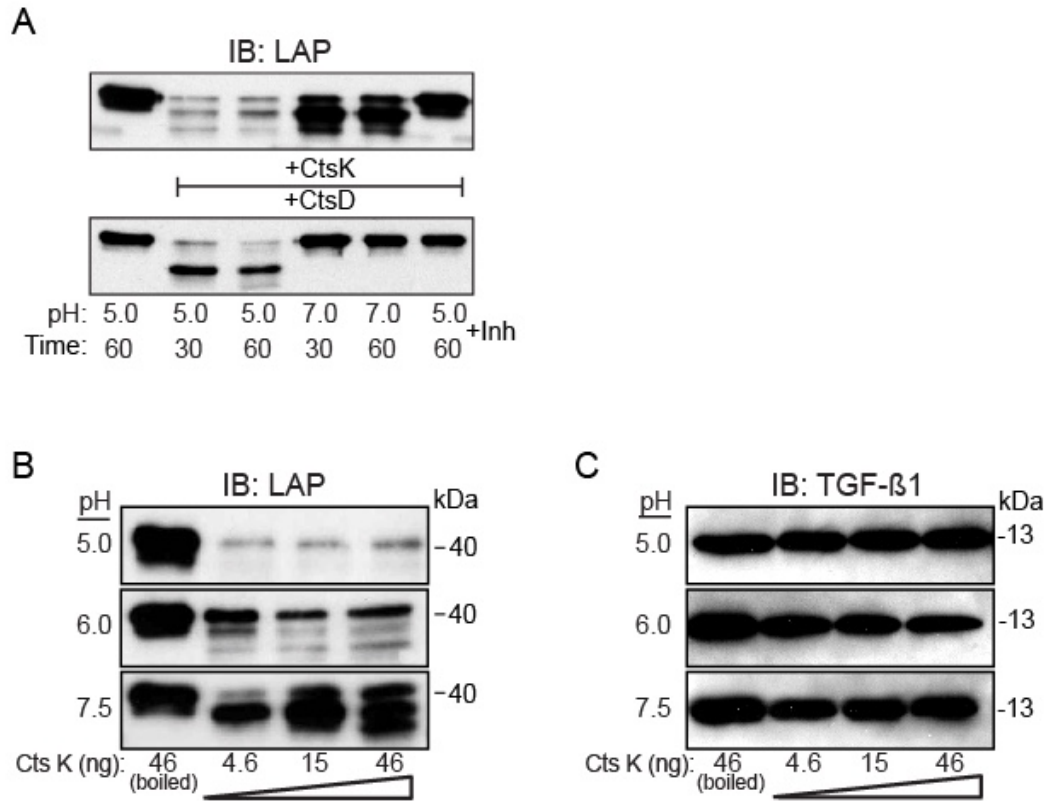


**Figure 2.2 CTSK preferentially cleaves LAP.** (A) Immunoblot of LAP following digestion with either CTSD or CTSK for 30 or 60 minutes at pH 5 or 7. (B) Immunoblot of LAP digested with CTSK. n=4 experiments. (C) Immunoblot of TGF $\beta$ 1 ligand with CTSK. n=4 experiments.

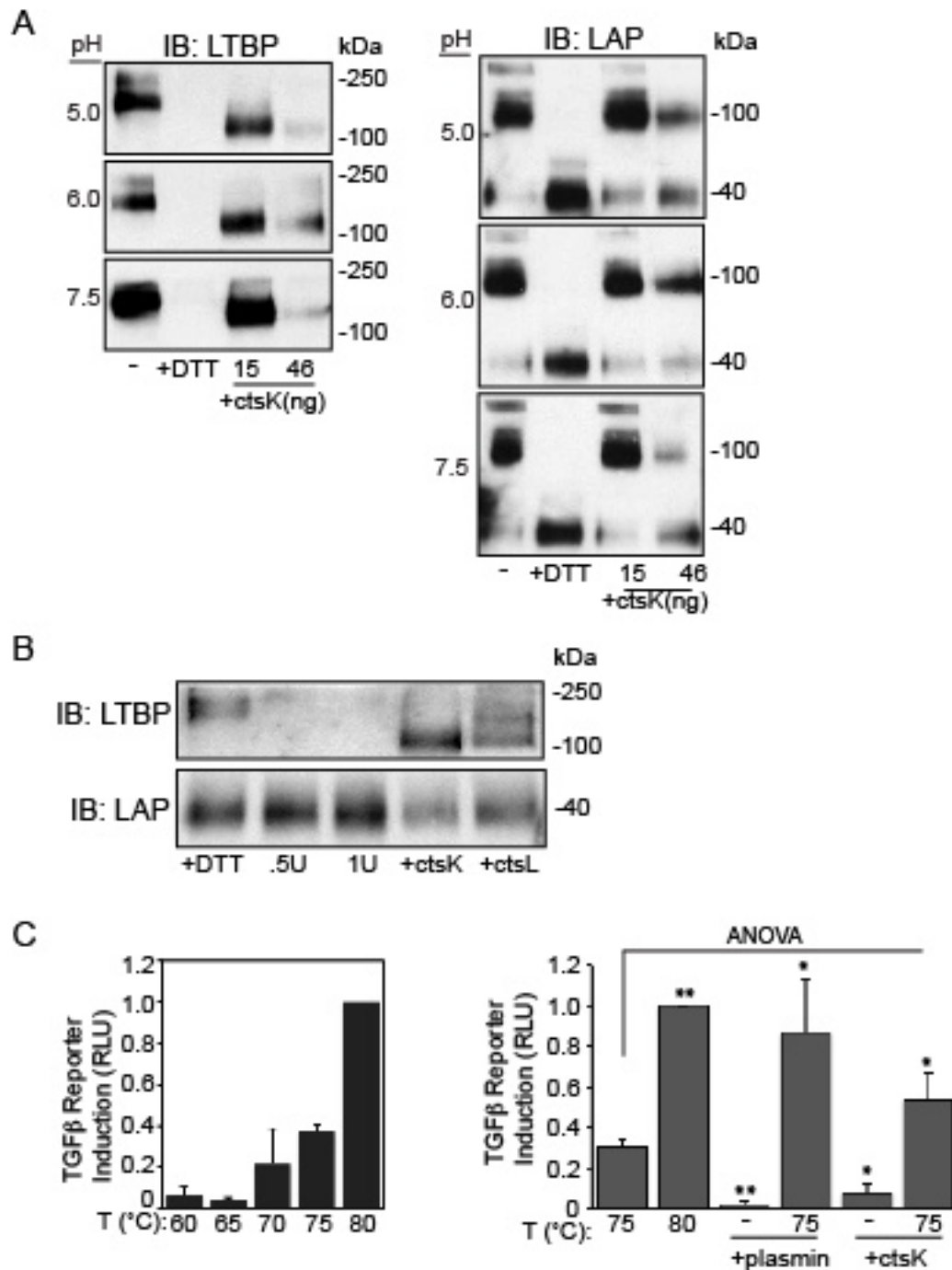


**Figure 2.3 CTSK lowers the activation barrier for TGFβ ligand liberation from the Large Latent Complex (LLC).** (A) Immunoblot of LTBP (non-reducing antibody) and LAP after CTSK digestion of LLC. n=4 experiments. (B) LTBP (reducing antibody) and LAP immunoblots of LLC digestions by plasmin, CTSK, and CTSL. n=4 experiments. (C) Luciferase induction of TGFβ reporter cells following heat treatment and or pre-activation of LLC by plasmin or CTSK. n=4 experiments.

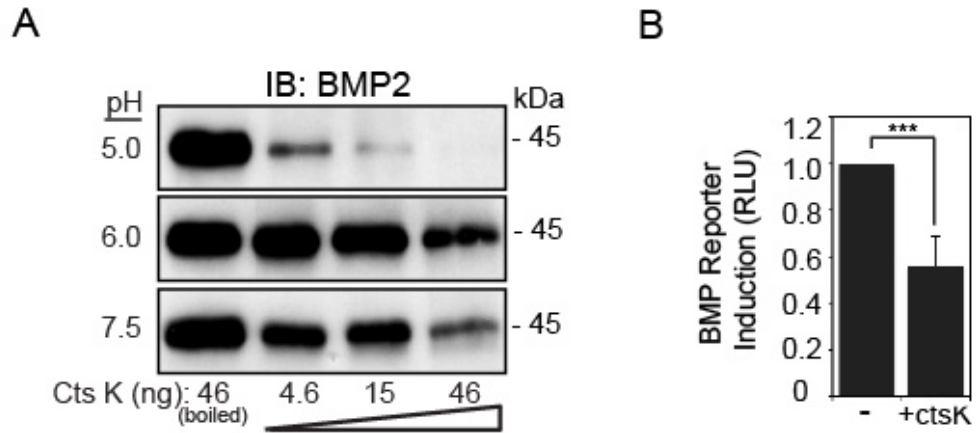


**Figure 2.4 CTSK degrades proBMP2.** (A) Immunoblot of BMP2 following CTSK digestion of proBMP2. n=4 experiments. (B) Luciferase induction of BMP reporter cells using CTSK digested proBMP2 n=3 experiments.

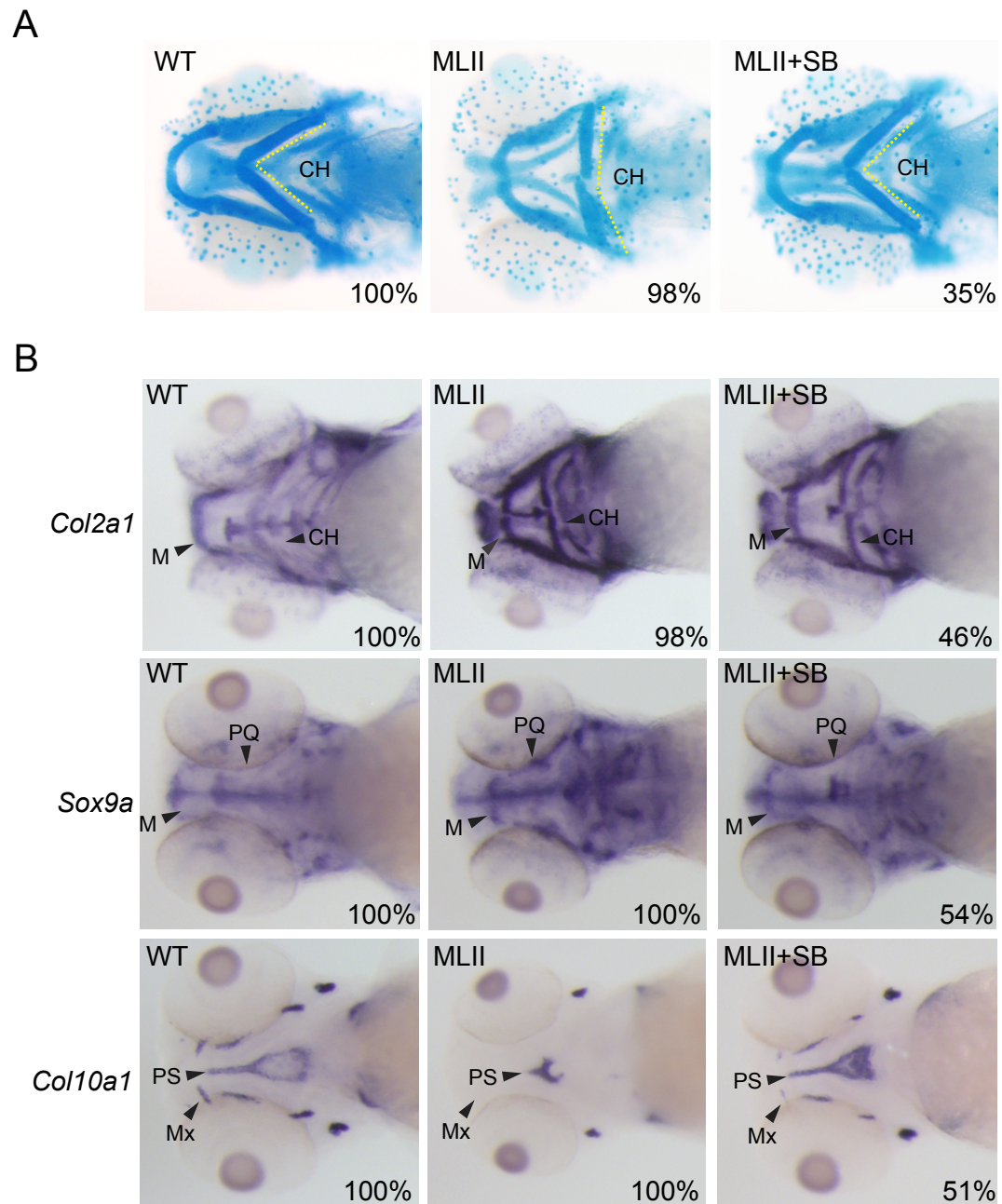
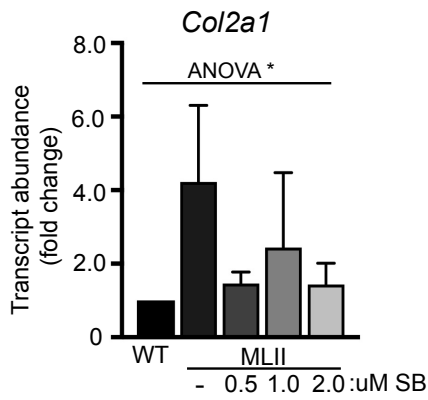
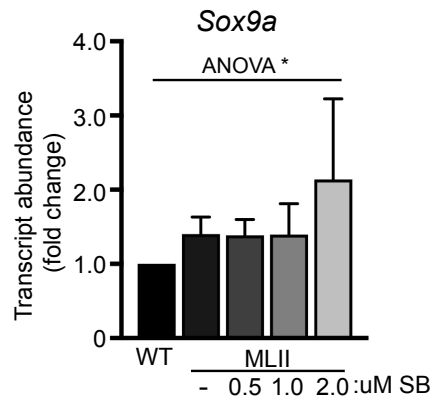


**Figure 2.5 Pharmacological inhibition of TGF $\beta$  in ML-II embryos rescues craniofacial morphology and chondrogenesis markers.** (A) Alcian blue staining of 4dpf WT, ML-II, and ML-II SB505124 treated embryos. Percentage values indicate the percentage of embryos that resemble the photograph. CH – ceratohyal. n=40. (B) In situ hybridization of *col2a1*, *sox9a*, and *col10a1* in 4dpf WT, ML-II, and ML-II treated with SB505124. M – Meckel’s cartilage; PQ – palatoquadrate; PS – parasphenoid; Mx – maxilla. n>50.

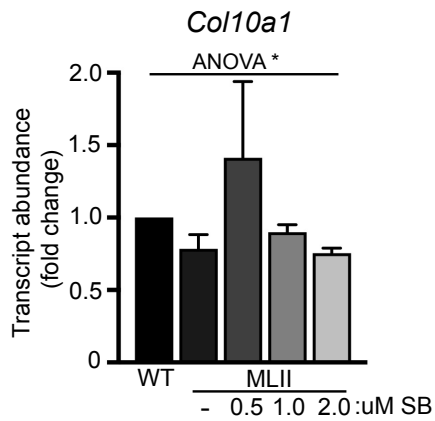
A



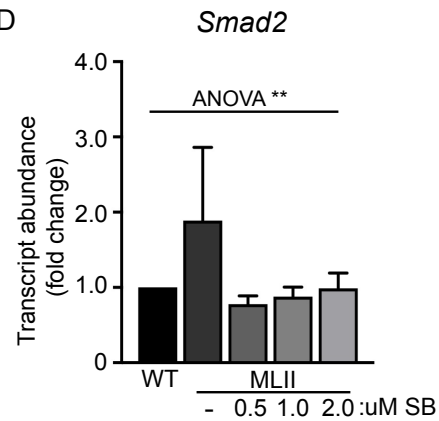
B



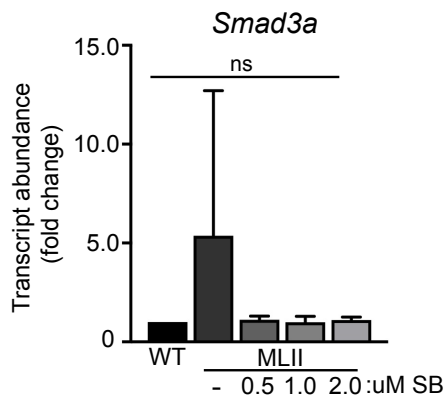
C



D



E



F

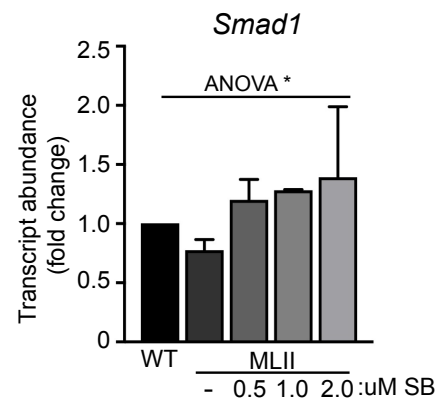


**Figure 2.6 TGF $\beta$  reduction in MLII embryos rescues TGF $\beta$  and BMP dependent genes and effectors.** (A) *Col2a1* (B) *sox9a* (C) *coll10a1* (D) *smad2* (E) *smad3a* (F) *smad1*, qPCR of 4dpf WT and ML-II embryos treated with three concentrations of SB505124. n=15 embryos/sample, at least 4 experiments. RPL4 was used as a normalizer. Transcript abundance is represented as a Log2 scale. \* p < 0.05, \*\* p < 0.01, \*\*\* p < 0.001.

**CHAPTER 3: ALTERED MET RECEPTOR PHOSPHORYLATION AND LRP1  
MEDIATED UPTAKE IN CELLS LACKING CARBOHYDRATE-DEPENDENT  
LYSOSOMAL TARGETING**

Megan Aarnio-Peterson, Peng Zhao, Courtney Christian, Seok-Ho Yu, Heather Flanagan-Steet, Lance Wells, and Richard Steet. Submitted to The Journal of Biological Chemistry 2017.

## ABSTRACT

Acid hydrolases utilize a carbohydrate-dependent mechanism for lysosomal targeting. These hydrolases acquire a mannose 6-phosphate tag by the action of the GlcNAc-1-phosphotransferase enzyme, allowing them to bind receptors and traffic to endosomes. Loss of GlcNAc-1-phosphotransferase results in hydrolase hypersecretion and profound lysosomal storage. Little, however, is known about how these cellular phenotypes affect the trafficking and localization of surface glycoproteins. To address this question, we profiled the abundance of surface glycoproteins in WT and CRISPR-mediated GNPTAB<sup>-/-</sup> HeLa cells and identified changes in numerous glycoproteins, including reduced levels of LRP1 and elevated abundance of multiple receptor tyrosine kinases. Decreased cell surface LRP1 in GNPTAB<sup>-/-</sup> cells corresponded with a reduction in its steady-state level and less Ab40 peptide uptake. GNPTAB<sup>-/-</sup> cells also displayed elevated activation of several kinases including Met receptor. We found increased Met phosphorylation, altered expression of Met-responsive genes and partial localization of the phosphorylated receptor to lysosomes. Deactivation of Met signaling is regulated by protein-tyrosine phosphatases such as PTPRJ, which showed reduced surface abundance in GNPTAB<sup>-/-</sup> cells. Moreover, lower concentrations of pervanadate were needed to cause an increase in phospho-Met in GNPTAB<sup>-/-</sup> cells, suggesting decreased phosphatase activity. GNPTAB<sup>-/-</sup> cells exhibited elevated levels of reactive oxygen species, known to inactivate phosphatases by oxidation of active site cysteine residues. Consistent with this mechanism, peroxide treatment of parental HeLa cells elevated phospho-Met levels while antioxidant treatment of GNPTAB<sup>-/-</sup> cells

**reduced phospho-Met levels. Collectively, these data identify new mechanisms whereby impaired lysosomal targeting can impact the activity and recycling of receptors.**

## **INTRODUCTION**

Soluble acid hydrolases are targeted to the lysosome via a carbohydrate dependent mechanism. This mechanism involves the addition of mannose 6-phosphate (M6P) tags on the N-glycans of newly made hydrolases by the heterohexameric enzyme, UDP-GlcNAc:lysosomal enzyme N-acetyl-glucosamine-1-phosphotransferase (GlcNAc-1-phosphotransferase; encoded by GNPTAB and GNPTG genes) (1,2). The GNPTAB gene encodes the  $\alpha/\beta$  subunits of the enzyme, involved in both hydrolase recognition and catalysis, while the GNPTG gene encodes the  $\gamma$  subunit, which plays a role in facilitating efficient mannose phosphorylation and enzyme stability (3-10). Defects in GNPTAB and GNPTG cause the lysosomal diseases, MLII, MLIII  $\alpha/\beta$ , and MLIII  $\gamma$ , characterized by hypersecretion of hydrolases, profound lysosomal storage in many mesenchymal cell types and a broad spectrum of clinical manifestations (3,11,12). The majority of lysosomal enzymes reach the lysosome via M6P dependent targeting but additional tissue and cell type specific mechanisms of carbohydrate independent sorting have been shown to exist (13). Lysosomal hydrolases can also be targeted to lysosomes via secretion and recapture. Receptors including LDLR and LRP1 have been implicated in trafficking of nonphosphorylated cathepsin D and B, and can function in the absence of GlcNAc-1-phosphotransferase (14).

While lysosomal storage remains the hallmark of the MLII, relatively little is known about how the localization and function of cell surface glycoproteins is affected upon the loss of lysosomal targeting. Several studies have reported abnormal recycling and trafficking of cell surface glycoproteins in cells with lysosomal storage (15-19). These trafficking defects can arise from multiple potential mechanisms, including the secondary storage of glycolipids or other molecules that interfere with the vesicle trafficking machinery or alter processes such as endocytosis or autophagy. Endosomal accumulation of glycoproteins was directly linked to abnormal recycling caused by cholesterol storage (15). Cell surface glycoproteins are also susceptible to the action of extracellular glycosidases, which mediate cell surface glycoprotein turnover (20). Thus, higher levels of secreted glycosidases in GNPTAB<sup>-/-</sup> cells due to loss of M6P targeting may result in increased processing and altered cell surface residence of glycoproteins by impacting their interaction with galectins or other factors (21,22). Defining these mechanisms is likely to provide important new clues to the molecular pathogenesis of lysosomal diseases.

In this study, we took advantage of chemical glycobiology methods to profile the abundance of cell surface glycoproteins in parental and CRISPR-mediated GNPTAB<sup>-/-</sup> HeLa cells in an effort to identify how loss of M6P-dependent lysosomal targeting impacts these glycoproteins. Our findings reveal changes in multiple cell surface glycoproteins, including reduced levels of the uptake receptor LRP1 and elevated abundance of multiple receptor tyrosine kinases. Characterization of the functional consequences and molecular basis for these changes revealed new mechanisms of action

whereby loss of lysosomal targeting and lysosomal storage alter receptor activity and receptor-mediated uptake.

## RESULTS

### **SEEL-based profiling of GNPTAB<sup>-/-</sup> HeLa cells reveals altered cell surface residence of multiple glycoprotein receptors.**

To address how loss of lysosomal hydrolase targeting affects cell surface sialoglycoproteins, their abundance was profiled in parental HeLa, GNPTG<sup>-/-</sup> and GNPTAB<sup>-/-</sup> cells using one-step selective exo-enzymatic labeling (SEEL) with the sialyltransferase ST6Gal1 (7,23,24). Cells were labeled with recombinant rat ST6Gal1 and biotinylated CMP-sialic acid in the presence or absence of neuraminidase and lysates analyzed by Western blot. Differences were noted in the profile of the major labeled glycoproteins, with the most striking changes noted between parental HeLa and GNPTAB<sup>-/-</sup> cells (**Figure 1A**). Higher reactivity was detected in GNPTAB<sup>-/-</sup> cells treated without neuraminidase, likely reflecting an increase in free terminal galactose acceptors. GNPTAB<sup>-/-</sup> cells also exhibited greater heterogeneity and increased mobility of the major labeled glycoproteins in the presence of neuraminidase.

Following neuraminidase-coupled SEEL, biotinylated glycoproteins were enriched by immunoprecipitation, resolved by SDS-PAGE and subjected to proteomic analysis by LC-MS-MS (**Figure 1B**). In light of the differences noted in the profile of labeled glycoproteins, we focused the proteomic analysis on the parental and GNPTAB<sup>-/-</sup> HeLa cells. Unlabeled HeLa and GNPTAB<sup>-/-</sup> cells were subjected to the same

enrichment procedure to control for glycoproteins that might be pulled down in a non-specific manner. A total of 211 proteins were identified across two biological replicates, with substantial overlap (>75%) observed between the parental and GNPTAB<sup>-/-</sup> lines (**Figure 1C**; see Table S1). Consistent with the ability of SEEL to only modify glycoproteins at the cell surface, the vast majority of assigned proteins were known cell surface glycoproteins including receptors, cell adhesion proteins and ion channels. For the most abundant glycoproteins, fold change between GNPTAB<sup>-/-</sup> and parental HeLa cells was plotted using a log<sub>2</sub> scale (**Figure 1D**). These data demonstrate lower cell surface abundance of multiple glycoproteins including the uptake receptor LRP1, the mucin MUC16 and receptor tyrosine phosphatases (PTPRK and PTPRJ). Increased abundance of several receptor tyrosine kinases (AXL, MET, EPH2A) and adhesion proteins (ITGB4, L1CAM, MCAM) was also noted in GNPTAB<sup>-/-</sup> cells.

#### **GNPTAB<sup>-/-</sup> cells exhibit reduced LRP1-dependent uptake.**

SEEL analysis identified a significant decrease in the LRP1 receptor on the cell surface of GNPTAB<sup>-/-</sup> cells (**Figure 1D**). This was of interest due to its proposed role in M6P-independent uptake and acid hydrolase sorting (14). To confirm LRP1's cell surface reduction, labeled lysates were immunoprecipitated with anti-biotin and LRP-1 subsequently analyzed by immunoblot (**Figure 2A**). These results show that the majority of LRP1 is present at the cell surface in the parental HeLa cells but less LRP1 is detected in both the input and eluted fractions of the GNPTAB<sup>-/-</sup> cells. This indicates that the reduced cell surface abundance of LRP1 in these cells likely stems from lower overall levels of this protein. The electrophoretic mobility of LRP1 was also increased in

GNPTAB<sup>-/-</sup> cells possibly reflecting abnormal glycan or protein processing. RT-PCR was performed next to ask whether this decrease corresponded with reduced transcript abundance but no differences were noted (**Figure 2B**). LRP1 not only mediates uptake and clearance of amyloid peptides in the brain (25-28), it also plays a role in M6P-independent recapture of lysosomal hydrolases. Therefore, decreased abundance of LRP1 may further exacerbate the cellular storage phenotype. To assess whether reduced LRP1 affects ligand uptake in GNPTAB<sup>-/-</sup> cells, we performed uptake assays using a fluorescently labeled b-amyloid peptide (AF647-Ab40). Parental HeLa and GNPTAB<sup>-/-</sup> cells were incubated with AF647-Ab40 overnight and peptide uptake measured in cell lysates. Consistent with LRP1's lower surface abundance, relative fluorescent units were 35% lower in GNPTAB<sup>-/-</sup> lysates (**Figure 2D**).

### **Increased phosphorylation of receptor tyrosine kinases was observed in GNPTAB<sup>-/-</sup> HeLa cells.**

SEEL-based proteomics also identified increased cell surface abundance of multiple receptor tyrosine kinases in GNPTAB<sup>-/-</sup> cells (**Figure 1D**). Using a phospho-receptor tyrosine kinase (RTK) array, we asked whether the increased cell surface abundance corresponded with altered receptor activation. As shown in **Figure 3A**, numerous RTKs – including several detected at elevated surface levels by SEEL - exhibited increased phosphorylation in GNPTAB<sup>-/-</sup> cells, suggesting increased activation and/or sustained activity. Quantification by densitometry of three independent runs demonstrated a 2-3-fold increase in the phosphorylation of c-Met, EphA7, EphB2, and Axl in the GNPTAB<sup>-/-</sup> (**Figure 3B**). Although SEEL labeling indicated more cell

surface EGFR, its activation was not significantly affected in GNPTAB<sup>-/-</sup> cells. Further, FGFR1, FGFR3, and insulin receptor were not detected on the surface of the cells using SEEL, but did display increased phosphorylation in GNPTAB<sup>-/-</sup> cells. Because c-Met showed both the largest difference in signal, and the largest difference in cell surface abundance between these between HeLa and GNPTAB<sup>-/-</sup>, the molecular basis for this elevation was explored in greater depth.

**GNPTAB<sup>-/-</sup> and GNPTG<sup>-/-</sup> exhibit increases in the steady-state level and phosphorylation of Met receptor.**

Western blot analysis of whole cell lysates demonstrated very low levels of Met receptor phosphorylation in parental HeLa cells while this was increased in both GNPTG<sup>-/-</sup> and GNPTAB<sup>-/-</sup> cells (**Figure 4A**). Quantitative analysis of Met and phospho-Met levels showed that Met levels were increased by nearly 3-fold in GNPTAB<sup>-/-</sup> cells compared to the parental HeLa line but phospho-Met levels were increased over 125-fold, indicating a high level of activation and/or sustained activity of this receptor (**Figure 4B**). An intermediate increase in Met receptor and phosphorylated Met receptor were noted in GNPTG<sup>-/-</sup> suggesting a relationship between Met receptor activation and the degree to which lysosomal targeting is impaired. Increased abundance of the Met receptor at the cell surface in GNPTAB<sup>-/-</sup> cells was confirmed by SEEL labeling followed by biotin immunoprecipitation and immunoblotting (**Figure 4C**). To examine the subcellular localization of phospho-Met, parental and GNPTAB<sup>-/-</sup> cells were immunohistochemically stained for Lamp1 and phospho-Met and analyzed by confocal microscopy. Phospho-Met was readily detected in both Lamp1 positive and negative

vesicular structures in GNPTAB<sup>-/-</sup> but not parental HeLa cells (**Figure 4D**). The substantial overlap between phospho-Met and the lysosomal marker Lamp1 in the GNPTAB<sup>-/-</sup> cells suggested a portion of phospho-Met localizes to this compartment. Because a detectable portion of phospho-Met was present in Lamp1-negative vesicles, we asked whether the increase in Met receptor phosphorylation correlated with an increase in the expression of Met-responsive genes (**Figure 4E**). The transcript abundance of ITGB1, a known Met-responsive gene (29), was increased 31% in GNPTAB<sup>-/-</sup>. Further, the transcript abundance of EPHX2 (whose expression is known to be negatively regulated by Met activity (30)) was decreased by 60%.

**GNPTAB<sup>-/-</sup> cells have decreased phosphatase activity towards Met and increased reactive oxygen species.**

Elevated Met receptor phosphorylation suggests its activity is sustained in the GNPTAB<sup>-/-</sup> cells whereas it is effectively deactivated in the parental HeLa cells. Met activity is partially regulated by the dephosphorylation of specific tyrosine residues on its C-terminus by protein-tyrosine phosphatases, such as PTPRJ/Dep-1 (31). Several protein-tyrosine phosphatases known to act on Met were detected following SEEL and proteomics in parental HeLa and GNPTAB<sup>-/-</sup> cells (PTPRJ and PTPRF) (**Figure 1D**). Notably, the primary phosphatase believed to downregulate Met activity, PTPRJ/Dep-1, was less abundant on the cell surface of GNPTAB<sup>-/-</sup> cells. To assess whether a reduction of phosphatase activity differentially impacts Met phosphorylation, cells were treated with increasing concentrations of the general phosphatase inhibitor pervanadate and immunoblotting for phospho-Met and Met receptor performed. As shown in **Figure 5A**,

inhibition of global phosphatase activity resulted in increased phospho-Met levels in all cell types but lower amounts of pervanadate were needed to raise phospho-Met levels in GNPTAB<sup>-/-</sup> cells, suggesting that less protein-tyrosine phosphatase activity. The ratio of phospho-Met to Met receptor was quantified in **Figure 5B**. Roughly the same ratio increase was noted at 1 μM in GNPTAB<sup>-/-</sup> as was seen at 10 μM in the parental HeLa cells supporting the idea that less active phosphatase is present to deactivate Met in GNPTAB<sup>-/-</sup>.

The maturation and cell surface residence of phosphatases has been linked to their enzymatic activation. High levels of reactive oxygen species (ROS) are known to inactivate many protein-tyrosine phosphatases (32-35). Oxidative inactivation of the catalytic cysteine corresponds with altered cell surface delivery and activity. Many lysosomal storage diseases are known to exhibit increased cellular ROS due to lysosomal storage and improper breakdown of mitochondria (36,37). Thus, elevated ROS in the GNPTAB<sup>-/-</sup> cells may account in part for the increase in phospho-Met levels. Using a fluorescent indicator of intracellular ROS, we examined ROS levels and found that GNPTAB<sup>-/-</sup> cells have a 50% increase in ROS compared to parental HeLa (**Figure 5C**). We next asked whether short-term treatment of parental HeLa cells with hydrogen peroxide (at concentrations previously shown to inactivate phosphatases and increased kinase phosphorylation (33)) was sufficient to elevate Met receptor phosphorylation. Hydrogen peroxide treatment was capable of increasing Met receptor phosphorylation in a dose-dependent manner with no appreciable change in Met receptor levels (**Figure 5D**), suggesting ROS-mediated inactivation of phosphatases is sufficient to raise phospho-Met levels in the parental HeLa line. Lastly, to assess whether increases in ROS are linked to

increases in phospho-Met levels in GNPTAB<sup>-/-</sup>, these cells were treated with the antioxidant Trolox for 96 hours followed by immunoblotting for phospho-Met and Met (**Figure 5E**). Trolox treatment consistently reduced phospho-Met levels in GNPTAB<sup>-/-</sup> cells without substantially altering Met receptor levels.

Lastly, we attempted to rescue GNPTAB<sup>-/-</sup> cells with WT GNPTAB cDNA to ask whether the biochemical alterations, including increased Met receptor activation, in the CRISPR-mediated knockout cells was specific to loss of lysosomal targeting. The glycosidases b-galactosidase and b-hexosaminidase are mannose 6-phosphorylated and trafficked to the lysosome in parental HeLa cells but not in GNPTAB<sup>-/-</sup> as evidenced by the reduction in intracellular activity of both glycosidases (**Figure 6A**). Following 120 hours of transient transfection, the intracellular glycosidase activities were measured to ensure that WT GlcNAc-1-phosphotransferase was functionally expressed. As shown in **Figure 6A**, transfection with WT GNPTAB increased intracellular glycosidase to near normal levels despite only an estimated 30-35% transfection efficiency. It is likely that the overexpression of WT GNPTAB results in hydrolase targeting to a greatly increased number of lysosomes in the GNPTAB<sup>-/-</sup> cells, thus exaggerating the effects of transient GNPTAB expression. We next asked whether the partial restoration of lysosomal targeting was sufficient to reduce Met receptor phosphorylation (**Figure 6B**). GNPTAB expression slightly lowered Met receptor phosphorylation in the GNPTAB<sup>-/-</sup> cells but this difference was not statistically significant in replicate experiments. Of note, levels of LAMP1 were also slightly reduced which indicates that transient GNPTAB expression may not be capable of fully reducing lysosomal storage in the transfected cell population.

## DISCUSSION

In this study, we expand the molecular phenotypes in GNPTAB-deficient cells to include altered receptor activity and uptake. Taking advantage of selective cell surface labeling to profile differences in the residence of sialoglycoproteins, we identified altered abundance of multiple receptors and cell adhesion molecules, including the sorting receptor LRP1 and the receptor tyrosine kinase, Met, on the surface of GNPTAB<sup>-/-</sup> cells. Our subsequent analysis of Met revealed an unexpected increase in its phosphorylation status. The mechanisms that underlie this phenotype were investigated, revealing a loss in the ability to deactivate Met, most likely due to ROS-mediated inactivation of protein tyrosine phosphatases and altered residence of receptor and phosphatase at the cell surface.

Prior work in MLII fibroblasts identified numerous alterations at the cellular levels when lysosomal targeting is impaired (16,38). For example, Otomo and colleagues demonstrated impaired endocytosis and receptor recycling in MLII fibroblasts that could be partially rescued by a total enzyme replacement strategy. This suggests that some of the differences in the cell surface abundance of receptors in the GNPTAB<sup>-/-</sup> HeLa cells may arise due to storage-dependent effects on receptor internalization and/or trafficking. Moreover, autophagic flux and mitochondrial defects were also detected in the MLII fibroblasts, which may explain the increase in ROS within the GNPTAB<sup>-/-</sup> HeLa cells. Impaired autophagy could allow damaged mitochondria to persist in these cells, providing a source of damaging ROS. One of the proteins exhibiting the greatest decrease in abundance at the cell surface of GNPTAB<sup>-/-</sup> cells was the sorting receptor

LRP1. This decrease corresponded with a functional reduction in uptake and internalization of its ligand AB40. Although the mechanistic basis for the decreased residence of this receptor is unclear, lower levels of LRP1 may reflect a recycling problem in these cells, consistent with effects on receptor recycling noted in other storage disease cells (15,17,19).

LRP1 has been shown to play a role in the reuptake of non-phosphorylated lysosomal hydrolases, although the steady-state levels of this receptor were not affected in mouse embryonic fibroblasts. It is plausible that reduction in its surface levels in some MLII cell types could potentiate lysosomal storage by preventing efficient recapture of secreted hydrolases. Further indication of reduced LRP1 as a disease modifier is evidenced in neurodegeneration and Alzheimer's disease (AD) pathology (39-41). LRP1 serves an essential role in brain lipid metabolism and loss of LRP1 leads to altered brain lipid homeostasis, causing global changes in brain function. Amyloid-beta, which is the main pathogenic molecule that accumulates in AD brains, is typically cleared by LRP1. Work by several groups suggests that reduction or inactivation of LRP1 leads to a decrease in amyloid-beta efflux across the blood-brain barrier (26,28,39). Interestingly, amyloid-beta induced oxidative modification of LRP1 can mediate LRP1 dysfunction (42). Since GNPTAB<sup>-/-</sup> cells exhibited increases in ROS, it is possible that the functional loss of LRP1 may be related to oxidative stress. We did not however detect any consistent elevation in LRP1 protein following treatment of GNPTAB<sup>-/-</sup> cells with the antioxidant Trolox.

Oxidative stress is a consequence of lysosomal storage, which can be caused by improper degradation of defective cellular components or organelles such as

mitochondria and can lead to many negative effects (37). Cellular increases in ROS affect the activity of protein tyrosine phosphatases by inactivation of the catalytic cysteine (33). The protein-tyrosine phosphatase, PTPRJ or Dep-1, has been shown to be susceptible to this kind of oxidative inactivation (32). SEEL followed by proteomics identified decreased abundance of Dep-1 in the GNPTAB<sup>-/-</sup> cells. Met receptor tyrosine kinase and its adaptor protein Gab1 are known substrates of Dep-1 (31). Thus it is possible that under the oxidative conditions in GNPTAB<sup>-/-</sup> cells, Dep-1 or other phosphatases are partially inactivated and unable to dephosphorylate Met, leading to sustained Met phosphorylation. This also provides a potential mechanism to explain the general increase in RTK phosphorylation that was noted upon loss of lysosomal targeting, although phosphorylation of EGFR, another Dep-1 substrate, was not affected. The relatively robust level of EGFR phosphorylation in both the parental and GNPTAB<sup>-/-</sup> HeLa cells could reflect constitutive activation of this receptor in the HeLa background or a high level of receptor ligand in the culture media.

The involvement of phosphatases may explain changes in cell surface abundance of other glycoproteins including cell adhesion molecules. For example, PTPRJ/Dep-1 and PTPRF have been shown to regulate integrin activation and recycling, respectively (43,44). Thus, a decrease in phosphatase activity or availability could lead to altered surface residence of these proteins. The detection of phosphorylated Met in the lysosome of the GNPTAB<sup>-/-</sup> cells suggests that this form of the receptor may traffic to this organelle and then fail to turnover due to a lack of necessary hydrolases and/or phosphatases. Nonetheless, the effects of sustained Met phosphorylation could be observed upon the expression of at least two Met-responsive genes so it is likely that at

least some of the phospho-Met is functionally active. The increase in Met phosphorylation may ultimately derive from a combination of decreased phosphatase-dependent inactivation and terminal storage of activated receptor in lysosomes.

Another intriguing possibility to consider is the fact that Met receptor levels are increased as a protective effect against oxidative stress. Work by several groups has shown that loss of c-Met in cells, particularly hepatocytes, results in loss of redox homeostasis and an acceleration of ROS-mediated damage (30,45-48). Thus, increased Met receptor expression or activity may reflect a compensatory response by the GNPTAB<sup>-/-</sup> cells to mitigate the impact of higher ROS levels.

Despite restoring glycosidase levels back to near normal levels, we were unable to achieve substantial rescue of the Met phosphorylation following introduction of WT GNPTAB. This is mostly likely attributed to the inability of transient GNPTAB transfection to correct the storage phenotype in these cells, as evidenced by only a slight decrease in LAMP1 levels following transfection, and to the low transfection efficiency of the large GNPTAB cDNA. An initial concern of ours was the possibility that elevated Met receptor activity was a result of clonal selection following CRISPR-Cas editing in the HeLa cells. The observation of an intermediate increase in phospho-Met levels in the GNPTG<sup>-/-</sup> cells makes this unlikely in our view and instead suggests that the effect on Met phosphorylation is tied directly (through trapping in this organelle) or indirectly (through ROS production) to the degree of lysosomal storage.

This study highlights another example whereby impaired lysosomal targeting leads to increased signaling of cell surface receptors. Studies in model organisms including zebrafish have identified increased TGF $\beta$  signaling as a function of the direct

action of secreted hydrolases on latent growth factors deposited within the ECM of tissues like cartilage (49). The present evidence for increased Met receptor activation appears to point instead to an intracellular mechanism of action. It is intriguing to speculate that ROS generation in lysosomes not only inactivates protein tyrosine phosphatases in the cytosol but may also reduce phosphatases in this compartment. This might explain why Met remains phosphorylated even after reaching the lysosome. The present study also highlights the ability of SEEL to identify changes in the abundance of cell surface glycoproteins and generate leads for further analysis. There are several candidates of interest for investigation including the wide range of cell adhesion molecules with altered abundance and/or expression in the GNPTAB<sup>-/-</sup> cells. Future studies will be focused on understanding whether altered glycan processing of cell surface glycoproteins by secreted glycosidases contribute to altered surface residence.

## **EXPERIMENTAL PROCEDURES**

**Reagents** – Recombinant rat  $\alpha$ -(2,6)-sialyltransferase (ST6Gal1) was prepared as previously published (50). CMP-sialic acid biotin was synthesized as previously reported (23). *Vibrio cholerae* neuraminidase (type II) (N6514) and protein G sepharose fast flow beads (P3296) were purchased from Sigma Aldrich. Alkaline phosphatase (FastAP) (EF0651), protease inhibitor mixture tablet (88666), and mass spectrometry compatible silver staining kit (24600) were purchased from Thermo Scientific. IgG fraction mouse monoclonal anti-biotin with or without HRP conjugation were purchased from Jackson Immuno Research (200-032-211, 200-00-211). Rabbit monoclonal anti-LRP1 was

purchased from Abcam (ab92544). Monoclonal rabbit anti-Met (DIC2) and rabbit anti-phospho-Met (Tyr1234/1235) (D26) were purchased from Cell Signaling Technology (8198 and 3077). For cellular uptake assays, human b-amyloid peptide (1-40), HiLyte Fluor 647-labeled was purchased from Anaspec (AS-60493), and was reconstituted in 100% DMSO at 500 $\mu$ M. The cell permeable vitamin E derivative, Trolox, was purchased from Enzo Scientific (AXL-270-267).

**Cell Lines and Culture** – GNPTG<sup>-/-</sup> and GNPTAB<sup>-/-</sup> HeLa cells were generously provided by Stuart Kornfeld (Washington University School of Medicine, St Louis, MO), and were generated by CRISPR/Cas9 genome editing (7). Cells were cultured in DMEM media with 4.5g/L glucose and L-glutamine (Lonza 12-604F) and supplemented with 10% fetal bovine serum (Seradigm 1500-500), and penicillin (100 IU/ml)/streptomycin (100  $\mu$ g/ml) (Corning 30-001-CI). Cells were cultured in a 5% CO<sub>2</sub> atmosphere, 37°C humid incubator.

**SEEL and proteomics** - *One-Step SEEL and proteomics* - Cell surface labeling was performed in serum free DMEM with 42  $\mu$ g/mL ST6Gal1 and 100  $\mu$ M CMP-Sia-C5-biotin, 12  $\mu$ L of BSA (2 mg/mL), 12  $\mu$ L of alkaline phosphatase, with or without 6  $\mu$ L of *Arthrobacter ureafaciens* (AU) neuraminidase for 2 h at 37 °C in total 1.8 mL of volume per 10 cm plate of confluent cells. After lysis of the labeled cells on plate with RIPA buffer, immunoprecipitation of 800  $\mu$ g of lysate was performed with anti-biotin antibody followed by SDS-PAGE, silver-stain, and in-gel digestion of proteins. Proteomic analysis was performed exactly as described previously (23).

**Western Blotting, Immunoprecipitation, and Phospho-Receptor Tyrosine Kinase Assay** – Cells were washed with DPBS and then lysed on ice with lysis buffer 17

(phospho-RTK kit) supplemented with protease inhibitor mixture. Lysed cells were centrifuged at 14,000 rpm for 8 minutes and the supernatant was removed and saved. Protein concentration was determined using the Micro BCA Protein Assay Kit (Thermo Scientific 23235). Immunoprecipitation with anti-biotin antibody coated protein G beads was performed as previously reported (24). Proteins were separated by SDS-polyacrylamide gels (161-0148), and transferred to 0.45  $\mu$ m nitrocellulose membranes (162-0115). Membranes were blocked with 5% non-fat dry milk in tris buffered saline plus 0.1% Tween 20 or with 5% bovine serum albumin in Tris buffered saline plus 0.1% tween 20 in the case of phospho-Met immunoblotting. Immunoreactive bands were identified with SuperSignal West Pico Chemiluminescent Substrate (Thermo Scientific 34080) and imaged and quantified using a Bio-Rad ChemiDoc MP imaging system. Human Phospho-RTK Arrays were performed according to manufacturer's instructions (R&D Systems ARY001B).

**Reverse transcriptase PCR and quantitative reverse transcriptase PCR** – For RT-PCR, RNA was extracted using Trizol (Life Technologies, cat# 15596026) from trypsinized cell pellets. For qPCR, RNA was extracted from cell pellets using a Qiagen RNeasy Plus Kit (cat#74134). cDNA was prepared using Quanta qScript XLT cDNA SuperMix (cat#95161). Thermo Scientific PCR Master Mix (2X) (K0171) was used for RTPCR reactions and Quanta PerfeCta Sybr Green FastMix (cat#95072). The primers used for RT-PCR or qPCR are shown in Table S2.

**b-Amyloid-40 uptake assay** –  $1 \times 10^4$  cells were plated per well in a 96-well tissue culture dish, and allowed to adhere overnight. The following day, cells were treated with 2 $\mu$ M human b-amyloid peptide (1-40), HiLyte Fluor 647-labeled (Anaspec) or DMSO in

complete DMEM growth media for 16 hours in 5% CO<sub>2</sub> atmosphere, 37°C humid incubator. Following 16 hours of incubation, media was removed and cells were rinse twice with DPBS. Cells were then lysed in RIPA buffer and fluorescence was read using a Synergy plate reader.

**Confocal Immunofluorescence Microscopy** – 6 X 10<sup>4</sup> cells were plated on gelatin coated coverslips in 12-well plates one day prior to staining. Immunofluorescence staining was performed according to manufacturer's instructions (Cell Signaling Technology), but 0.15% Triton X-100 was used instead of 0.3%.

**Pervanadate and Trolox treatment** – 6 X 10<sup>4</sup> cells were plated in 12-well plates one day prior to treatment. Cells were incubated for 20 minutes at 37°C with 1 μM, 5 μM, or 10 μM of pervanadate. Following treatment, cells were rinse and SDS-PAGE and Western blotting were performed as described. For Trolox experiments, cells were plated at 50% confluence and treated with 5 μM of Trolox dissolved in DMSO. Trolox incubations were performed for 96 hours, with media change and Trolox replacement after 48 hours, followed by Western blot analysis.

**Analysis of Cellular ROS Levels** – Reactive oxygen species (ROS) levels were determined using the ROS indicator dye carboxy-H<sub>2</sub>DCFDA. Cells were seeded at 75% confluence one day prior to ROS measurement. 2mM carboxy-H<sub>2</sub>DCFDA in DMSO was prepared fresh before each experiment. Cells were trypsinized and resuspended in DMEM containing 0.1% BSA and incubated with 20 μM carboxy-H<sub>2</sub>DCFDA for 45 minutes in a rocking 37°C chamber. Cells were quickly pelleted and resuspended in DPBS and ROS levels were read using a Synergy plate reader.

**Rescue Experiments with WT GlcNAc-1-phosphotransferase – GNPTAB<sup>-/-</sup>** HeLa cells were transfected with 1 $\mu$ g of WT GlcNAc-1-phosphotransferase using Lipofectamine 3000 (Invitrogen) several hours after plating at 75% confluence in 6-well plates. Following overnight incubation, transfection media was removed and replaced with fresh growth media. Enzyme assays or SDS-PAGE and Western blotting were performed 120 hours after transfection.

## **ACKNOWLEDGEMENTS**

This work was supported by grants from the National Institutes of Health (GM086524 and GM107012) and the Yash Gandhi Foundation. We are grateful to Dr. Stuart Kornfeld (Washington University in St. Louis) for providing the GNPTAB<sup>-/-</sup> and GNPTG<sup>-/-</sup> HeLa cell lines and to Dr. Frederick Domann (University of Iowa-Carver College of Medicine) for advice analyzing ROS levels in cells. We wish to acknowledge Dr. Kelley Moremen's laboratory for providing recombinant ST6Gal1 and the laboratory of Dr. Geert-Jan Boons for the CMP-sialic acid-biotin reagent.

## **CONFLICT OF INTEREST**

The authors declare that they have no conflicts of interest with the contents of this article.

## **AUTHOR CONTRIBUTIONS**

MA conceived the study and designed, performed and analyzed the experiments. PZ and LW designed, performed and analyzed all the proteomics experiments shown in Figure 1. SY provided technical assistance and contributed to the analysis of the proteomics data.

HFS contributed to the study design and performed all confocal microscopy. RS conceived the study and coordinated the research. RS and MA wrote the paper. All authors reviewed the results and approved the final version of the manuscript.

## REFERENCES

1. Kornfeld, S. (1986) Trafficking of lysosomal enzymes in normal and disease states. *The Journal of Clinical Investigation* **77**, 1-6
2. Reitman, M. L., and Kornfeld, S. (1981) Lysosomal enzyme targeting. N-Acetylglucosaminylphosphotransferase selectively phosphorylates native lysosomal enzymes. *The Journal of Biological Chemistry* **256**, 11977-11980
3. Kollmann, K., Pohl, S., Marschner, K., Encarnacao, M., Sakwa, I., Tiede, S., Poorthuis, B. J., Lubke, T., Muller-Loennies, S., Storch, S., and Braulke, T. (2010) Mannose phosphorylation in health and disease. *European Journal of Cell Biology* **89**, 117-123
4. Lee, W. S., Payne, B. J., Gelfman, C. M., Vogel, P., and Kornfeld, S. (2007) Murine UDP-GlcNAc:lysosomal enzyme N-acetylglucosamine-1-phosphotransferase lacking the gamma-subunit retains substantial activity toward acid hydrolases. *The Journal of Biological Chemistry* **282**, 27198-27203
5. Pohl, S., Encarnacao, M., Castrichini, M., Muller-Loennies, S., Muschol, N., and Braulke, T. (2010) Loss of N-acetylglucosamine-1-phosphotransferase gamma subunit due to intronic mutation in GNPTG causes mucopolipidosis type III gamma: Implications for molecular and cellular diagnostics. *American Journal of Medical Genetics. Part A* **152A**, 124-132
6. Qian, Y., van Meel, E., Flanagan-Steet, H., Yox, A., Steet, R., and Kornfeld, S. (2015) Analysis of mucopolipidosis II/III GNPTAB missense mutations identifies domains of UDP-GlcNAc:lysosomal enzyme GlcNAc-1-phosphotransferase involved in catalytic function and lysosomal enzyme recognition. *The Journal of Biological Chemistry* **290**, 3045-3056
7. van Meel, E., Lee, W. S., Liu, L., Qian, Y., Doray, B., and Kornfeld, S. (2016) Multiple Domains of GlcNAc-1-phosphotransferase Mediate Recognition of Lysosomal Enzymes. *The Journal of Biological Chemistry* **291**, 8295-8307
8. De Pace, R., Coutinho, M. F., Koch-Nolte, F., Haag, F., Prata, M. J., Alves, S., Braulke, T., and Pohl, S. (2014) Mucopolipidosis II-related mutations inhibit the exit from the endoplasmic reticulum and proteolytic cleavage of GlcNAc-1-phosphotransferase precursor protein (GNPTAB). *Human Mutation* **35**, 368-376
9. De Pace, R., Velho, R. V., Encarnacao, M., Marschner, K., Braulke, T., and Pohl, S. (2015) Subunit interactions of the disease-related hexameric GlcNAc-1-phosphotransferase complex. *Human Molecular Genetics* **24**, 6826-6835
10. Pohl, S., Tiede, S., Marschner, K., Encarnacao, M., Castrichini, M., Kollmann, K., Muschol, N., Ullrich, K., Muller-Loennies, S., and Braulke, T. (2010) Proteolytic processing of the gamma-subunit is associated with the failure to form GlcNAc-1-phosphotransferase complexes and mannose 6-phosphate residues on lysosomal enzymes in human macrophages. *The Journal of Biological Chemistry* **285**, 23936-23944
11. Kudo, M., Brem, M. S., and Canfield, W. M. (2006) Mucopolipidosis II (I-cell disease) and mucopolipidosis IIIA (classical pseudo-hurler polydystrophy) are caused by mutations in the GlcNAc-phosphotransferase alpha / beta -subunits precursor gene. *American journal of human genetics* **78**, 451-463

12. Tiede, S., Storch, S., Lubke, T., Henrissat, B., Bargal, R., Raas-Rothschild, A., and Braulke, T. (2005) Mucopolidosis II is caused by mutations in GNPTA encoding the alpha/beta GlcNAc-1-phosphotransferase. *Nature Medicine* **11**, 1109-1112
13. Dittmer, F., Ulbrich, E. J., Hafner, A., Schmahl, W., Meister, T., Pohlmann, R., and von Figura, K. (1999) Alternative mechanisms for trafficking of lysosomal enzymes in mannose 6-phosphate receptor-deficient mice are cell type-specific. *Journal of Cell Science* **112 ( Pt 10)**, 1591-1597
14. Markmann, S., Thelen, M., Cornils, K., Schweizer, M., Brocke-Ahmadinejad, N., Willnow, T., Heeren, J., Gieselmann, V., Braulke, T., and Kollmann, K. (2015) Lrp1/LDL Receptor Play Critical Roles in Mannose 6-Phosphate-Independent Lysosomal Enzyme Targeting. *Traffic* **16**, 743-759
15. Mbua, N. E., Flanagan-Steet, H., Johnson, S., Wolfert, M. A., Boons, G. J., and Steet, R. (2013) Abnormal accumulation and recycling of glycoproteins visualized in Niemann-Pick type C cells using the chemical reporter strategy. *Proceedings of the National Academy of Sciences of the United States of America* **110**, 10207-10212
16. Otomo, T., Higaki, K., Nanba, E., Ozono, K., and Sakai, N. (2011) Lysosomal storage causes cellular dysfunction in mucopolidosis II skin fibroblasts. *The Journal of Biological Chemistry* **286**, 35283-35290
17. Cox, T. M., and Cachon-Gonzalez, M. B. (2012) The cellular pathology of lysosomal diseases. *The Journal of Pathology* **226**, 241-254
18. Devlin, C., Pipalia, N. H., Liao, X., Schuchman, E. H., Maxfield, F. R., and Tabas, I. (2010) Improvement in lipid and protein trafficking in Niemann-Pick C1 cells by correction of a secondary enzyme defect. *Traffic* **11**, 601-615
19. Fukuda, T., Ewan, L., Bauer, M., Mattaliano, R. J., Zaal, K., Ralston, E., Plotz, P. H., and Raben, N. (2006) Dysfunction of endocytic and autophagic pathways in a lysosomal storage disease. *Annals of Neurology* **59**, 700-708
20. Yang, W. H., Aziz, P. V., Heithoff, D. M., Mahan, M. J., Smith, J. W., and Marth, J. D. (2015) An intrinsic mechanism of secreted protein aging and turnover. *Proceedings of the National Academy of Sciences of the United States of America* **112**, 13657-13662
21. Brewer, C. F., Miceli, M. C., and Baum, L. G. (2002) Clusters, bundles, arrays and lattices: novel mechanisms for lectin-saccharide-mediated cellular interactions. *Current Opinion in Structural Biology* **12**, 616-623
22. Sacchettini, J. C., Baum, L. G., and Brewer, C. F. (2001) Multivalent protein-carbohydrate interactions. A new paradigm for supermolecular assembly and signal transduction. *Biochemistry* **40**, 3009-3015
23. Sun, T., Yu, S. H., Zhao, P., Meng, L., Moremen, K. W., Wells, L., Steet, R., and Boons, G. J. (2016) One-Step Selective Exoenzymatic Labeling (SEEL) Strategy for the Biotinylation and Identification of Glycoproteins of Living Cells. *Journal of the American Chemical Society* **138**, 11575-11582
24. Yu, S. H., Zhao, P., Sun, T., Gao, Z., Moremen, K. W., Boons, G. J., Wells, L., and Steet, R. (2016) Selective Exo-Enzymatic Labeling Detects Increased Cell Surface Sialoglycoprotein Expression upon Megakaryocytic Differentiation. *The Journal of Biological Chemistry* **291**, 3982-3989

25. Fuentealba, R. A., Liu, Q., Zhang, J., Kanekiyo, T., Hu, X., Lee, J. M., LaDu, M. J., and Bu, G. (2010) Low-density lipoprotein receptor-related protein 1 (LRP1) mediates neuronal Abeta42 uptake and lysosomal trafficking. *PLoS One* **5**, e11884
26. Kanekiyo, T., Liu, C. C., Shinohara, M., Li, J., and Bu, G. (2012) LRP1 in brain vascular smooth muscle cells mediates local clearance of Alzheimer's amyloid-beta. *The Journal of Neuroscience* **32**, 16458-16465
27. Kanekiyo, T., Zhang, J., Liu, Q., Liu, C. C., Zhang, L., and Bu, G. (2011) Heparan sulphate proteoglycan and the low-density lipoprotein receptor-related protein 1 constitute major pathways for neuronal amyloid-beta uptake. *The Journal of Neuroscience* **31**, 1644-1651
28. Storck, S. E., Meister, S., Nahrath, J., Meissner, J. N., Schubert, N., Di Spiezio, A., Baches, S., Vandenbroucke, R. E., Bouter, Y., Prikulis, I., Korth, C., Weggen, S., Heimann, A., Schwaninger, M., Bayer, T. A., and Pietrzik, C. U. (2016) Endothelial LRP1 transports amyloid-beta(1-42) across the blood-brain barrier. *The Journal of Clinical Investigation* **126**, 123-136
29. Gujdar, A., Sipeki, S., Bander, E., Buday, L., and Farago, A. (2004) Protein kinase C modulates negatively the hepatocyte growth factor-induced migration, integrin expression and phosphatidylinositol 3-kinase activation. *Cellular Signalling* **16**, 505-513
30. Kaposi-Novak, P., Lee, J. S., Gomez-Quiroz, L., Coulouarn, C., Factor, V. M., and Thorgeirsson, S. S. (2006) Met-regulated expression signature defines a subset of human hepatocellular carcinomas with poor prognosis and aggressive phenotype. *The Journal of Clinical Investigation* **116**, 1582-1595
31. Palka, H. L., Park, M., and Tonks, N. K. (2003) Hepatocyte growth factor receptor tyrosine kinase met is a substrate of the receptor protein-tyrosine phosphatase DEP-1. *The Journal of Biological Chemistry* **278**, 5728-5735
32. Godfrey, R., Arora, D., Bauer, R., Stopp, S., Muller, J. P., Heinrich, T., Bohmer, S. A., Dagnell, M., Schnetzke, U., Scholl, S., Ostman, A., and Bohmer, F. D. (2012) Cell transformation by FLT3 ITD in acute myeloid leukemia involves oxidative inactivation of the tumor suppressor protein-tyrosine phosphatase DEP-1/ PTPRJ. *Blood* **119**, 4499-4511
33. Meng, T. C., Fukada, T., and Tonks, N. K. (2002) Reversible oxidation and inactivation of protein tyrosine phosphatases in vivo. *Molecular Cell* **9**, 387-399
34. van der Wijk, T., Overvoorde, J., and den Hertog, J. (2004) H<sub>2</sub>O<sub>2</sub>-induced intermolecular disulfide bond formation between receptor protein-tyrosine phosphatases. *The Journal of Biological Chemistry* **279**, 44355-44361
35. Yang, J., Groen, A., Lemeer, S., Jans, A., Slijper, M., Roe, S. M., den Hertog, J., and Barford, D. (2007) Reversible oxidation of the membrane distal domain of receptor PTPalpha is mediated by a cyclic sulfenamide. *Biochemistry* **46**, 709-719
36. Tseng, W. L., Chou, S. J., Chiang, H. C., Wang, M. L., Chien, C. S., Chen, K. H., Leu, H. B., Wang, C. Y., Chang, Y. L., Liu, Y. Y., Jong, Y. J., Lin, S. Z., Chiou, S. H., Lin, S. J., and Yu, W. C. (2017) Imbalanced Production of Reactive Oxygen Species and Mitochondrial Antioxidant SOD2 in Fabry Disease-Specific Human Induced Pluripotent Stem Cell-Differentiated Vascular Endothelial Cells. *Cell Transplantation* **26**, 513-527

37. Vazquez, M. C., del Pozo, T., Robledo, F. A., Carrasco, G., Pavez, L., Olivares, F., Gonzalez, M., and Zanlungo, S. (2011) Alteration of gene expression profile in Niemann-Pick type C mice correlates with tissue damage and oxidative stress. *PloS one* **6**, e28777
38. Otomo, T., Higaki, K., Nanba, E., Ozono, K., and Sakai, N. (2009) Inhibition of autophagosome formation restores mitochondrial function in mucopolipidosis II and III skin fibroblasts. *Molecular Genetics and Metabolism* **98**, 393-399
39. Liu, C. C., Hu, J., Zhao, N., Wang, J., Na, W., Cirrito, J. R., Kanekiyo, T., Holtzman, D. M., and Bu, G. (2017) Astrocytic LRP1 Mediates Brain Abeta Clearance and Impacts Amyloid Deposition. *The Journal of Neuroscience* **37**, 4023-31
40. Liu, Q., Trotter, J., Zhang, J., Peters, M. M., Cheng, H., Bao, J., Han, X., Weeber, E. J., and Bu, G. (2010) Neuronal LRP1 knockout in adult mice leads to impaired brain lipid metabolism and progressive, age-dependent synapse loss and neurodegeneration. *The Journal of Neuroscience* : **30**, 17068-17078
41. Zlokovic, B. V., Deane, R., Sagare, A. P., Bell, R. D., and Winkler, E. A. (2010) Low-density lipoprotein receptor-related protein-1: a serial clearance homeostatic mechanism controlling Alzheimer's amyloid beta-peptide elimination from the brain. *Journal of Neurochemistry* **115**, 1077-1089
42. Owen, J. B., Sultana, R., Aluise, C. D., Erickson, M. A., Price, T. O., Bu, G., Banks, W. A., and Butterfield, D. A. (2010) Oxidative modification to LDL receptor-related protein 1 in hippocampus from subjects with Alzheimer disease: implications for Abeta accumulation in AD brain. *Free Radical Biology & Medicine* **49**, 1798-1803
43. Walser, M., Umbricht, C. A., Frohli, E., Nanni, P., and Hajnal, A. (2017) beta-Integrin de-phosphorylation by the Density-Enhanced Phosphatase DEP-1 attenuates EGFR signaling in *C. elegans*. *PLoS Genetics* **13**, e1006592
44. Mana, G., Clapero, F., Panieri, E., Panero, V., Bottcher, R. T., Tseng, H. Y., Saltarin, F., Astanina, E., Wolanska, K. I., Morgan, M. R., Humphries, M. J., Santoro, M. M., Serini, G., and Valdembri, D. (2016) PPFIA1 drives active alpha5beta1 integrin recycling and controls fibronectin fibrillogenesis and vascular morphogenesis. *Nature Communications* **7**, 13546
45. Clavijo-Cornejo, D., Enriquez-Cortina, C., Lopez-Reyes, A., Dominguez-Perez, M., Nuno, N., Dominguez-Meraz, M., Bucio, L., Souza, V., Factor, V. M., Thorgeirsson, S. S., Gutierrez-Ruiz, M. C., and Gomez-Quiroz, L. E. (2013) Biphasic regulation of the NADPH oxidase by HGF/c-Met signaling pathway in primary mouse hepatocytes. *Biochimie* **95**, 1177-1184
46. Gomez-Quiroz, L. E., Factor, V. M., Kaposi-Novak, P., Coulouarn, C., Conner, E. A., and Thorgeirsson, S. S. (2008) Hepatocyte-specific c-Met deletion disrupts redox homeostasis and sensitizes to Fas-mediated apoptosis. *The Journal of Biological Chemistry* **283**, 14581-14589
47. Gomez-Quiroz, L. E., Seo, D., Lee, Y. H., Kitade, M., Gaiser, T., Gillen, M., Lee, S. B., Gutierrez-Ruiz, M. C., Conner, E. A., Factor, V. M., Thorgeirsson, S. S., and Marquardt, J. U. (2016) Loss of c-Met signaling sensitizes hepatocytes to lipotoxicity and induces cholestatic liver damage by aggravating oxidative stress. *Toxicology* **361-362**, 39-48

48. Takami, T., Kaposi-Novak, P., Uchida, K., Gomez-Quiroz, L. E., Conner, E. A., Factor, V. M., and Thorgeirsson, S. S. (2007) Loss of hepatocyte growth factor/c-Met signaling pathway accelerates early stages of N-nitrosodiethylamine induced hepatocarcinogenesis. *Cancer Research* **67**, 9844-9851
49. Flanagan-Steet, H., Aarnio, M., Kwan, B., Guihard, P., Petrey, A., Haskins, M., Blanchard, F., and Steet, R. (2016) Cathepsin-Mediated Alterations in TGF $\beta$ -Related Signaling Underlie Disrupted Cartilage and Bone Maturation Associated With Impaired Lysosomal Targeting. *Journal of Bone and Mineral Research* **31**, 535-548
50. Meng, L., Forouhar, F., Thieker, D., Gao, Z., Ramiah, A., Moniz, H., Xiang, Y., Seetharaman, J., Milaninia, S., Su, M., Bridger, R., Veillon, L., Azadi, P., Kornhaber, G., Wells, L., Montelione, G. T., Woods, R. J., Tong, L., and Moremen, K. W. (2013) Enzymatic basis for N-glycan sialylation: structure of rat  $\alpha$ 2,6-sialyltransferase (ST6GAL1) reveals conserved and unique features for glycan sialylation. *The Journal of Biological Chemistry* **288**, 34680-34698

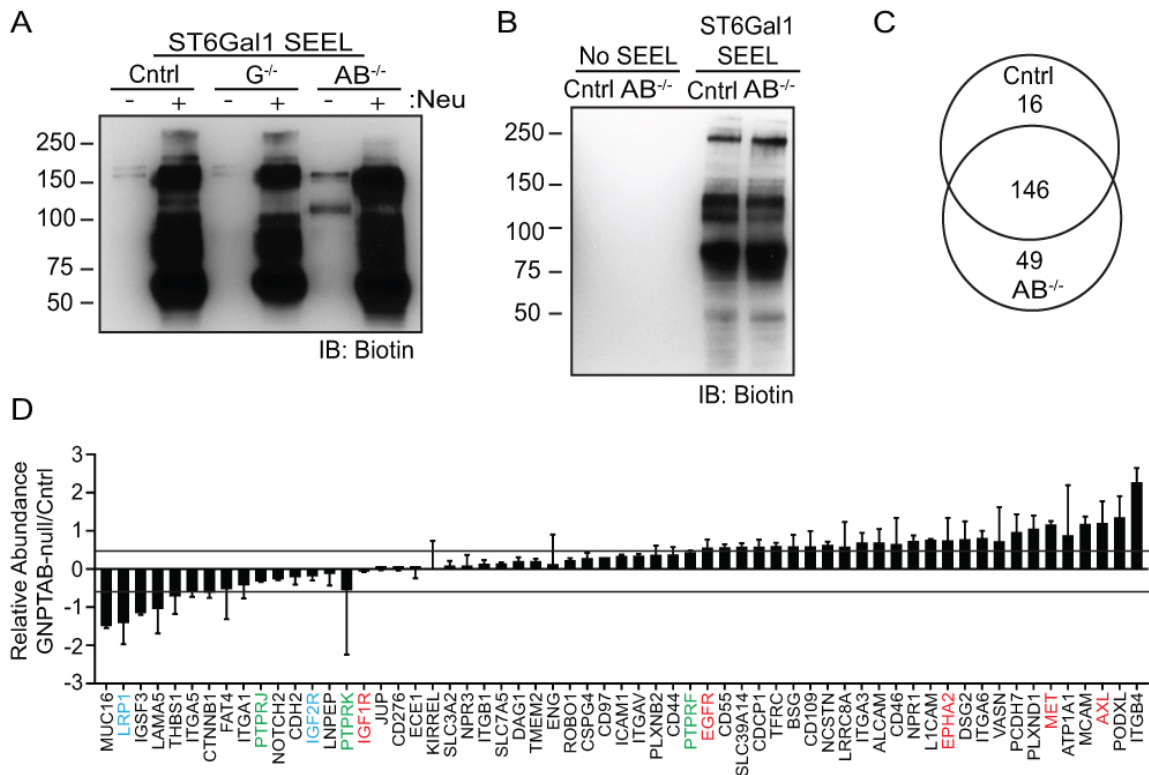


**Figure 3.1: GNPTAB<sup>-/-</sup> cells have dynamic changes in cell surface sialoglycoproteins.** (A) Representative immunoblot using an anti-biotin antibody of parental HeLa, GNPTG<sup>-/-</sup>, and GNPTAB<sup>-/-</sup> cells following ST6Gal1 SEEL in the presence or absence of neuraminidase. (n=3) (B) Biotin immunoblot of parental HeLa and GNPTAB<sup>-/-</sup> cells used for subsequent MS analysis. Samples either received no SEEL or ST6Gal1 SEEL in the presence of neuraminidase. (C) Venn diagram comparing the total number proteins identified in two biological replicates following ST6Gal1 SEEL and proteomic analysis. (D) Fold change comparing GNPTAB<sup>-/-</sup> to parental HeLa of the most abundant assigned proteins plotted using a log<sub>2</sub> scale. Blue indicates uptake receptors, green indicates protein-tyrosine phosphatases, and red indicates receptor tyrosine kinases (RTKs). Error bars indicate standard error of the mean calculated from two independent labeling experiments.

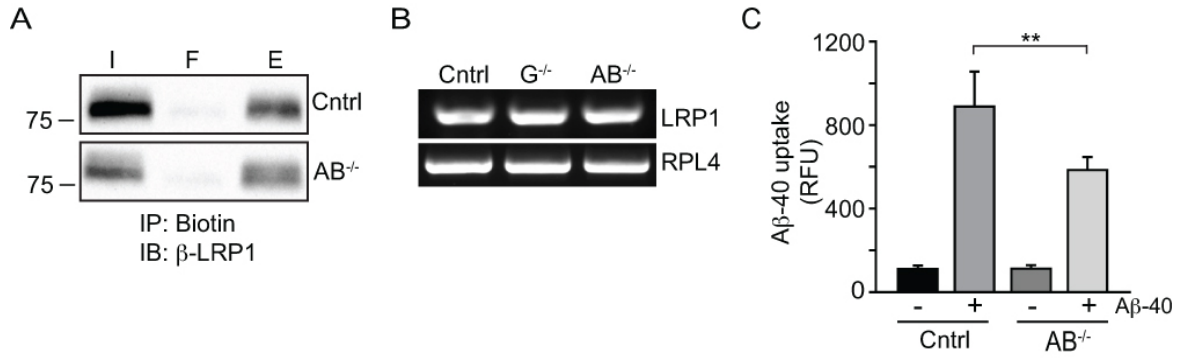


**Figure 3.2: Surface reduction of the reuptake receptor LRP1, results in decreased ligand uptake in GNPTAB<sup>-/-</sup> cells.** (A) Representative β-LRP1 immunoblot following biotin immunoprecipitation of ST6Gal1 SEEL labeled parental HeLa and GNPTAB<sup>-/-</sup> cells (n=5). 20 μg of protein was loaded for input (I) and flowthrough (F) fractions, and 100ug of protein was loaded for the elute (E) fraction. (B) RT-PCR of LRP1 from parental HeLa, GNPTG<sup>-/-</sup>, and GNPTAB<sup>-/-</sup> cells with RPL4 as a control gene. (C) Amyloid-β-40-647 cellular uptake represented in relative fluorescent units (RFU). Cells were treated with 2 μM Aβ-40 for 16 hours. Mean and standard deviation values obtained from four biological replicates with at least three technical replicates for each experiment. \*\*p<0.01

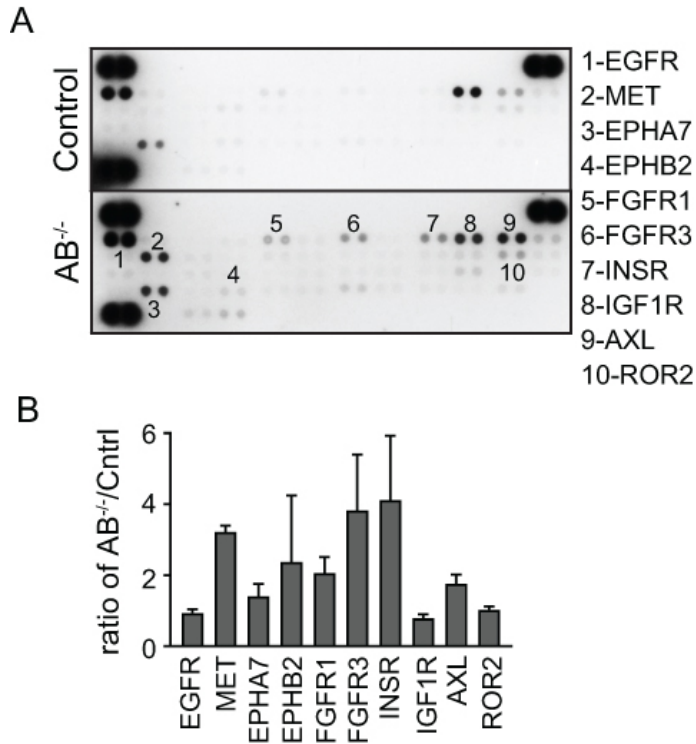


**Figure 3.3: GNPTAB<sup>-/-</sup> cells have increased levels of multiple phosphorylated receptor tyrosine kinases.** (A) Representative image of a human phospho-RTK array analysis of HeLa parental control and GNPTAB<sup>-/-</sup> cells (n=3). Receptors with high signal or large change in signal between HeLa parental control and GNPTAB<sup>-/-</sup> are labeled. (B) Fold change of the signal intensity of individual spots comparing GNPTAB<sup>-/-</sup> to HeLa parental control obtained from three biological replicates. Error bars denote standard deviation.

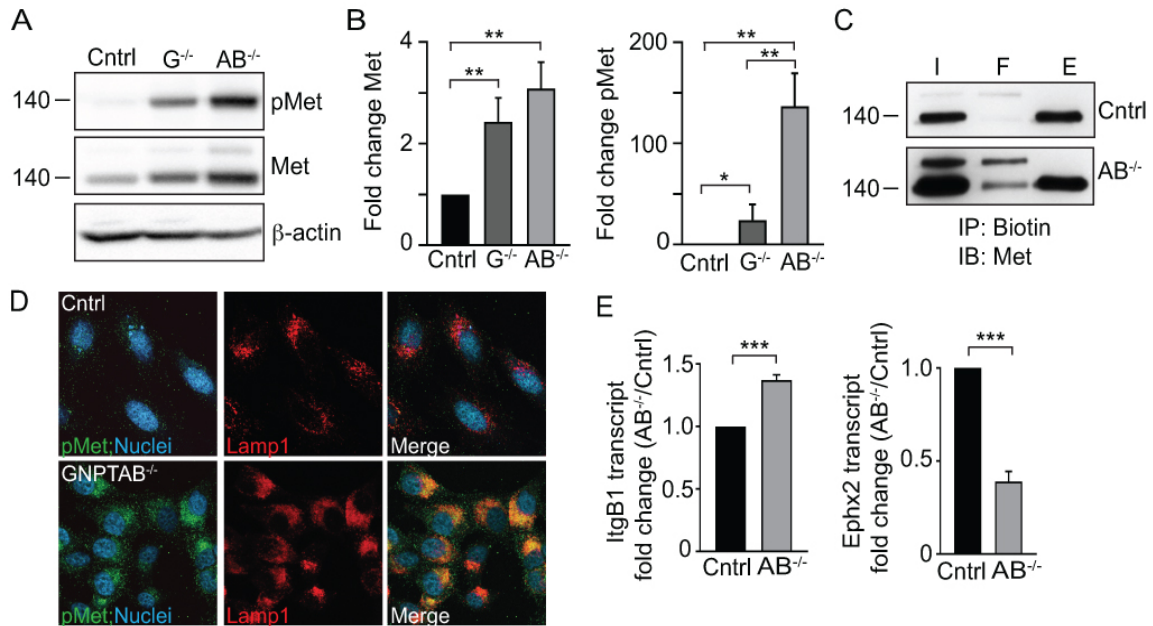


**Figure 3.4: Met and phospho-Met levels are increased in GNPTAB<sup>-/-</sup> cells.** (A) Whole cell lysates (100 μg) immunoblotted for pMet or Met, with β-actin as a loading control (n=4). (B) Fold change of GNPTAB<sup>-/-</sup> to HeLa parental control densitometry calculated from four biological replicates. \*p<0.05 and \*\*p<0.01. (C) Met immunoblots following anti-biotin immunoprecipitation of parental HeLa control and GNPTAB<sup>-/-</sup> SEEL labeled cells (n=4). 40 μg of protein was loaded for input (I), flowthrough (F), and elute (E) fractions. (D) Confocal microscopy of HeLa parental control and GNPTAB<sup>-/-</sup> cells stained for pMet (green) and Lamp1 (red) with nuclei labeled in blue. (E) qPCR transcript abundance measured in fold change of GNPTAB<sup>-/-</sup> to HeLa parental control of two Met target genes from three biological replicates. \*\*\*p<0.001.

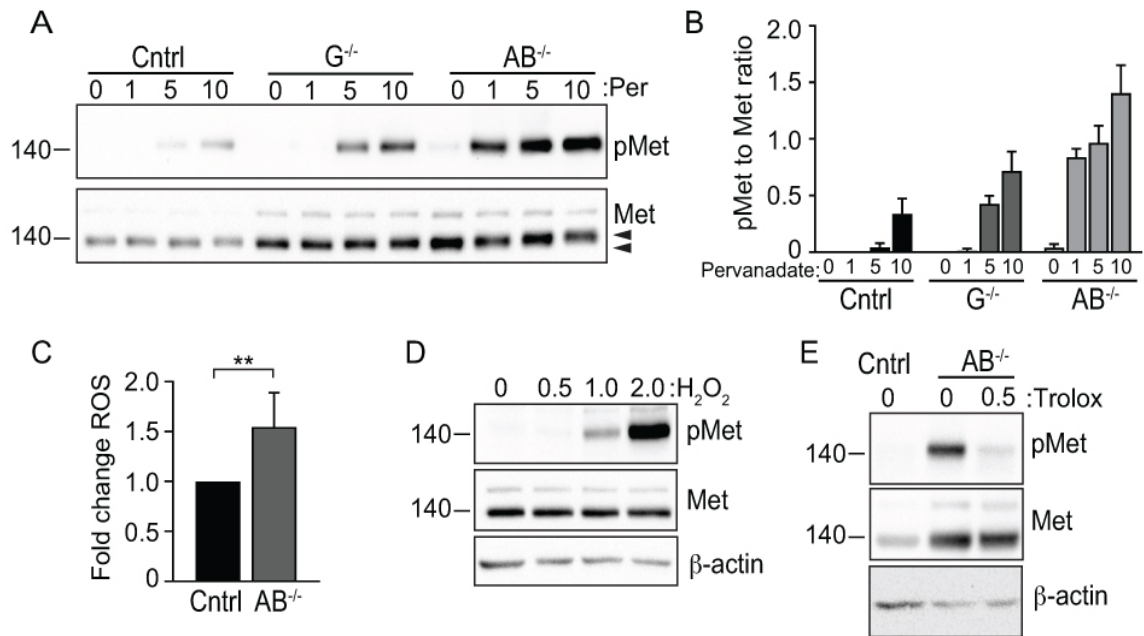


**Figure 3.5: pMet increases are tied to elevated ROS in GNPTAB<sup>-/-</sup> cells.** (A) Whole cell lysates (100  $\mu$ g) immunoblotted for pMet or Met following 20 min treatment with sodium pervanadate (n=2). Arrowheads indicate size shift of Met. (B) Densitometric analysis of the pMet to Met ratio. Error bars indicate standard error of the mean from two biological replicate experiments. (C) ROS levels were measured following a 45 min incubation of trypsinized cells with 2 mM carboxy-H<sub>2</sub>DCFDA (n=4). The fold change of ROS was calculated as the ratio of GNPTAB<sup>-/-</sup> to the parental HeLa control, setting the parental control value to 1. \*\*p<0.01. (D) Representative immunoblot of pMet and Met following 5 min treatment of parental HeLa cells with variable concentrations of hydrogen peroxide (n=4). (E) Total cell lysates from GNPTAB<sup>-/-</sup> cells treated for 96 hours with 0.5 mM Trolox were immunoblotted for pMet and Met, with  $\beta$ -actin serving as a loading control. A representative image of four biological replicates is shown.

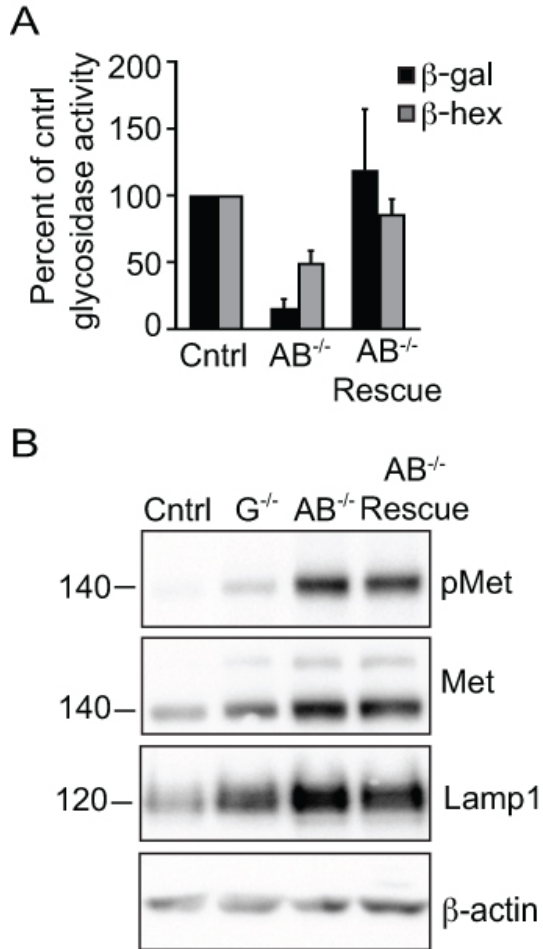


**Figure 3.6: Wild type GlcNAc-1-phosphotransferase partially rescues lysosomal function in GNPTAB<sup>-/-</sup> cells.** (A) GNPTAB<sup>-/-</sup> cells were transfected with wild type GlcNAc-1-phosphotransferase and cultured for 120 hours and then intracellular glycosidase activities of  $\beta$ -galactosidase and  $\beta$ -hexosaminidase were measured. Mean and standard deviation values obtained from parental HeLa cells are set to 100% (n=4). (B) Following 120 hours transfection, 100  $\mu$ g of whole cell lysates were immunoblotted for pMet, Met, and Lamp1.  $\beta$ -actin was used as a loading control (n=3).

## **CHAPTER 4: DISCUSSION AND FUTURE PERSPECTIVES**

Alterations in signaling pathways can lead to developmental abnormalities, and cancer at later stages in life. Often, signaling changes occur as a direct result of mutations affecting either growth factor ligands or their receptors. For example, in some cancers, receptor tyrosine kinases (RTKs) remain constitutively active in the absence of ligand stimulation due to transforming mutations [1]. Mutations in growth factors are not solely the cause of enhanced signaling, but seem to be the main focus of study. The research presented in this dissertation provides two mechanisms by which growth factor signaling is enhanced through loss of carbohydrate mediated lysosomal targeting.

### **The Contribution of Extracellular Cathepsins to Mucopolysaccharidosis II Pathology**

This research provides a direct mechanism whereby the extracellular activity of a cathepsin protease can drive disease pathology. Using a zebrafish model of MLII we show that cathepsin K (CtsK) has increased and sustained activity localized outside of chondrocytes. Further, we provide evidence to support an in vitro mechanism of latent growth factor activation. Based on in vitro digestions combining CtsK with latent TGF $\beta$ , we show that CtsK preferentially cleaves the latency associated peptide of TGF $\beta$  (Figure 2.2B). Interestingly, mature TGF $\beta$  ligand appears to be less susceptible to CtsK activity. Digestions with the LLC show that CtsK preferentially cleaves LTBP. There are several

possibilities for this, first that CtsK has a higher preference for LTBP, or cleavage is conformation based. It is possible that the CTSK cleavage sites for LAP need to be uncovered from LTBP first. These findings support a direct mechanism of latent TGF $\beta$  activation, which could be occurring *in vivo*. Further, determining the sequence specific cleavages of LAP and LTBP by CtsK would be informative, and provide information about the specificity of CtsK. Previous experiments in the lab were aimed at mapping the cleavage pattern of LAP following CtsK digestion using Edman Sequencing. Ultimately these experiments proved problematic and were not completed, but future studies could be completed by proteomic analysis of digested LAP.

Previous studies indicated that the C-terminal glycan of zebrafish CtsK is the primary site of N-glycosylation and removal of this site leads to enhanced activity. To assess the contribution of mannose phosphorylation to CtsK secretion and activity *in vivo*, N-glycan deleted CtsK mRNA was injected into WT embryos. mRNA injection lead to inconclusive results, as there were several limitations to this experiment: CtsK overexpression was systemic and endogenous CtsK was still present, further embryos displayed severe phenotypes uncharacteristic of MLII. These findings do not conclude that hypersecretion of cathepsin K is sufficient to recapitulate ML-II. Therefore, to delineate the interaction between extracellular CtsK and latent TGF $\beta$  *in vivo*, our lab is generating transgenic zebrafish expressing N-glycan deleted CtsK. Additionally, CtsK will be under the control of a tissue specific promoter to ensure expression in cartilage. These experiments will provide further support that hypersecretion of CtsK is the causative mechanism of craniofacial abnormalities in morphants.

Cathepsins K and L are two cathepsin proteases that have increased and sustained activity in MLII embryos. Both cathepsins contain putative N-glycan sites, indicative of M6P modification and potential hypersecretion in MLII. Cathepsin proteases are synthesized as inactive zymogens, with a propeptide region that must be removed to yield a functional enzyme [2-4]. In the lysosome, cathepsins are activated by low pH and proteolysis by other cathepsins. Our data shows that the majority of CtsK activity in MLII morphants is localized outside of chondrocytes, with CtsK existing in the active mature form. Thus if cathepsin L (CtsL) is hypersecreted in morphants, it could contribute to CtsK activation. The reverse is also true, that CtsK could activate CtsL in the ECM. This idea is supported by the fact that inhibition of CtsK activity in morphants leads to a concomitant reduction in CtsL activity as well. This suggests a correlation between elevated CtsK activity and other cathepsin activity in MLII zebrafish.

Future studies looking at the contribution of CtsL to disease pathology would be beneficial. Interestingly, LLC digestions with CTSL yielded a distinct cleavage pattern of LTBP (Figure 2.3B). Since these digestions were performed at a neutral pH, this suggests that CtsL has a broader pH range than previously published [5-7]. Early studies in the lab aimed at reducing CtsL expression in morphants. One drawback to this line of work is the fact that zebrafish have several CtsL genes and isoforms, which have very high homology. Upon reduction of one CtsL gene, the other CtsL genes responded. Specific morpholinos or pharmacological inhibitors will be needed to assess the specific contribution of each gene in regards to MLII pathogenesis.

There is an interesting link between TGF $\beta$  signaling and CtsL transcript abundance. A study in activated stromal fibroblasts showed that increased TGF $\beta$

signaling leads to elevated CtsL transcript abundance [8]. This is relevant to MLII zebrafish because CtsL1a and CtsL1b transcripts are increased as seen through qPCR analysis (see figure 4.1). It is currently unknown as to whether this is because of enhanced TGF $\beta$  signaling or from some other mechanism, but data suggests that elevated CtsL transcript is related to TGF $\beta$ . As seen in figure 4.1, reduction of TGF $\beta$  signaling in morphants reduces CtsL1a and CtsL1b transcript abundance. This data supports a tie between elevated TGF $\beta$  signaling and CtsL transcript abundance in morphant embryos.

### **Excessive TGF $\beta$ Signaling: A Hallmark of Disease**

Growth factor signaling regulation is essential for proper chondrogenesis, and imbalance leads to pathogenesis. This is evidenced by increased activated Smad2,3 and decreased Smad1,5,8, which impairs chondrocyte differentiation. Notably, the growth factor imbalance in morphants is also seen in the growth plates of MLII kittens [9]. In long bones, mesenchymal progenitors give rise to chondrocytes and osteoblasts, which is controlled through TGF $\beta$  and BMP signaling. Smad2,3 in coordination with Sox9 drive chondrogenesis while Smad1,5,8 induction of Osx induces an osteogenic fate. Figure 4.4 shows a schematic of this process. Based on immunohistochemical analysis, MLII kittens have increased Sox9 expression in hypertrophic chondrocytes. Further, osteoblasts expressed more pSmad3 and less pSmad1. These findings support imbalanced growth factor signaling is a disease mediator in both a zebrafish model of MLII and in a naturally occurring feline model.

Excessive TGF $\beta$  signaling is implicated in several other genetic disorders, including osteogenesis imperfecta, Marfan syndrome, and Camurati-Engelmann Disease.

Osteogenesis imperfecta (OI) is heritable in both a dominant and recessive manner, with mutations in type I collagen or the cartilage-associated protein (CRTAP) respectively [10]. In OI, hypomorphic mutations of CRTAP lead to collagen overmodification and alterations in the signal-modulating function of the bone matrix. Specifically, TGF $\beta$  signaling is increased as a product of reduced sequestration of TGF $\beta$  in the ECM. The authors of a 2014 study on OI, suggest that reduced collagen binding of decorin leads to defects in decorin's ability to sequester TGF $\beta$  [11]. These findings are interesting and could relate to the increased TGF $\beta$  signaling seen in zebrafish morphants. It is possible that the presence of extracellular cathepsins destabilizes the ECM. CtsK is a potent collagenase known to cleave the triple-helical region of type II collagen [12]. Thus extracellular localized CtsK could degrade type II collagen and affect its interaction with other matrix components and growth factors. Further, decorin expression is reduced in morphant embryos based on in situ analysis and qPCR transcript abundance [9]. Therefore, it is possible that CtsK mediates TGF $\beta$  signaling both directly and indirectly by altering the ECM to enable easier liberation of latent growth factors.

Marfan syndrome is an autosomal dominant genetic disorder characterized by increased TGF $\beta$  signaling. It is caused by mutations in the ECM glycoprotein fibrillin-1 [13]. Fibrillin is a matrix protein that mediates LTBP incorporation into the ECM [14]. As described in detail in the introduction section, LTBP is the latent TGF $\beta$  binding protein that forms the large latent complex with LAP-TGF $\beta$ . In Marfan syndrome, mutations in the fibrillin-1 gene leads to increased liberation of TGF $\beta$  from the matrix, due to impaired interaction with LTBP. Analogous to MLII, there does not appear to be an increase in TGF $\beta$  ligand, but rather an increase in activation. In MLII zebrafish there

is no change in transcript abundance of TGF $\beta$  or BMP genes compared to WT embryos. This suggests that the signaling imbalance in morphants is caused by post-translational activation of latent growth factors. Parallels with other genetic disorders causing increased TGF $\beta$  signaling, support a model of increased liberation of active TGF $\beta$  from latent forms.

### **MLII Therapy**

There is currently no cure for MLII, and treatment options are aimed at symptom relief rather than combating disease pathology. Gene therapy for genetic disorders is still far from becoming a reality; therefore it is essential to develop other treatment options. Recently, CtsK inhibitors have proven effective for treatment of osteoporosis and osteoarthritis. Osteoporosis is caused by an imbalance of bone resorption and bone formation, leading to low bone mineral density and increased bone fragility and fracture risk [15]. Current osteoporosis therapies are designed to inhibit osteoclast-mediated bone resorption. Similar to osteoporosis, ML-II patients suffer from elevated bone resorption. The CtsK inhibitor, odanocatib, has shown much potential as an osteoporosis therapy, and could be useful for treating MLII [16, 17]. Other osteoporosis drugs function in an antiresorptive manner to reduce osteoclast activity, and can reduce osteoclast number. Clinical trials with odanocatib show that it does not affect osteoclast viability and cellular activity.

Studies in our lab use odanocatib as a potent CtsK inhibitor to treat morphant embryos. Odanocatib yields comparable results to genetic knockdown of CtsK, indicating it's potential as a therapeutic drug in zebrafish. Based on similarities between human

MLII and morphants, odanacatib could be a potential drug to treat patients. While odanacatib reduces CtsK activity and rescues the signaling imbalance in MLII zebrafish, it does not correct the misslocalization of CtsK. One of the main drivers of pathogenesis in MLII human patients is the persistent accumulation of lysosomal storage. This differs from zebrafish morphants, as they do not develop storage during the early developmental time points studied. Therefore pathology in morphants is caused by the extracellular presence of hypersecreted cathepsins. Based on this, odanacatib treatment in patients may not address the issue of lysosomal storage. Thus studies in cell culture and other animal models that have storage would be beneficial.

As we have shown in our zebrafish model of ML-II, TGF $\beta$  signaling is greatly increased causing altered craniofacial cartilage development. The previous section addressed elevated TGF $\beta$  signaling in other genetic disorders, such as Marfan syndrome. A 2006 study published in Science detailed research using Losartan, an angiotensin II type I receptor (AT1) antagonist to treat a mouse model of Marfan's [18]. Losartan is a competitive inhibitor of angiotensin II, and has been shown to reduce TGF $\beta$  signaling [19, 20]. Zebrafish experiments in our lab have used Losartan to decrease TGF $\beta$  signaling in morphant embryos. Based on Alcian Blue analysis, Losartan treatment rescued the craniofacial phenotype of morphant embryos. Further analysis by in situ hybridization showed that Losartan rescued the TGF $\beta$  dependent gene Col2a1. Interestingly, losartan also rescued the BMP dependent gene, Col10a in morphant embryos. Based on qPCR analysis, losartan treatment also appears to rescue the TGF $\beta$  effectors Smad2,3, which have increased abundance in morphants. Based on our findings in zebrafish and studies

on Marfan syndrome, Losartan is an effective TGF $\beta$  antagonist. Future experiments in zebrafish should address Smad activation levels following Losartan treatment.

### **SEEL Applications and Future Studies in GNPTAB-null HeLa Cells**

Using a GNPTAB knockout HeLa cell line, we profiled cell surface sialoglycoproteins by selective exo-enzymatic labeling (SEEL). This one step process combines recombinant glycosyltransferases with labeled sugar nucleotides in the presence of a sialidase to provide terminal galactose acceptors [21]. In chapter three we used the sialyltransferase ST6Gal1, which transfers sialic acid to N-glycans by a 2,6 linkage [22]. SEEL has the added advantage of labeling proteins with slow turnover, which can be missed when using metabolic labeling. Further, in metabolic labeling, azide sugars compete with endogenous sugar precursors. SEEL is efficient and does not require the synthesis of new glycoproteins or the biosynthetic machinery of the cell. Therefore, SEEL provides an accurate real time profile of cell surface sialoglycoproteins.

In chapter three, SEEL followed by proteomic analysis identified decreased abundance of uptake receptors and increased abundance of receptor tyrosine kinases (RTKs) on the cell surface of GNPTAB<sup>-/-</sup> cells. The reduction of the uptake receptor LRP1 was especially interesting because of its role in enzyme reuptake. LRP1 functions to reuptake non-phosphorylated lysosomal enzymes from the cell surface [23]. The reduction of LRP1 in GNPTAB<sup>-/-</sup> cells is functionally relevant as measured by reduced uptake of the ligand AB-40. It is possible that this is a disease modifier in GNPTAB<sup>-/-</sup> cells since mistargeted lysosomal hydrolases may not be taken up as efficiently.

Proteomics also revealed reduced surface abundance of several RTKs in GNPTAB<sup>-/-</sup> cells. Interestingly, this reduced surface abundance did not correlate to reduced activation. Based on human phospho-RTK analyses, RTKs from GNPTAB<sup>-/-</sup> cells were globally increased in phosphorylation status. This presents an intriguing finding that suggests these RTKs are either not being turned over or their dephosphorylation status is deregulated. Our findings support both of these mechanisms with respect to the c-Met receptor. We show that it has increased expression within lysosomes as evidenced by colocalization with the lysosomal marker LAMP1. Further, the main protein-tyrosine phosphatase (PTP) that acts on phospho-Met (PTPRJ/Dep-1) has reduced abundance on the cell surface of GNPTAB<sup>-/-</sup> cells based on proteomic analysis. This is coupled to an increase in reactive oxygen species (ROS), which has been shown to inactivate PTPs [24, 25]. We show that treatment with an antioxidant reduces phospho-Met levels, tying activated Met to increases in ROS.

Multiple types of ROS (peroxides, superoxide, hydroxyl radical) can cause oxidative stress, and in this study we used a pan-ROS indicator dye that does not differentiate between species [26]. Future experiments using specific ROS indicators would be useful to determine which species are increased in GNPTAB<sup>-/-</sup> cells. Based on this, antioxidant treatment can be tailored to the specific ROS upregulated in GNPTAB<sup>-/-</sup> cells. The cause of the global increase in phospho-RTKs in GNPTAB<sup>-/-</sup> cells is another intriguing question. Is this global activation caused by increases in ROS, and if so can activation be reduced through antioxidant treatment? Future experiments will address these questions.

Additional studies looking at PTP activity would be useful to determine their activity level in GNPTAB<sup>-/-</sup> cells. Another way to look at the affects of PTP activity on Met activation would be to reduce PTP activity or expression in HeLa parental cells. This could be done through siRNA knockdown of Dep-1, which is known to act on Met [27]. We would expect knockdown of Dep-1 to show an increase in Met phosphorylation similar to GNPTAB<sup>-/-</sup> levels. Reduction of storage is another way to potentially rescue Met signaling, unfortunately previous studies using total enzyme replacement therapy in GNPTAB<sup>-/-</sup> cells were unsuccessful.

### **Receptor Function and Activity is Modified by Glycosylation**

Lysosomal storage and enzyme secretion are hallmark features of MLII, but little is know about the affects of secreted glycosidases. Further, how are cell surface glycoproteins affected by secreted glycosidases? Research from Yang and colleagues defines a mechanism whereby endogenous circulating glycosidases remove terminal saccharides from secreted proteins, leading to their internalization and turnover [28]. As proteins age and are in circulation they are exposed to endogenous extracellular glycosidases leading to the sequential removal of sugar moieties. Removal of terminal sugars generates ligands for lectin recognition and binding. This natural process could be potentiated in GNPTAB<sup>-/-</sup> cells due to the increased secretion of glycosidases. To support this idea, ST6Gal SEEL shows increased labeling of GNPTAB<sup>-/-</sup> cells in the absence of neuraminidase, indicating exposed terminal galactose residues (Figure 3.1A). Further the increased presence of exposed saccharides could increase lead to an increase in protein internalization. Based on the storage burden of these cells, endocytosis and

turnover and most likely affected. Future experiments treating GNPTAB<sup>-/-</sup> cells with a sialidase inhibitor would be interesting to see how reducing glycan trimming affects receptor internalization. Further, we could learn if glycan trimming affects RTK phosphorylation status and signaling by looking at Met receptor phosphorylation.

Glycosylation status affects the function of many proteins by mediating their recognition and binding ability. This is evidenced by the cooperative action of LRP1 and heparan sulfate proteoglycan (HSPG) in amyloid-beta uptake [29]. Both LRP1 and HSPG colocalize to amyloid plaques in Alzheimer's disease (AD) and coimmunoprecipitate as a complex from the cell surface. Further HSPG deficiency or heparin treatment decreases amyloid-beta binding and uptake.

Based on experiments detailed in chapter three, we show a functional decrease in LRP1 dependent uptake of the ligand AB-40 in GNPTAB<sup>-/-</sup> cells. We believe this decrease stems from reduced abundance of LRP1 at the surface. While we do not have information regarding the glycosylation status of LRP1 in GNPTAB<sup>-/-</sup> cells, it could affect its binding and uptake ability. Glycan analysis of LRP1 in GNPTAB<sup>-/-</sup> cells and parental HeLa cells would be beneficial.

## REFERENCES

1. Nishikawa, R., et al., A mutant epidermal growth factor receptor common in human glioma confers enhanced tumorigenicity. *Proc Natl Acad Sci U S A*, 1994. 91(16): p. 7727-31.
2. Menard, R., et al., Autocatalytic processing of recombinant human procathepsin L. Contribution of both intermolecular and unimolecular events in the processing of procathepsin L in vitro. *J Biol Chem*, 1998. 273(8): p. 4478-84.
3. Pungercar, J.R., et al., Autocatalytic processing of procathepsin B is triggered by proenzyme activity. *FEBS J*, 2009. 276(3): p. 660-8.
4. Turk, V., et al., Cysteine cathepsins: from structure, function and regulation to new frontiers. *Biochim Biophys Acta*, 2012. 1824(1): p. 68-88.
5. Smith, S.M. and M.M. Gottesman, Activity and deletion analysis of recombinant human cathepsin L expressed in *Escherichia coli*. *J Biol Chem*, 1989. 264(34): p. 20487-95.
6. Mason, R.W., G.D. Green, and A.J. Barrett, Human liver cathepsin L. *Biochem J*, 1985. 226(1): p. 233-41.
7. Mason, R.W. and A.J. Barrett, Properties of human liver cathepsin L. *Prog Clin Biol Res*, 1985. 180: p. 217-9.
8. Yin, M., et al., TGF-beta signaling, activated stromal fibroblasts, and cysteine cathepsins B and L drive the invasive growth of human melanoma cells. *Am J Pathol*, 2012. 181(6): p. 2202-16.
9. Flanagan-Steet, H., et al., Cathepsin-Mediated Alterations in TGF $\beta$ s-Related Signaling Underlie Disrupted Cartilage and Bone Maturation Associated With Impaired Lysosomal Targeting. *J Bone Miner Res*, 2016. 31(3): p. 535-48.
10. Baldrige, D., et al., Generalized connective tissue disease in *Crtap*<sup>-/-</sup> mouse. *PLoS One*, 2010. 5(5): p. e10560.
11. Grafe, I., et al., Excessive transforming growth factor-beta signaling is a common mechanism in osteogenesis imperfecta. *Nat Med*, 2014. 20(6): p. 670-5.
12. Dejica, V.M., et al., Cleavage of type II collagen by cathepsin K in human osteoarthritic cartilage. *Am J Pathol*, 2008. 173(1): p. 161-9.
13. Neptune, E.R., et al., Dysregulation of TGF-beta activation contributes to pathogenesis in Marfan syndrome. *Nat Genet*, 2003. 33(3): p. 407-11.
14. Kaartinen, V. and D. Warburton, Fibrillin controls TGF-beta activation. *Nat Genet*, 2003. 33(3): p. 331-2.
15. Otomo, T., et al., Elevated Bone Turnover in an Infantile Patient with Mucopolysaccharidosis II; No Association with Hyperparathyroidism. *Clin Pediatr Endocrinol*, 2011. 20(1): p. 7-12.
16. Bone, H.G., et al., Odanacatib, a cathepsin-K inhibitor for osteoporosis: a two-year study in postmenopausal women with low bone density. *J Bone Miner Res*, 2010. 25(5): p. 937-47.
17. Gauthier, J.Y., et al., The discovery of odanacatib (MK-0822), a selective inhibitor of cathepsin K. *Bioorg Med Chem Lett*, 2008. 18(3): p. 923-8.

18. Habashi, J.P., et al., Losartan, an AT1 antagonist, prevents aortic aneurysm in a mouse model of Marfan syndrome. *Science*, 2006. 312(5770): p. 117-21.
19. Nataatmadja, M., et al., Angiotensin II Receptor Antagonism Reduces Transforming Growth Factor Beta and Smad Signaling in Thoracic Aortic Aneurysm. *Ochsner J*, 2013. 13(1): p. 42-8.
20. Bar-Klein, G., et al., Losartan prevents acquired epilepsy via TGF-beta signaling suppression. *Ann Neurol*, 2014. 75(6): p. 864-75.
21. Yu, S.H., et al., Selective Exo-Enzymatic Labeling Detects Increased Cell Surface Sialoglycoprotein Expression upon Megakaryocytic Differentiation. *J Biol Chem*, 2016. 291(8): p. 3982-9.
22. Mbua, N.E., et al., Selective exo-enzymatic labeling of N-glycans on the surface of living cells by recombinant ST6Gal I. *Angew Chem Int Ed Engl*, 2013. 52(49): p. 13012-5.
23. Markmann, S., et al., Lrp1/LDL Receptor Play Critical Roles in Mannose 6-Phosphate-Independent Lysosomal Enzyme Targeting. *Traffic*, 2015. 16(7): p. 743-59.
24. Godfrey, R., et al., Cell transformation by FLT3 ITD in acute myeloid leukemia involves oxidative inactivation of the tumor suppressor protein-tyrosine phosphatase DEP-1/ PTPRJ. *Blood*, 2012. 119(19): p. 4499-511.
25. Meng, T.C., T. Fukada, and N.K. Tonks, Reversible oxidation and inactivation of protein tyrosine phosphatases in vivo. *Mol Cell*, 2002. 9(2): p. 387-99.
26. Ray, P.D., B.W. Huang, and Y. Tsuji, Reactive oxygen species (ROS) homeostasis and redox regulation in cellular signaling. *Cell Signal*, 2012. 24(5): p. 981-90.
27. Palka, H.L., M. Park, and N.K. Tonks, Hepatocyte growth factor receptor tyrosine kinase met is a substrate of the receptor protein-tyrosine phosphatase DEP-1. *J Biol Chem*, 2003. 278(8): p. 5728-35.
28. Yang, W.H., et al., An intrinsic mechanism of secreted protein aging and turnover. *Proc Natl Acad Sci U S A*, 2015. 112(44): p. 13657-62.
29. Kanekiyo, T., et al., Heparan sulphate proteoglycan and the low-density lipoprotein receptor-related protein 1 constitute major pathways for neuronal amyloid-beta uptake. *J Neurosci*, 2011. 31(5): p. 1644-51.

## FIGURES

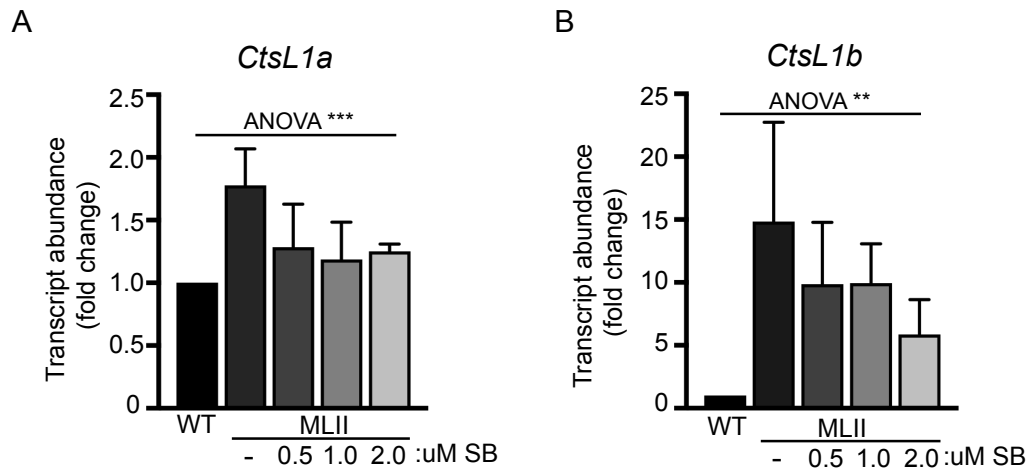


**Figure 4.1 TGF $\beta$  reduction in ML-II embryos reduces CtsL transcript.** (A) CtsL1a (B) CtsL1b, qPCR of 4dpf WT and ML-II embryos treated with three concentrations of SB505124. n=15 embryos/sample, at least 3 experiments. RPL4 was used as a normalizer. \*\* p < 0.01, \*\*\* p < 0.001.

APPENDIX: SUPPLEMENTAL TABLE

Replicate 1				Replicate 2				Average Fold Change
Gene	HeLa	GNPTAB	Fold change	Gene	HeLa	GNPTAB	Fold Change	
ABCC1	25	46	1.84	ABCC1	31	29	0.94	1.39
ADAM15	10	12	1.20	ADAM15	14	10	0.71	0.96
AGRN	6	14	2.33	AGRN	15	3	0.20	1.27
ALCAM	97	187	1.93	ALCAM	122	168	1.38	1.65
AMIGO2	8	23	2.88	AMIGO2	14	14	1.00	1.94
ANXA2	7	13	1.86	ANXA2	11	7	0.64	1.25
ATP1A1	35	123	3.51	ATP1A1	126	123	0.98	2.25
ATP1B1	13	30	2.31	ATP1B1	48	43	0.90	1.60
ATP1B3	29	73	2.52	ATP1B3	43	45	1.05	1.78
AXL	24	73	3.04	AXL	28	49	1.75	2.40
BCAM	26	18	0.69	BCAM	22	14	0.64	0.66
BSG	138	242	1.75	BSG	185	241	1.30	1.53
BST2	23	27	1.17	BST2	28	34	1.21	1.19
BTN2A1	11	17	1.55	BTN2A1	11	13	1.18	1.36
CACNA2D1	45	23	0.51	CACNA2D1	32	31	0.97	0.74
CD109	79	145	1.84	CD109	86	107	1.24	1.54
CD276	92	90	0.98	CD276	89	90	1.01	0.99
CD44	120	143	1.19	CD44	110	158	1.44	1.31
CD46	30	66	2.20	CD46	60	68	1.13	1.67
CD55	41	59	1.44	CD55	48	74	1.54	1.49
CD82	8	10	1.25	CD82	14	14	1.00	1.13
CD97	83	103	1.24	CD97	91	113	1.24	1.24
CDCP1	64	88	1.38	CDCP1	56	92	1.64	1.51
CDH2	115	108	0.94	CDH2	111	87	0.78	0.86
CELSR1	11	30	2.73	CELSR1	18	15	0.83	1.78
CLU	8	12	1.50	CLU	17	12	0.71	1.10
CNNM3	22	30	1.36	CNNM3	34	23	0.68	1.02
CNNM4	8	18	2.25	CNNM4	17	11	0.65	1.45
CSPG4	174	227	1.30	CSPG4	171	197	1.15	1.23
CTNNB1	136	94	0.69	CTNNB1	130	79	0.61	0.65
CXADR	22	37	1.68	CXADR	38	33	0.87	1.28
DAG1	75	91	1.21	DAG1	126	139	1.10	1.16
DCBLD1	18	12	0.67	DCBLD1	21	18	0.86	0.76
DSG2	74	160	2.16	DSG2	122	167	1.37	1.77

ECE1	84	93	1.11	ECE1	88	78	0.89	1.00
EDIL3	45	30	0.67	EDIL3	70	16	0.23	0.45
EGFR	136	181	1.33	EGFR	105	172	1.64	1.48
ENG	40	64	1.60	ENG	69	52	0.75	1.18
EPHA2	68	86	1.26	EPHA2	37	83	2.24	1.75
EPHA7	27	6	0.22	EPHA7	34	4	0.12	0.17
EPHB4	26	38	1.46	EPHB4	38	62	1.63	1.55
ERBB2	21	23	1.10	ERBB2	17	19	1.12	1.11
FAP	8	23	2.88	FAP	13	11	0.85	1.86
FAS	14	10	0.71	FAS	16	11	0.69	0.70
FAT1	6	23	3.83	FAT1	22	20	0.91	2.37
FAT4	68	69	1.01	FAT4	72	34	0.47	0.74
GPC1	39	28	0.72	GPC1	52	33	0.63	0.68
GPR56	28	43	1.54	GPR56	40	41	1.03	1.28
ICAM1	40	50	1.25	ICAM1	45	58	1.29	1.27
IGF1R	57	54	0.95	IGF1R	53	51	0.96	0.95
IGF2R	217	201	0.93	IGF2R	193	160	0.83	0.88
IGSF3	75	33	0.44	IGSF3	68	31	0.46	0.45
IGSF8	25	45	1.80	IGSF8	25	42	1.68	1.74
IL1RAP	16	13	0.81	IL1RAP	25	15	0.60	0.71
ITFG1	10	9	0.90	ITFG1	10	4	0.40	0.65
ITFG3	19	26	1.37	ITFG3	30	24	0.80	1.08
ITGA1	81	51	0.63	ITGA1	57	50	0.88	0.75
ITGA2	7	27	3.86	ITGA2	6	18	3.00	3.43
ITGA3	118	170	1.44	ITGA3	104	191	1.84	1.64
ITGA5	116	79	0.68	ITGA5	115	71	0.62	0.65
ITGA6	137	220	1.61	ITGA6	115	222	1.93	1.77
ITGAV	134	175	1.31	ITGAV	121	151	1.25	1.28
ITGB1	314	331	1.05	ITGB1	275	318	1.16	1.11
ITGB4	36	209	5.81	ITGB4	45	182	4.04	4.93
ITGB5	29	40	1.38	ITGB5	30	46	1.53	1.46
JUP	114	112	0.98	JUP	130	130	1.00	0.99
KIAA1161	31	19	0.61	KIAA1161	34	17	0.50	0.56
KIRREL	32	46	1.44	KIRREL	50	35	0.70	1.07
L1CAM	174	293	1.68	L1CAM	146	251	1.72	1.70
LAMA5	38	25	0.66	LAMA5	51	18	0.35	0.51
LAMB1	20	32	1.60	LAMB1	13	14	1.08	1.34
LAMC1	21	37	1.76	LAMC1	29	20	0.69	1.23
LDLR	12	29	2.42	LDLR	18	21	1.17	1.79
LNPEP	68	72	1.06	LNPEP	66	52	0.79	0.92
LRP1	186	91	0.49	LRP1	182	52	0.29	0.39
LRRC8A	50	103	2.06	LRRC8A	62	68	1.10	1.58
LRRC8C	16	18	1.13	LRRC8C	21	8	0.38	0.75

LRRC8D	14	24	1.71	LRRC8D	25	25	1.00	1.36
MCAM	93	232	2.49	MCAM	120	249	2.08	2.28
MET	91	195	2.14	MET	75	176	2.35	2.24
MRC2	43	14	0.33	MRC2	25	4	0.16	0.24
MSLN	7	11	1.57	MSLN	11	6	0.55	1.06
MUC16	55	19	0.35	MUC16	33	12	0.36	0.35
MYOF	9	12	1.33	MYOF	14	17	1.21	1.27
NCSTN	31	50	1.61	NCSTN	26	39	1.50	1.56
NOTCH2	89	73	0.82	NOTCH2	72	60	0.83	0.83
NPR1	42	75	1.79	NPR1	41	64	1.56	1.67
NPR3	50	61	1.22	NPR3	58	54	0.93	1.08
NPTN	9	22	2.44	NPTN	20	18	0.90	1.67
NRP1	19	40	2.11	NRP1	15	35	2.33	2.22
PCDH7	45	71	1.58	PCDH7	54	133	2.46	2.02
PDCD6IP	12	29	2.42	PDCD6IP	14	31	2.21	2.32
PIEZO1	19	40	2.11	PIEZO1	20	21	1.05	1.58
PLXDC2	20	17	0.85	PLXDC2	26	13	0.50	0.68
PLXNA1	8	22	2.75	PLXNA1	9	16	1.78	2.26
PLXNA2	5	15	3.00	PLXNA2	11	14	1.27	2.14
PLXNB2	135	197	1.46	PLXNB2	151	175	1.16	1.31
PLXND1	29	51	1.76	PLXND1	15	37	2.47	2.11
PODXL	44	86	1.95	PODXL	31	104	3.35	2.65
PTGFRN	25	12	0.48	PTGFRN	22	14	0.64	0.56
PTK7	43	40	0.93	PTK7	32	25	0.78	0.86
PTPRA	12	32	2.67	PTPRA	8	19	2.38	2.52
PTPRD	11	20	1.82	PTPRD	10	3	0.30	1.06
PTPRF	106	140	1.32	PTPRF	77	107	1.39	1.36
PTPRJ	83	66	0.80	PTPRJ	72	57	0.79	0.79
PTPRK	37	11	0.30	PTPRK	43	67	1.56	0.93
PTPRS	21	30	1.43	PTPRS	24	23	0.96	1.19
PVR	38	37	0.97	PVR	41	36	0.88	0.93
PVRL3	10	15	1.50	PVRL3	19	10	0.53	1.01
ROBO1	58	70	1.21	ROBO1	45	52	1.16	1.18
ROR2	13	23	1.77	ROR2	31	20	0.65	1.21
SCARB1	31	44	1.42	SCARB1	34	38	1.12	1.27
SEMA3C	17	31	1.82	SEMA3C	21	20	0.95	1.39
SERPINE1	10	15	1.50	SERPINE1	16	11	0.69	1.09
SLC12A2	23	32	1.39	SLC12A2	27	22	0.81	1.10
SLC1A5	32	41	1.28	SLC1A5	39	33	0.85	1.06
SLC2A1	12	36	3.00	SLC2A1	22	22	1.00	2.00
SLC39A10	10	16	1.60	SLC39A10	11	20	1.82	1.71
SLC39A14	35	55	1.57	SLC39A14	32	46	1.44	1.50
SLC39A6	9	15	1.67	SLC39A6	10	7	0.70	1.18

SLC3A2	909	1030	1.13	SLC3A2	1113	1123	1.01	1.07
SLC44A2	16	23	1.44	SLC44A2	14	32	2.29	1.86
SLC7A5	137	154	1.12	SLC7A5	172	188	1.09	1.11
SLITRK4	15	17	1.13	SLITRK4	25	15	0.60	0.87
ST6GAL1	22	26	1.18	ST6GAL1	33	79	2.39	1.79
TFRC	417	660	1.58	TFRC	428	622	1.45	1.52
THBS1	42	32	0.76	THBS1	35	17	0.49	0.62
TMEM132A	20	28	1.40	TMEM132A	21	15	0.71	1.06
TMEM2	48	54	1.13	TMEM2	36	43	1.19	1.16
TPBG	15	13	0.87	TPBG	14	16	1.14	1.00
VASN	30	77	2.57	VASN	62	66	1.06	1.82

**Supplemental Table 1: Spectral counts and fold change of GNPTAB<sup>-/-</sup> to HeLa.** Data represents proteins detected after ST6Gal1 SEEL and biotin immunoprecipitation by MS/MS. Proteins listed were detected in two biological replicates and have spectral counts above 10.